TECHNISCHE UNIVERSITÄT WIEN

DIPLOMA THESIS

Modification of Preceramic Polymers and Investigation of their Porosity Development

TU Wien

Institute of Chemical Technologies and Analytics

Getreidemarkt 9/164

1060 Wien

under instructions of Assistant Prof. Dipl.-Ing. Dr.techn. Thomas Konegger and
Ao.Univ.Prof. Dipl.-Ing. Dr.techn. Roland Haubner

by

Matthias Nebel BSc

Seckendorfstraße 2/2/2
1140 Wien

Wien, April 2019

Abstract

The topic of this work was the modification of preceramic polymers, as well as the investigation of porosity in the ceramics obtained by thermal conversion of these modified polymers. It was the objective of this work to produce porous ceramics with pores in the size range of 1 nanometer or smaller and to determine ways to influence the porosity of these ceramics by changing parameters. These microporous ceramics are meant to be used subsequently as material for selective layers in gas separation membranes.

For the production of these microporous ceramics, the polymer precursor route was used in this work, which, in contrast to the conventional powder route, starts from a preceramic polymer, which is converted to a ceramic by a thermal polymer-to-ceramic conversion process.

The precursor used in this work was a commercially available poly(vinyl)silazane, which is converted into a microporous ceramic with pores in the size range of 1 nanometer by a two-stage thermal conversion process (cross-linking at 250 °C and pyrolysis at 600 °C, both under an nitrogen atmosphere).

For a further increase in the number of pores, the poly(vinyl)silazane was chemically modified prior to thermal conversion by the addition of different bromides, resulting in the substitution of organic groups on the poly(vinyl)silazane. The idea behind this is that these organic groups are split off during the thermal conversion process and thus lead to an increase in porosity.

To characterize the products and their preliminary products (crosslinked and uncrosslinked polymers), these were, as far as possible, examined with IR, NMR and elemental analysis (carbon and oxygen). The porosity investigations were carried out by nitrogen physisorption. These investigations showed that the modification lead to a significant increase in the BET surface area while maintaining the pore size, which in turn shows that the number of pores has increased.

By variation of the precursor/bromide ratio in the reaction mixture of the chemical modification, it was also possible to influence the number of pores, which shows that it's possible to control the porosity with this approach.

The objectives of this work were therefore achieved. It was possible to increase the number of micropores in the desired size range. On the other hand, a clearly too high oxygen content of the samples turned out to be undesirable, the reduction of which could not be achieved in this work.

Kurzfassung

Das Thema dieser Arbeit war die Modifikation von präkeramischen Polymeren, sowie die Untersuchung der Porosität in den Keramiken, die durch thermische Umwandlung dieser modifizierten Polymere erhalten werden. Dabei war es das Ziel Keramiken mit Poren im Größenbereich von 1 Nanometer oder kleiner herzustellen und zu versuchen die Porosität dieser Keramiken gezielt zu beeinflussen. Diese mikroporösen Keramiken sollen in weiterer Folge als Material für selektive Schichten in Gastrennmembranen zur Anwendung kommen.

Zur Herstellung der mikroporösen Keramiken kam in dieser Arbeit die Polymerprecursorroute zur Anwendung, die im Gegensatz zur konventionellen Pulverroute nicht von einem keramischen Pulver ausgeht, sondern von einem präkeramischen Polymer, welches durch ein thermisches Umwandlungsverfahren zu einer Keramik umgewandelt wird.

Als Precursor wurde in dieser Arbeit ein kommerziell erhältliches Poly(vinyl)silazan eingesetzt, welches durch ein zweistufiges thermisches Umwandlungsverfahren (Vernetzung bei 250 °C und Pyrolyse bei 600 °C, jeweils unter Stickstoffatmosphäre) in eine mikroporöse Keramik mit Poren im Größenbereich von 1 Nanometer umgewandelt werden kann.

Um die Anzahl der Poren zusätzlich zu erhöhen, wurde das Poly(vinyl)silazan vor der thermischen Umwandlung chemisch modifiziert. Dabei wurden durch Zugabe unterschiedlicher Bromide organische Gruppen an das Poly(vinyl)silazan substituiert. Die Idee dahinter ist, dass diese organischen Gruppen bei der thermischen Umwandlung wieder abgespalten werden und so für eine Erhöhung der Porosität sorgen.

Zur Charaktersierung der Produkte, sowie deren Vorstufen (vernetzte und unvernetzte Polymere), wurden diese, soweit möglich, mittels IR, NMR und Elementanalyse (Kohlenstoff und Sauerstoff) untersucht. Die Porositätsuntersuchungen wurden mittels Stickstoff-Physisorption durchgeführt. Dabei konnte eine deutliche Erhöhung der BET-Oberfläche bei gleichzeitiger Beibehaltung der Porengröße (um 1 nm) erreicht werden, was wiederum zeigt, dass die Anzahl der Poren gestiegen ist.

Durch Variation des Precursor/Bromid-Verhältnisses im Reaktionsansatz der chemischen Modifikation konnte außerdem die Anzahl der Poren beeinflusst werden, was zeigt, dass über diesen Ansatz die Steuerung der Porosität möglich ist.

Die Ziele dieser Arbeit wurden daher erreicht, durch den gewählten Ansatz war es möglich die Anzahl an Mikroporen im gewünschten Größenbereich zu erhöhen. Als unerwünscht stellte sich dagegen ein deutlich zu hoher Sauerstoff-Gehalt der Proben heraus, dessen Verringerung im Rahmen dieser Arbeit nicht erreicht werden konnte.

Table of contents

1. Introduction

Global challenges in the field of energy and the environment lead to an increasing demand of materials with improved and novel properties to enable alternative industrial processes with increased efficiency and lower environmental impact. Novel ceramic materials derived from silicon-based polymers with microporosity in the size range smaller than 1 nanometer are expected to possess promising properties in the field of high-temperature gas separation. Focus of recent investigations is the clarification of the origin and the collapse of microporosity in these materials, as well as an analysis of the influence of the microporous structure on their interaction with gases.

The hypothesis is that through a comprehensive consideration of all relevant process steps an identification of the factors influencing the structure and thermal stability of the microporous final material is possible. It is assumed that this will allow the development of a strategy to control the material properties so that it enables well-defined gas transport, which is of high relevance for establishing new membrane materials.

This work focuses mainly on the modification of the preceramic polymer and how this modification subsequently affects the porosity of the resulting ceramics. The used approach is that organic groups are added to the polymer by a nucleophilic substitution, which are subsequently split off during the polymer-to-ceramic conversion, leaving behind pores in the resulting gaps.

The objective of this work was in a first step to determine if and to which extent this approach increases the number of pores in the polymer-derived ceramics and how the use of different bromides influences the results (see 4.1).

In a second step parameters were varied to get a better understanding of the process and to optimize it (see 4.2, 4.3 and 4.4).

2. Theoretical background

2.1 Porous ceramics

The word *pore* originates from the greek word *πόρος (póros)*, which translates into "passage". Pores can be defined as minute openings through which gases, liquids, or microscopic particles may pass [1]. Combined with the greek word *póros*, pores can be therefore seen as passages for material exchange.

However, it has to be mentioned that this definition is not exact, as it does not include closed pores. A more accurate definition is therefore that pores are those parts of a solid that are not occupied by solid material [2].

In ceramic science pores are considered as defects and are often undesirable because of their strength-reducing effect [3]. In many areas of technology, it is therefore a target to produce components with little or no porosity. For example, during casting, pores (also called voids in special cases) are considered as casting defects, and sintering is primarily a process to eliminate pores for better strength.

However, pores are not always considered as negative. In many applications, porosity is introduced to influence the properties of a material. For example, pores can be used to reduce the density (to lower weight and cost), to increase the specific surface area (e.g. to increase the reactivity), to influence thermal and electrical properties (such as thermal shock resistance, thermal and electrical conductivity or heat capacity) and to control the permeability (which is important for membrane applications) [4].

While the targeted introduction of porosity into other classes of materials is widely-used, this was not the case for ceramics, with the exception of the refractory industry, for a long time [4], because to their inherently brittle nature [5]. However, ceramics combine some properties that are highly relevant in technical applications, such as good chemical stability, great specific strength and rigidity and high thermal stability [6].

It is therefore not surprising that the interest in porous ceramics has increased in recent decades, especially for applications where the components are exposed to high temperatures, extensive wear and corrosive environments [5]. These applications include filtration (e.g. diesel particulate, molten metal and hot gas filtration), absorption, membrane supports (e.g. for hydrogen separation), separation membranes, porous bioimplants, sensors, etc [7].

2.1.1 Gas separation membranes

There are several substantial arguments for further development of gas separation membranes, which are membranes able to separate different gases from each other.

On the one hand, the separation of gases is an important part of process optimization, nowadays often referred to as process intensification (PI). According to Stankiewicz and Moulijn [8], PI *comprises novel equipment, processing techniques, and process development methods that, compared to conventional ones, offer substantial improvements in (bio)chemical manufacturing and processing.*

One of the technologies supporting this objective is according to Fig. 1 the "Separation Technology", because in-situ separation process steps are essential for the construction of multi-functional reactors, which combine different functions that conventionally would be performed in separate pieces of equipment [9].

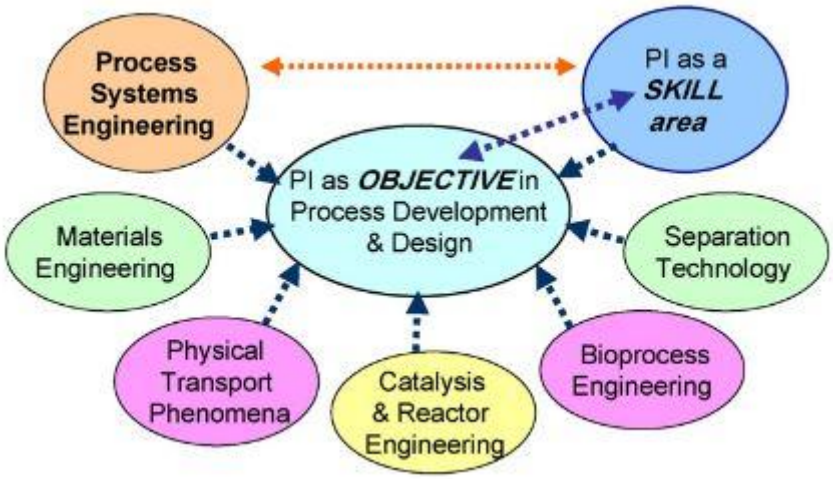

Fig. 1 Process intensification (PI) as objective and as skill area [27]
©2008 by Elsevier. Reprinted with permission.

Especially the production or purification of hydrogen represents a key technology for future developments. Nowadays hydrogen is e.g. used for the reduction of metal oxides, for the production of ammonia or as a coolant (due to its high heat capacity). However, due to increasing demand for energy the most promising application for hydrogen is the use as an source of energy. The power consumption is predicted to almost double until 2050 to around 30 TW as compared to 17 TW in 2017 [10]. Hydrogen could play an important role as alternative energy source to overcome these global challenges.

2.1.2 Ceramics as membrane material

Hydrogen is mainly produced today through steam reforming or catalytic reforming. Both techniques operate in presence of low molecular weight hydrocarbons. This means that the separation of hydrogen can only be accomplished at high temperatures (>80 °C) to avoid condensation of hydrocarbons on the membrane. These temperatures can affect the performance of polymer membranes, which are used today. Furthermore, they are very sensitive to variations of gas composition, which can lead to their failure [11].

The use of ceramic membranes represents an interesting alternative, since they possess higher thermal, mechanical and chemical stability and can therefore be used at temperatures above 300 °C and in harsh chemical environments [12].

However, the production of ceramic membranes is problematic and cannot be achieved satisfactorily through the conventional powder processing route, since the sintering process eliminates the porosity. Lowering the sintering temperature would contain porosity, although it would also lower the mechanical strength of the resulting ceramics [13].

Therefore other production methods must be used to obtain ceramics with the desired permeability, while maintaining the required mechanical strength. An interesting alternative is the use of PDCs (polymer-derived ceramics), which are ceramics derived from preceramic polymers.

2.1.3 Structure of gas separation membranes

The construction of a gas separation membrane should be discussed briefly at this point: A highly-selective layer is responsible for the separation of the gases. These selective layers tend to have very low permeation rates. Therefore the selective layer has to be extremely thin (often less than 0.1 µm), which however leads to another problem. Such thin layers wouldn't be mechanically stable enough, which is why this selective layer is supported by a microporous low-selectivity substrate, which doesn't affect the separation process but provides mechanical strength [11].

The selective layer can be directly applied on the substrate, but usually these gas separation membranes also contain an intermediate gutter layer as shown in Fig. 2. This gutter layer provides a smooth surface for the selective layer and serves to conduct the permeating gas to the pores of the microporous support [11].

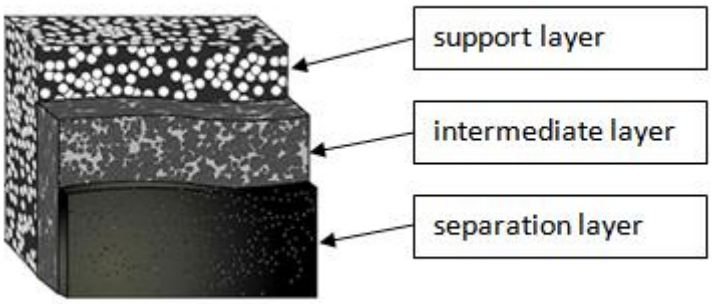

Fig. 2 Typical structure of a gas separation membrane [14]

This work focuses on the production of materials that can be used for the selective layer of such gas separation membranes. For this purpose a considerable amount of pores in the size around or beneath 1 nanometer are required.

2.2 Polymer-derived ceramics

While ceramics are traditionally derived through sintering of pressed powders, PDCs (polymer-derived ceramics) are derived through a thermal polymer-to-ceramic conversion process. This conversion process consists usually of two steps: First, the polymer gets cross-linked, this occurs usually at low temperatures between 200 and 300 °C, but the required temperature can be lowered significantly through the addition of a radical initiator (e.g. dicumyl peroxide). In a consecutive step the cross-linked polymer gets pyrolyzed at higher temperatures [15] [16].

The biggest advantage of this processing method is that the shaping takes place at a time when the substance is still of a polymeric nature, which is why shaping processes can be used which are difficult or impossible to access in the conventional powder route such as injection molding, extrusion, meltspinning, blowing or 3-D printing [7]. Furthermore it is possible to control the micro- and nanostructure of the resulting ceramics [16], allowing the introduction of well-defined microporosity, which is a requirement for the production of gas separation membranes.

There are several possibilities to introduce porosity into PDCs, including direct foaming or the use of sacrificial fillers [17]. It was also shown that it's possible to introduce microporosity without the presence of additives, for example through pyrolysis of low molecular weight polysilazane precursor polymers in NH_3 with low heating rates to form an amorphous, covalent ceramic [18].

Another advantage is that the processing takes place at significantly lower temperatures than the conventional production route, which is due to the lower energy consumption an economic and ecological advantage [16].

The precursors used to obtain PDCs are usually silicon-based polymers. Some of the commonly used preceramic polymer systems are summarized in Fig. 3.

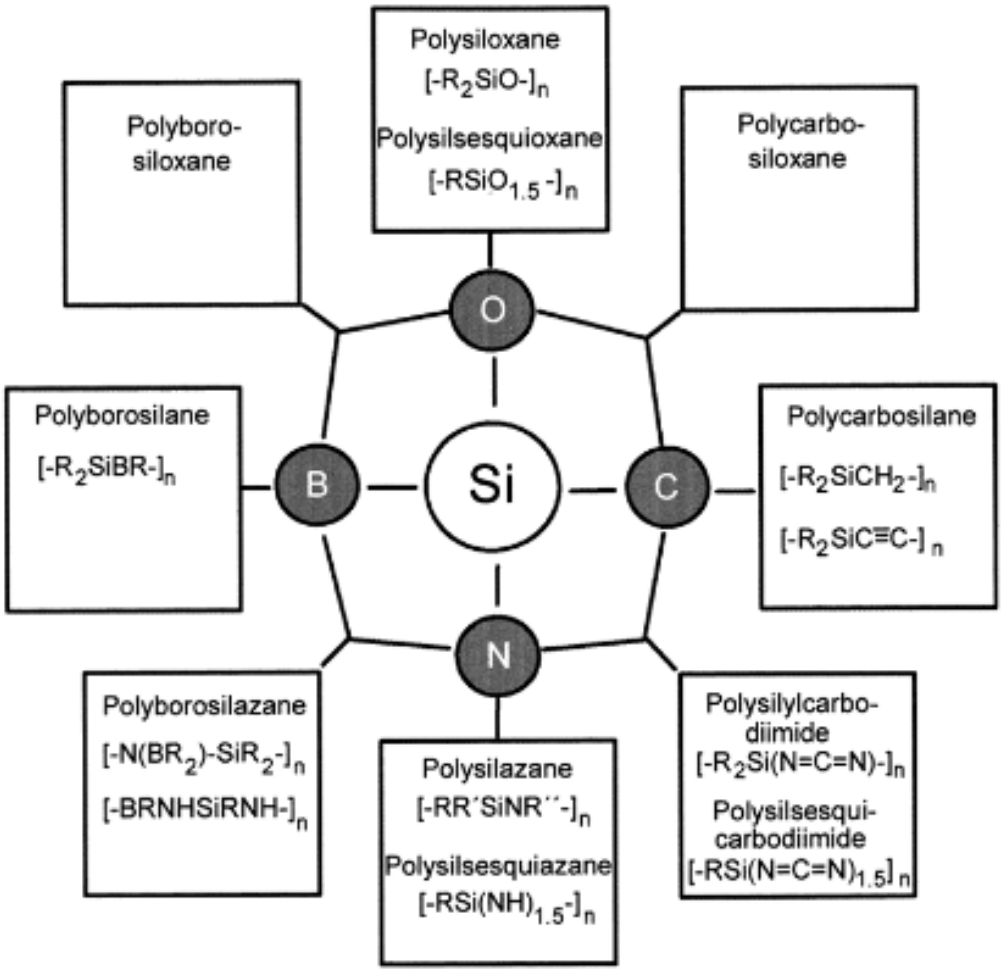

Fig. 3 Preceramic polymer compositions in the system Si-O-C-N-B [19]

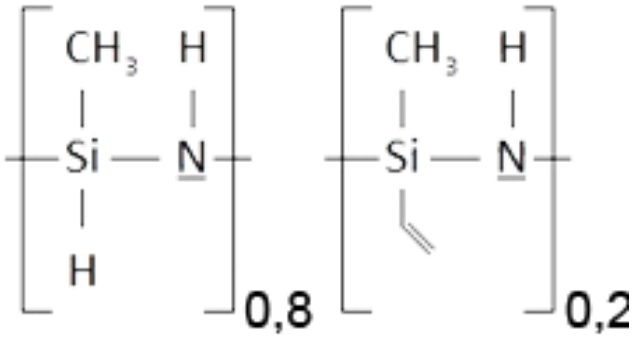

Fig. 4 Structural formula of Durazane 1800

The precursor material used in this work is a poly(vinyl)silazane (Durazane 1800, durXtreme GmbH, Germany), the structural formula of this polymer is shown in Fig. 4. Due to its vinyl moieties it can be cross-linked at temperatures around 250 °C, while the polymer-to-ceramic conversion process takes place at temperatures above 400 °C [12] [15].

Two points must be considered for the heat treatment: First, the insertion of oxygen into the polymer must be avoided, because high oxygen contents lead to a reduced high-temperature stability [16], while Si-O-C bonds are considered to be hydrothermally unstable [12]. Therefore the thermal conversion processes must be carried out under an inert atmosphere.

Secondly, an excessively high pyrolysis temperature results in a collapse of the pore structure as shown in Fig. 5. Temperatures above 600 °C must therefore be avoided to maintain high specific surface areas.

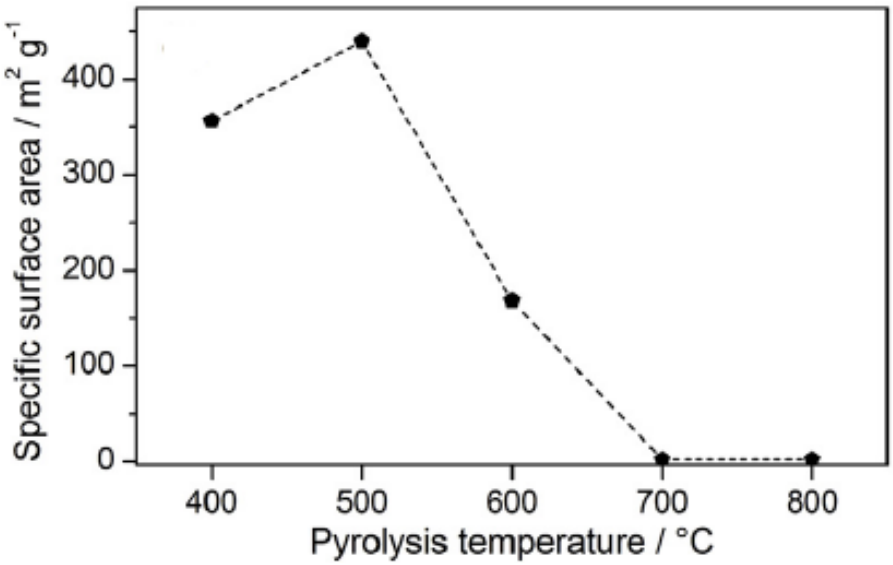

Fig. 5 Specific surface area of PVS-derived materials as a function of pyrolysis temperature [12]

2.3 Modification of the precursor

Several approaches can be found in the literature to modify precursor materials to change the properties of the resulting ceramics. Many of these approaches use metallic components as additives to give magnetic properties to the resulting ceramics [20] [21] or to build micro- and mesoporous nanocomposites [22] [23].

The approach of this work to introduce micropores into the polymer-derived ceramics is to modify the poly(vinyl)silazane through a nucleophilic substitution, as shown in Fig. 6, prior to cross-linking/pyrolysis. For the realization of this modification a work of Moore et al. [24] was used as a reference, which focuses on the synthesis of tertiary amines through direct alkylation of secondary amines with alkyl halides.

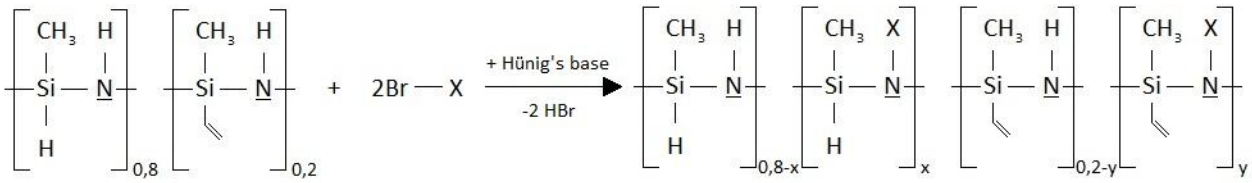

Fig. 6 Modification of a poly(vinyl)silazane by nucleophilic substitution

The polysilazane contains secondary nitrogen atoms, which react in a nucleophile substitution with the alkyl bromide to ternary nitrogen atoms and hydrogen bromide as byproduct. The addition of Hünig's base is necessary to prevent side reactions by building a quarternary ammonium salt with hydrogen bromide. Without the addition of Hünig's base hydrogen bromide would react with the polysilazane, building undesired byproducts, which would strongly decrease the yield.

The idea behind this approach is that the added organic groups are split off during pyrolysis, leaving pores behind. The objective of this work is to determine if this approach works as expected and how the porosity of the resulting ceramics can be manipulated. For example, to investigate if the size of the organic substituent (labelled as X in Fig. 6) influences the resulting pore size.

3. Experimental procedure

3.1 Materials

A commercially available poly(vinyl)silazane (Durazane 1800, durXtreme GmbH, Germany) was used as precursor material. Under normal conditions this polysilazane is a colourless liquid with a comparatively low viscosity (22 mPa.s at 25 °C [12]). The polysilazane was stored in the refrigerator, due to its hydrolysis sensitivity under nitrogen atmosphere.

The other reagents were stored under normal storage conditions in a dark and dry area. The solvent (acetonitrile) was additionally dried with a molecular sieve with a diameter of 3 Å. The molecular sieve was regenerated from time to time at 110 °C. An overview of all reagents that were used in this work is shown in Tab. 1.

The gases employed in this work were supplied by Air Liquide and used as supplied: N_2 ($\geq$ 99.999 %), He ($\geq$ 99.999 %) and O_2 ($\geq$ 99.995 %).

Tab. 1 Overview of the used reagents

Reagent	CAS number	Mol mass, $g.mol^{-1}$	Density at 20 °C, $g.cm^{-3}$	Manufacturer	Purity, %
Durazane 1800	/	64.28	1.00	durXtreme, GmbH	$\geq$ 99
acetonitrile	75-05-8	41.05	0.78	Sigma-Aldrich	$\geq$ 99.8
Hünig's base (N,N-diisopropylethylamine)	7087-68-5	129.25	0.74	Sigma-Aldrich	$\geq$ 99.5
benzyl bromide	100-39-0	171.04	1.44	Sigma-Aldrich	$\geq$ 98
α-bromo-p-xylene	104-81-4	185.06	1.32	Sigma-Aldrich	$\geq$ 99
allyl bromide	106-95-6	120.98	1.40	Sigma-Aldrich	$\geq$ 97
1-bromobutane	109-65-9	137.03	1.28	Sigma-Aldrich	$\geq$ 99
1-bromooctane	111-83-1	193.13	1.11	Sigma-Aldrich	$\geq$ 99

3.2 Synthesis of materials

3.2.1. Modification of precursors

The modification of the precursor polymer carried out in this work is based on the work of Moore et al. [24] (see also 2.3). To modify the poly(vinyl)silazane, it was mixed with the respective bromide and N,N-diisopropylethylamine (Hünig's base). The molar ratio was typically 1:2:2, in which 1 is the amount of the polysilazane, while 2 represents the amount of bromide and Hünig's base. For some experiments the molar ratio was varied (see 4.2).

Because of the hydrolysis-sensitivity of the polysilazane and the objective to keep the oxygen content as low as possible the equipment was baked out overnight at 110 °C before each experiment to remove water residues.

Furthermore the reactions were executed under inert atmosphere (N_2). For this purpose, the apparatus was flushed with nitrogen for at least five minutes before the beginning of the experiment (and before the reagents were weighed in). Thereafter, the apparatus was closed and at each further opening of the apparatus it was operated under nitrogen counterflow. Before the start of the reaction, the apparatus was sealed with a nitrogen-filled balloon to avoid overpressure and to monitor if the apparatus is air-tight sealed.

When handling the reagents, the toxicity of the bromides (especially allyl bromide) and the occurrence of lachrymatory vapors (in the case of benzyl bromide and α -bromo-p-xylene) must be taken into account. Therefore, weighing and addition of the reagents have to be carried out with suitable protective clothing (safety glasses and protective gloves).

In Fig. 7 the construction of the apparatus can be seen. After addition of the reagents, the apparatus was heated through a oil bath, the temperature of the oil bath was controlled by a Heidolph temperature sensor, which was connected with the magnetic stirrer-heater and automatically adjusted the heating. The set temperature was 60 ° C, the actual temperature of the oil bath fluctuated between 60-70 °C.

The stirring of the oil bath and the reaction mixture was carried out with magnetic stirbars and a magnetic stirrer, the reaction was executed under reflux with a reflux condenser.

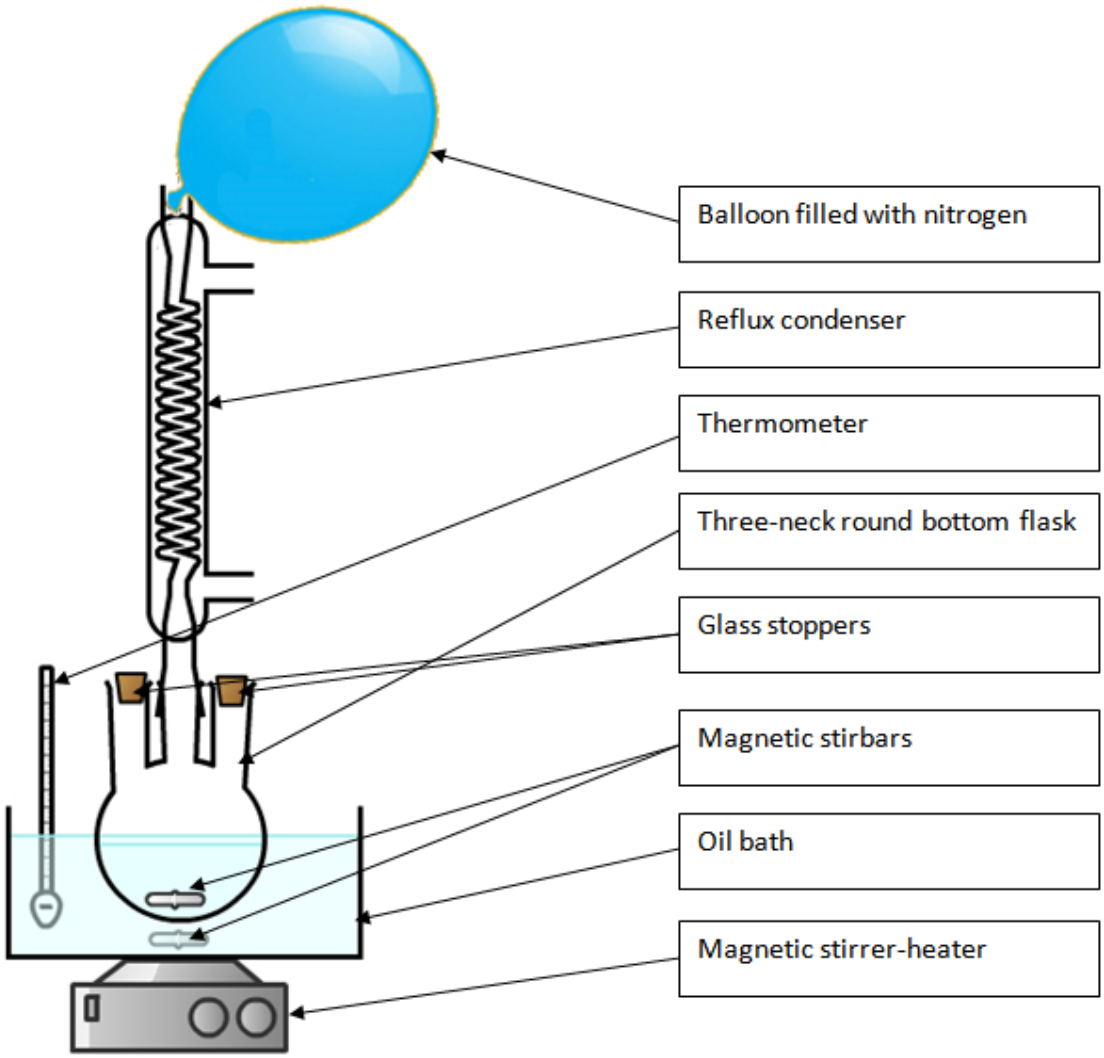

Fig. 7 Schematic illustration of the apparatus for the modification of the precursor

The weighed in amounts of reagents for the respective experiments are summarized in Tab. 2. The sample names refer to the used polymer (which was the same for all experiments) and the added bromide. The numbers included after the bromide of some sample names represent the precursor/bromide ratio (see 4.2.1), while the two experiments labeled with "dichloromethane" were processed differently (see 4.3). In a typical experiment to 0.75 g of the polysilazane around 10 mL acetonitrile were added. Also shown is the duration of the reactions, which was chosen due to the reaction rate, which differed depending on which bromide was used (for further explanation see 4.1.2).

Tab. 2 Overview of weighed in amounts of reagents

Sample	PSZ, g	Hünig's base, g	Bromide, g	Duration, d
PSZ + benzyl bromide	1.51	6.07	5,74	3
PSZ + α-bromo-p-xylene	0.77	3.09	4.1	3
PSZ + allyl bromide	0.86	3.66	3.31	3
PSZ + 1-bromobutane	0.87	3.54	3.29	7
PSZ + 1-bromooctane	0.73	3.16	3.9	7
PSZ + benzyl bromide 1:0.25	0.8	0.76	0.53	3
PSZ + benzyl bromide 1:0.5	0.75	1.5	1.01	3
PSZ + benzyl bromide 1:1	0.75	2.01	1.99	3
PSZ + benzyl bromide 1:2	0.77	3.13	4.35	3
PSZ + 1-bromobutane 1:0.5	1.5	3.03	1.43	7
PSZ + 1-bromobutane 1:2	1.51	6.07	5,74	7
PSZ + benzyl bromide dichlormethane	1.54	6.1	8.05	3
PSZ + 1-bromobutane dichlormethane	1.51	6.17	5.72	7

After the reaction was finished the solution was cooled down to room temperature and the reaction mixture was transferred into a evaporation flask and the solvent was evaporated. To keep the contact with humidity as low as possible the rotary evaporator was beforehand evacuated and filled with N_2, the installation of the evaporation flask was executed under nitrogen counterflow.

To the residual solid material approximately 30 mL n-hexane were added. The resulting suspension was stirred at room temperature for at least 1 hour, solubilizing the polysilazane and the unreacted educts, while the quaternary ammonium salt remained solid. The stirring was carried out under nitrogen atmosphere. For this purpose the flask was flushed with nitrogen prior to stirring and closed leak-tight with a glass stopper.

Next, solution and residue were separated by centrifugation. The centrifugation tubes were again flushed with nitrogen to reduce contact with moisture.

The received liquid was vacuum distilled in two steps: In the first step n-hexane was removed at 100 °C and 300 mbar, in the second step the unreacted educts were removed at 110 °C and 5-10 mbar. The second step was executed for at least 1 hour to dry the product thoroughly. The distillation was carried out without the addition of nitrogen. To prevent contact with humidity at high temperatures, the distillation apparatus was first evacuated and then heated.

The resulting solid adhered to the glass wall of the distillation flask and had to be scraped off with a laboratory spatula. The obtained solids were weighed into glass vials, which were purged with nitrogen before sealing and stored in the refrigerator.

To achieve higher yields, the processing was optimized in the further course of this work. For this purpose additional acetonitrile was used to transfer the residues in the reaction flask to the evaporation flask. In addition, the solving process with n-hexane was improved by crushing the solid into small pieces with a laboratory spatula before the stirring.

3.2.2. Thermal conversion

Next, the modified samples were subjected to a two-stage thermal conversion process (cross-linking and pyrolysis). These thermal conversions were performed in a HZS 12/600 three zone horizontal tube furnace from Carbolite, whose heat length is divided into three zones, each with its own controller and thermocouple, to accomplish a better temperature uniformity in the furnace.

In addition, the tube furnace unit was equipped on one side with a gas inlet and on the other side with a gas outlet to perform the heat treatment under an inert gas atmosphere. The furnace is opened on the side of the outlet, which means that the samples can be put into the furnace under nitrogen counterflow.

Before beginning of operation (and before the samples were put into the furnace) the furnace was purged with nitrogen for about 30 minutes at a nitrogen flow of 2 l/min. After the samples were placed into the middle of the furnace and the furnace was closed, the nitrogen flow was throttled to 0.35 l/min.

3.2.2.1 Cross-linking

For cross-linking the modified samples were heated under nitrogen atmosphere to 250 °C, which results in the formation of cross-links between the polymer chains due to the presence of vinyl moieties.

The heating schedule of the furnace, which was identical for all three zones of the furnace, is shown in Fig. 8. After heating to 250 °C with a heating rate of 1 K min^{-1}, the temperature was held for 150 minutes and afterwards the samples were cooled down to room temperature with a cooling rate of 3 K min^{-1}. However, it must be mentioned that the used furnace contains no active cooling system, meaning that the cooling rate was, especially at lower temperatures, much slower than 3 K min^{-1}.

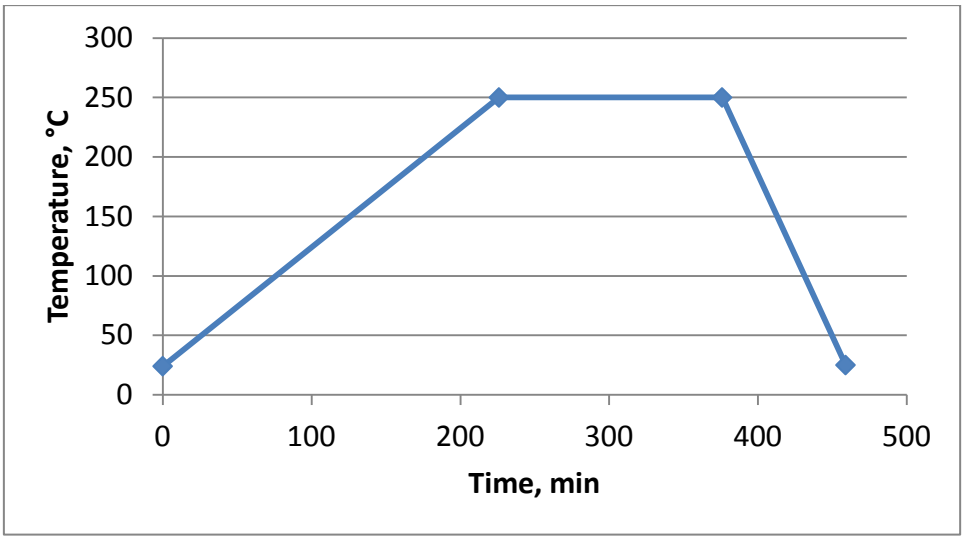

Fig. 8 Heating schedule for cross-linking

3.2.2.2 Pyrolysis

The cross-linked polymers were heated under nitrogen atmosphere up to 600 °C. This leads to a polymer-to-ceramic conversion process, including chemical decomposition and molecular rearrangement processes, resulting in a microporous ceramic.

The heating schedule for the central zone of the furnace is shown in Fig. 9, the target temperature of the two side zones was constantly set 20 °C higher. The heating was started with a rather quick heating rate (3 K min^{-1}) up to 300 °C, followed by a slower heating rate (1 K min^{-1}) up to the holding temperature (600 °C). This temperature was maintained for 4 hours and subsequently it was cooled down to room temperature with a cooling rate of 3 K min^{-1}.

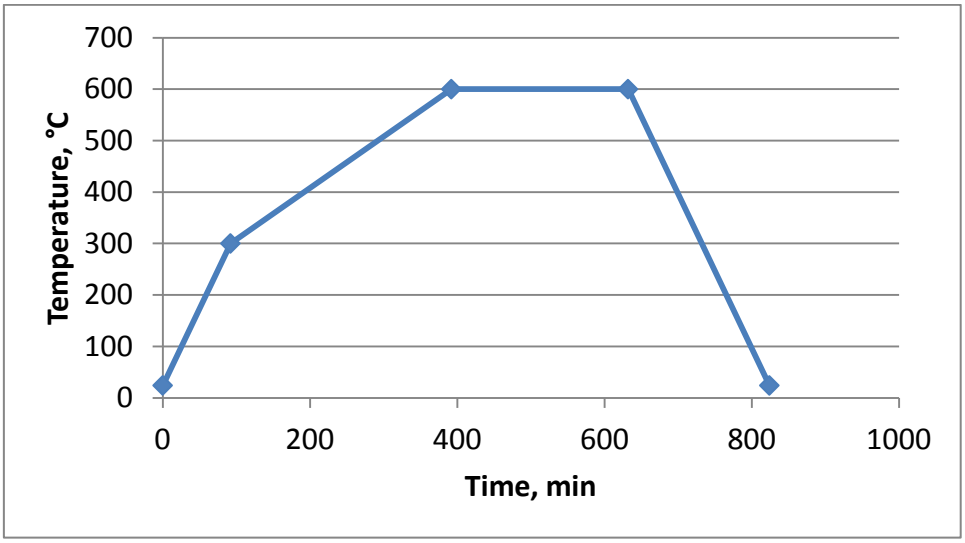

Fig. 9 Heating schedule for pyrolisis

After thermal conversion, the pyrolyzed samples were stored as before heat treatment. They were transferred to glass vials, which were purged with nitrogen, sealed and stored in the refrigerator.

3.3 Characterization

3.3.1. Elemental analysis

The elemental composition of the samples was measured with two LECO elemental analyzers: A CS230 for the determination of carbon and sulfur and a TC400 for the determination of oxygen and nitrogen.

In the CS230 Carbon/Sulfor Determinator a pre-weighed sample of ~10 mg with tungsten powder as accelerator is combusted in a stream of purified oxygen. The carbon in the sample is oxidized primarily to carbon dioxide (CO_2) with some carbon monoxide (CO) possibly being produced. The sulfur is oxidized to sulfur dioxide (SO_2). These gases are swept, along with oxygen, through a dust filter and a drying reagent into an infrared cell (IR) where sulfur is detected as SO_2. The gases are then routed through a heated catalyst which converts CO to CO_2 and SO_2 to sulfur trioxide (SO_3). The SO_3 is removed by a filter and CO_2 is measured in a separate IR cell. Based on the measured amounts of CO_2 and SO_2 it can be recalculated to the carbon and sulfur content. For the calibration of carbon analysis the reference material BAM-S003 (SiC powder, carbon mass fraction 29.89 %) was used, while the sulfur analysis wasn't calibrated since the determination of the sulfur content was irrelevant for this work.

The TC400 Nitrogen/Oxygen Determinator uses the inert gas fusion method for oxygen analysis. For this purpose, the sample was weighed in a tin capsule, which was compressed, so that as little air as possible was included with the sample. Subsequently the tin capsule was completely burned in a graphite crucible under helium atmosphere at very high temperatures (~ 3000 °C). At these temperatures the oxygen in the sample reacts with the carbon in the crucible to form CO or CO_2, which is then measured by infrared detection, while the nitrogen in the sample reacts to N_2, which is quantified with a thermal conductivity detector. As in the case of carbon/sulfur, the contents of oxygen and nitrogen were then calculated. For the calibration of oxygen analysis the reference material JK 47 (iron powder, oxygen mass fraction 1.09 %) was used, while the nitrogen measurement was calibrated with the reference material ED101 (Si_3N_4, nitrogen mass fraction 38.1 %).

At least 3 measurements were taken per sample, in the case of outliers further measurements were executed, and from these average und standard deviation were calculated. For samples with very high oxygen contents, the measurements on the O/N-LECO had to be carried out with smaller amounts of sample, because otherwise the amounts of oxygen were outside the measurement range, resulting in significantly higher values with high standard deviations.

3.3.2. Infrared spectroscopy

For quick qualitative analysis of the samples, an ATR-FTIR Spectrometer, Model: 5500 from Intech was used. For this purpose, a small amount of sample was applied to the measuring surface and then the ATR crystal was pressed onto the sample.

The samples were measured in a wavenumber range from 400 to 4000 cm^{-1} with a resolution of 2 cm^{-1} and the spectra were recorded as absorption spectra. Per measurement 50 scans were taken to gain more accurate data.

3.3.3. Nuclear magnetic resonance spectroscopy

The modified samples were analyzed by NMR spectroscopy. For this purpose, about 10 mg of the respective sample were transferred to an NMR sample tube and dissolved in 500-600 µL D-chloroform.

^{1}H and ^{13}C (CPD and DEPT-135) NMR spectra were obtained at 295 K on a Bruker Avance III HD spectrometer (Bruker BioSpin GmbH, Rheinstetten, Germany) equipped with a 5 mm Cryoprobe™ Prodigy BBO, operating at 600.15 MHz for ^{1}H and 150.90 MHz for ^{13}C.

NMR data were recorded and evaluated using TopSpin 4.0.2 (Bruker BioSpin GmbH). Chemical shifts were established based on the $CDCl_3$ peaks at 7.24 ppm (^{1}H-NMR) and 77.0 ppm (^{13}C-NMR). Subsequently, all clearly recognizable peaks were marked manually, whereby the ppm number becomes visible above each peak.

Thereafter, the peaks were integrated. The peak of the three hydrogen atoms of the Si-CH_3 peak at approximately 0 ppm was used for calibration of the integral sizes. For better illustration, the structural formula of the respective sample was inserted into a screenshot of the evaluated spectrum and the hydrogen atoms and the associated peaks were each marked in the same color.

3.3.4. Nitrogen physisorption

To determine size and volume of the pores, as well as the specific surface area, the pyrolyzed samples were analyzed by nitrogen physisorption. For this purpose, the pyrolyzed samples were pulverized in a glove box under nitrogen atmosphere and 30-50 mg of the resulting powder were weighed in a sample tube.

The analysis of the samples was carried out in an ASAP2020 device from Micromeritic, which is shown in Fig. 10. For this purpose, the sample was first degassed for 1 hour at 100 °C and 3-4 µbar and subsequently degassed for 12 hours at 250 °C and the same pressure. The degassing took place at a degas port of the device. Afterwards the sample tube was assembled to the analysis port, again manually degassed for 1 hour at 250 °C and 3-4 µbar.

Subsequently an adsorption-desorption isotherm was recorded with nitrogen as the adsorption gas under cooling with liquid nitrogen at 77K. For this purpose, the adsorbed quantity of nitrogen was measured at 50 points in the relative pressure range between $5*10^{-6}$ and 1, while subsequently the desorbed quantity of nitrogen was measured at 17 points in the relative pressure range between 1 and 0.15.

This isotherm served as a basis for further calculations. The equilibrium interval was 10 seconds, measuring at each point until the pressure in this interval changed by a maximum of 0.01 %.

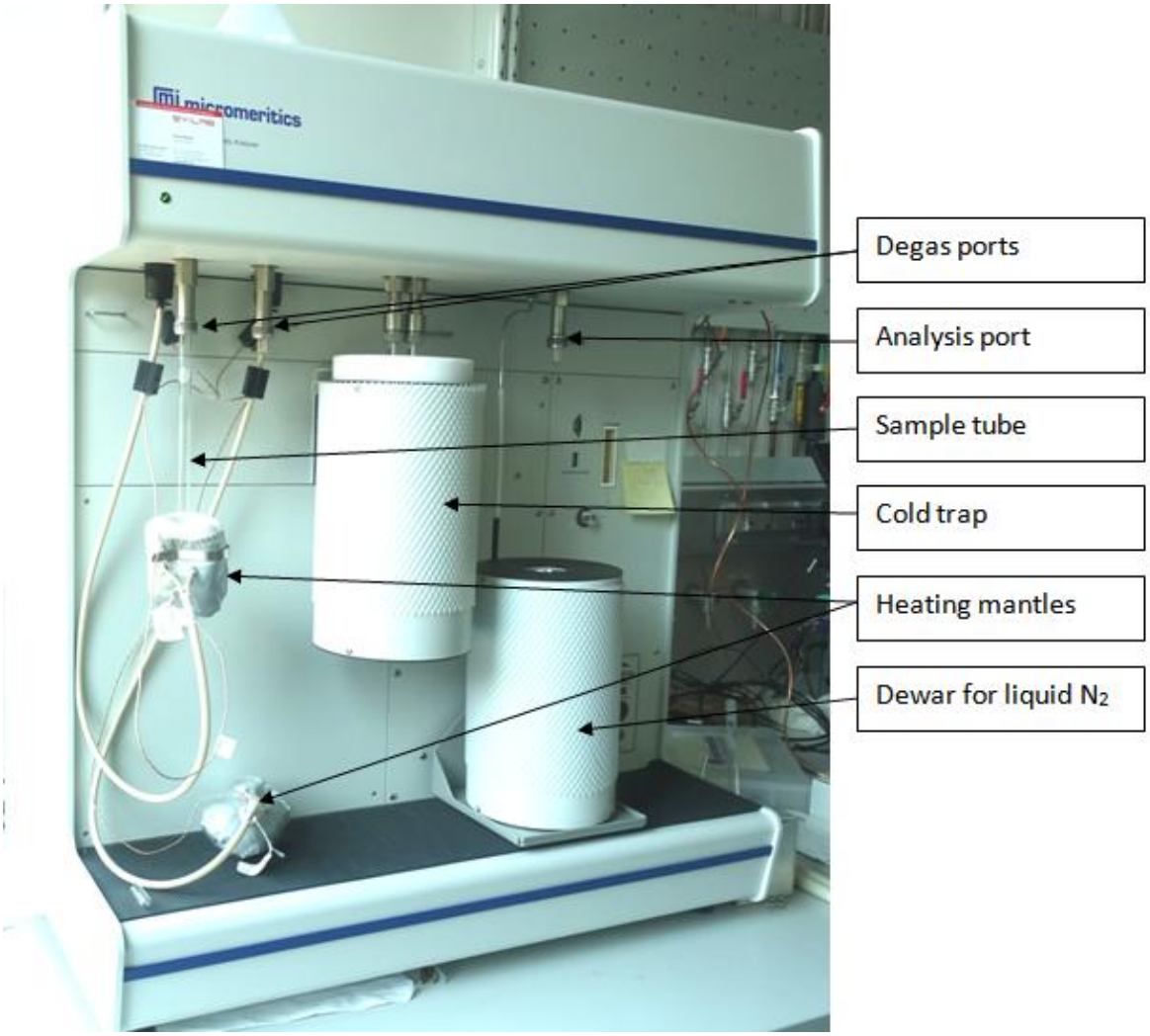

Fig. 10 ASAP2020 from Micromeritics

For the calculation of the BET surface area, five points in the relative pressure range between 0.05 and 0.3 were used. The pore size distribution (PSD) was calculated by applying the Non-Local Density Functional Theory (NLDFT) standard slit model to the nitrogen adsorption isotherms, using the data reduction software SAEIUS. The regularization parameter λ was set to 1 for all samples because this resulted in relatively smooth distribution graphs with low standard deviations.

3.4 Calculations

3.4.1 Yield

The yield of the chemical modification was calculated with Eq. 1, which is based on the assumption that the maximum possible degree of substitution is achieved. The degree of substitution is the proportion of nitrogen atoms of the precursor to which an organic group has been substituted. A degree of substitution of 50 % means therefore that the nucleophilic substitution (see Fig. 6) took place for half of the nitrogen atoms of the precursor, while the other half of nitrogen atoms are still secondary nitrogen atoms bound to one hydrogen atom.

Which degree of substitution is achievable depends on the precursor/bromide ratio and is therefore for all samples (except those in section 4.2) 100 %, because the bromide has been added in excess. The maximum possible degrees of substitution of the samples of section 4.2 are summarized in Tab. 3

Tab. 3 Theoretical possible degrees of substiution of samples modified with different precursor/bromide ratios

Sample	Theoretical possible degree of substitution, %
PSZ + benzyl bromide 1:0.25	25
PSZ + benzyl bromide 1:0.5	50
PSZ + benzyl bromide 1:1	100
PSZ + benzyl bromide 1:2	100
PSZ + 1-bromobutane 1:0.5	50
PSZ + 1-bromobutane 1:2	100

$$Y = \frac{W}{W_{th.}} = \frac{W}{\frac{m_{PSZ} * M_M}{M_p}} = \frac{W}{\frac{m_{PSZ} * (M_p + d * X)}{M_p}} \qquad \textbf{Eq. 1}$$

Y .....yield, %

W.....received mass of product, g

$W_{th.}$.....theoretically achievable mass of product, g

$m_{PSZ.}$.....weighed in mass of precursor polymer, g (see Tab. 2)

M_M .....molar mass of modified polymer based on one monomer unit, $g.mol^{-1}$

M_P .....molar mass of unmodified polymer based on one monomer unit (= 64.28 $g.mol^{-1}$)

d. .....molar mass of the respective substituted group - 1, $g.mol^{-1}$

X.....degree of substitution, %

The values of d for the respective bromides are summarized in Tab. 4. The molar masses of the bromides are also illustrated because the values of d were calculated by subtracting 81 $g.mol^{-1}$ from the molar mass of the respective bromide. 81 $g.mol^{-1}$ is the molar mass of hydrogen bromide, which is separated during the nucleophilic substitution (see Fig. 6).

Tab. 4 Molar masses of used bromides and of the respective substitution groups

Bromide	Molar mass, $g.mol^{-1}$	Molar mass of substituted group - 1, $g.mol^{-1}$
benzyl bromide	171	90
α-bromo-p-xylene	185	104
1-bromobutane	137	56
1-bromooctane	193	112
allyl bromide	121	40

In addition to the yield, the received mass of product and the theoretical receivable amount of product were also calculated in section 4.2.1. To be able to compare these numbers with each other, they are independent of the weighed-in amount of poly(vinyl)silazane (PSZ). The received mass of product per g PSZ was calculated with Eq.2, for the calculation of the theoretical receivable amount of product per g PSZ Eq.3 was used. Both equations can be easily derived from Eq.1.

$$W_{rel.} = \frac{W}{m_{PSZ}} \qquad \textbf{Eq. 2}$$

W_{rel}.....received mass of product per g PSZ (educt), $g.g^{-1}$

$$W_{rel.th.} = \frac{W_{th.}}{m_{PSZ}} = \frac{M_p + d * X}{M_p} \qquad \textbf{Eq. 3}$$

$W_{rel.th.}$.....theoretically achievable mass of product per g PSZ (educt), $g.g^{-1}$

3.4.2 Mass change

The mass change was calculated with Eq.4 for both cross-linking and pyrolysis.

$$relative\ mass\ change = 1 - \frac{mass\ after\ crosslinking/pyrolysis}{mass\ before\ crosslinking/pyrolysis} \quad \textbf{Eq. 4}$$

The theoretical mass losses were calculated with Eq.5:

$$Z = \frac{M_M - M_P}{M_M} = \frac{(M_P + d * X) - M_P}{M_P + d * X} = \frac{d * X}{M_P + d * X} \quad \textbf{Eq. 5}$$

Z .....theoretical mass loss, %

M_M .....molar mass of modified polymer based on one monomer unit, g.mol^{-1}

M_P .....molar mass of unmodified polymer based on one monomer unit (= 64.28 g.mol^{-1})

d. .....molar mass of the respective substituted group - 1, g.mol^{-1} (see Tab. 4)

X.....degree of substitution, %

3.4.3 Theoretical carbon content

The theoretical carbon content was calculated with Eq.6. The degree of substitution used for these calculations is again the maximum possible degree of substitution.

$$C_{th.} = \frac{m_C}{M_M} = \frac{16.8 + 12 * z * X}{M_P + d * X} \quad \textbf{Eq. 6}$$

$C_{th.}$.....theoretical carbon content, %

m_C.....mass of carbon atoms based on one monomer unit, g.mol^{-1}

M_M .....molar mass of modified polymer based on one monomer unit, g.mol^{-1}

M_P .....molar mass of unmodified polymer based on one monomer unit (= 64.28 g.mol^{-1})

z.....number of carbon atoms in the respective bromide

d. .....molar mass of the respective substituted group - 1, g.mol^{-1} (see Tab. 4)

X.....degree of substitution, %

3.4.4 Degree of substitution

In order to be able to estimate the degree of substitution, a formula for the calculation of the degree of substiution, based on the carbon content, was derived. The derivation of this formula will be discussed below.

To derive a formula with which the degree of substitution can be calculated, a formula for the carbon content should first be formulated. By definition, the carbon content of a polymer is generally calculated as follows:

$$C = \frac{mass\ of\ carbon\ atoms}{mass\ of\ polymer}$$

C.....measured carbon content, %

The mass of the carbon atoms is calculated in this case as follows:

$$mass\ of\ carbon\ atoms = 16.8 + 12 * z * X$$

X.....degree of substitution, %
z.....number of carbon atoms in the respective bromide

In this 16.8 is the mass of carbon atoms in an average unit of the unmodified polymer and is calculated as follows: 12 * 0.8 + 36 * 0.2 = 16.8 g.mol^{-1}. 12, on the other hand, is the mass of one carbon atom in g.mol^{-1}.

The mass of the polymer is calculated as follows:

$$mass\ of\ polymer = 64.28 + d * X$$

d.....molar mass of the respective substituted group - 1, g.mol^{-1}

64.28 is the molecular weight of the unsubstituted polymer, 1 must be subtracted from the molar mass of the substituted group, because during the nucleophilic substitution a hydrogen atom is split off the polymer (see Fig. 6).

This results in this formula for the carbon content:

$$C = \frac{16.8 + 12 * z * X}{64.28 + d * X}$$

This formula now has to be converted into a formula for X. For this purpose, the denominator is first brought to the other side:

$C * (64.28 + d * X) = 16.8 + 12 * z * X$
$64.28 * C + d * X * C = 16.8 + 12 * z * X$

By further transformation is obtained:

$64.28 * C - 16.8 = 12 * z * X - d * X * C$

Now X is singled out and the rest is moved to the other side, which finally gives the formula for calculation of the degree of substitution:

$64.28 * C - 16.8 = X * (12 * z - d * C)$

$$X = \frac{64.28 * C - 16.8}{12 * z - C * d} \qquad \textbf{Eq. 7}$$

4. Results and discussion

In this chapter the results of all experiments and their interpretation will be discussed. It is divided into four sections: In the first section (see 4.1) the effect of the bromide choice for the modification of the precursor will be discussed, while section 4.2 focuses on two of these bromides (benzyl bromide and 1-bromobutane) and investigates how the precursor/bromide ratio affects the results of the experiments. In section 4.3 experiments with a different processing method are examined and the last section (4.4) discusses the observations made with different storage durations of the samples.

4.1 Choice of bromide-containing compound

First, the influence of the choice of the bromide used for the modification was studied. On the one hand to test with which bromides the substitution reaction works best, on the other hand to find out how size and type of substituents affect the pore structure in the resulting ceramic.

For this purpose, five bromides of different types and sizes were selected, which can be seen in Fig. 11. Two linear bromides of different length (1-bromobutane and 1-bromooctane), two aromatic bromides (benzyl bromide and α-bromo-p-xylene) and one bromide with a double bond (allyl bromide), by which additional crosslinking sites can be introduced.

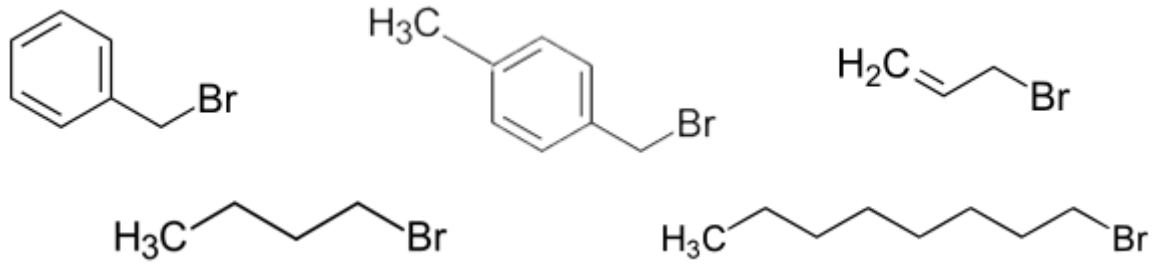

Fig. 11 Bromides used in this work (top f.l.t.r.: benzyl bromide, α-bromo-p-xylene and allyl bromide; bottom f.l.t.r.: 1-bromobutane and 1-bromooctane)

4.1.1 Observations during the reactions and their processing

All reactions were colorless to slightly yellowish at the beginning of the reaction and changed their color during the reaction to dark red to brownish. In the batches with the two aromatic bromides (benzyl bromide and α-bromo-p-xylene) and the mixtures with allyl bromide, a change in color to yellow-orange was noticeable after just a few hours. After 24 hours, the solutions were dark red and the color didn't change any further until the end of the reaction.

In the experiments with the linear bromides (1-bromobutane and 1-bromooctane) the color change was much slower. After 24 hours it was between yellow and orange, after two to four days the colors of the solutions changed to brown (1-bromobutane) or dark red (1-bromoctane).

Furthermore, it should be pointed out that in the experiments with 1-bromooctane two phases were visible, which indicates that 1-bromooctane is not completely soluble in acetonitrile.

After the wet chemical processing the products were initially liquid (with the exception of the allyl bromide samples) and crystallized during cooling as orange to brown solids. The products from the batches of the aromatic bromides were generally lighter in color than the other products. Special mention should be made of the products from the allyl bromide batches, which had a very sticky consistency, indicating that cross-linking might already have taken place during the substitution reaction.

4.1.2 Yield

First, the reactions were carried out with all five bromides with a reaction time of three days (for the procedure of the experiments see 3.2.1). The yields of these experiments were calculated with Eq.1 (see 3.4.1) and are illustrated in Fig. 12.

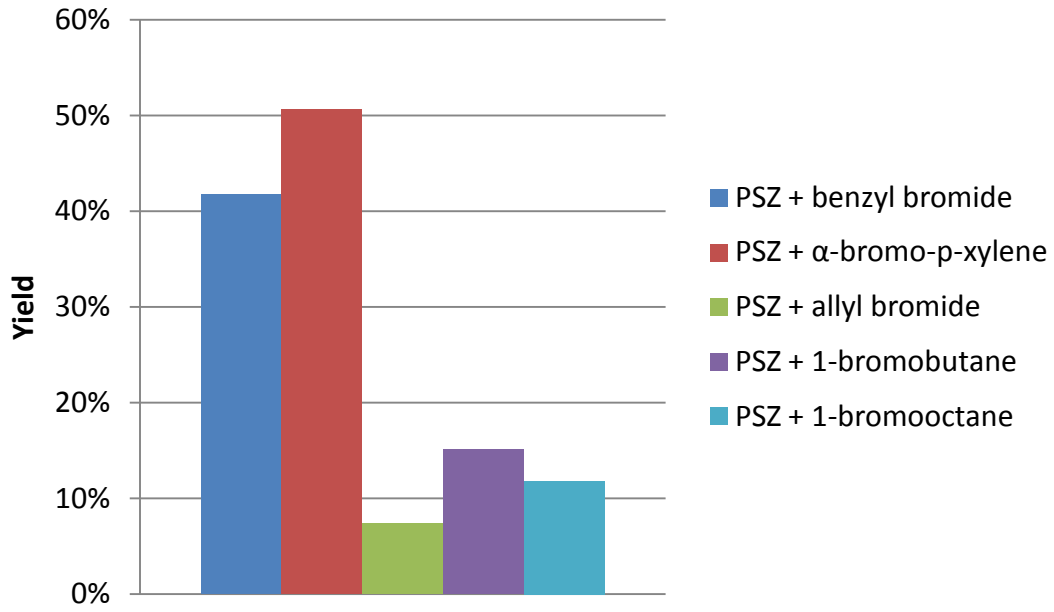

Fig. 12 Yields of reactions with different bromides after 3 days

As can be seen in this figure, these experiments resulted in insufficient yield for the experiments of three bromides (1-bromobutane, 1-bromooctane and allyl bromide), the experiments with these bromides were therefore repeated with a reaction time of seven days, which lead to a significant increase in the yields.

All yields of the experiments in this section are summarized in Tab. 5. From this table it can be concluded that the reactions with the two aromatic bromides proceed much faster than with the three non-aromatic bromides. Slowest were the experiments with 1-bromooctane, which may also be related to the fact that 1-bromooctane was not completely soluble in acetonitrile.

Tab. 5 Yields of reactions with five different bromides and varying reaction durations

Sample	Reaction time, d	Yield, %
PSZ + benzyl bromide	3	41.8
PSZ + α-bromo-p-xylene	3	50.6
PSZ + allyl bromide	3	7.4
	7	39.4
PSZ + 1-bromobutane	3	15.1
	7	34.8
PSZ + 1-bromooctane	3	11.8
	7	24.5

When looking at yields, it should be mentioned that these should only be considered as approximate values, but not as absolutely reliable measurements. In the course of this work, the processing steps were optimized (see 3.2.1) to such an extent that yields of about 60 % were achieved in experiments with benzyl bromide (see Tab. 12), which is significantly higher than in the first experiment with the same bromide, which is shown in Tab. 5.

4.1.3 IR analysis

From the modified samples and the unmodified polymer, IR spectra were recorded, which are shown in Fig. 13. The spectra were normalized with the peak of the bending vibrations of the silicon-carbon bonds at a wavenumber of about 1250 cm^{-1} (marked in green in the figure), since this peak should not be influenced by the nucleophilic substitution and was used therefore as a reference for the intensity of the other peaks.

Based on the IR spectra it can be concluded that in all cases a reaction has occurred. In the case of the two samples which were modified with aromatic bromides, the four bands typical for benzene in the wavenumber range between 1300-1550 cm^{-1} (marked in turquoise) are well recognizable, which indicates that the benzene ring was successfully incorporated into the polymer. These samples also show peaks in the wavenumber range of 3000-3100 cm^{-1} (marked in blue) indicating unsaturated carbon-carbon bonds, further confirmation for the presence of the benzene ring.

The sample "PSZ + allyl bromide" shows no peaks suggestive of additional carbon-carbon double bonds, confirming the theory that these double bonds already react during nucleophilic substitution and lead to cross-linking of the samples (see 4.1.1).

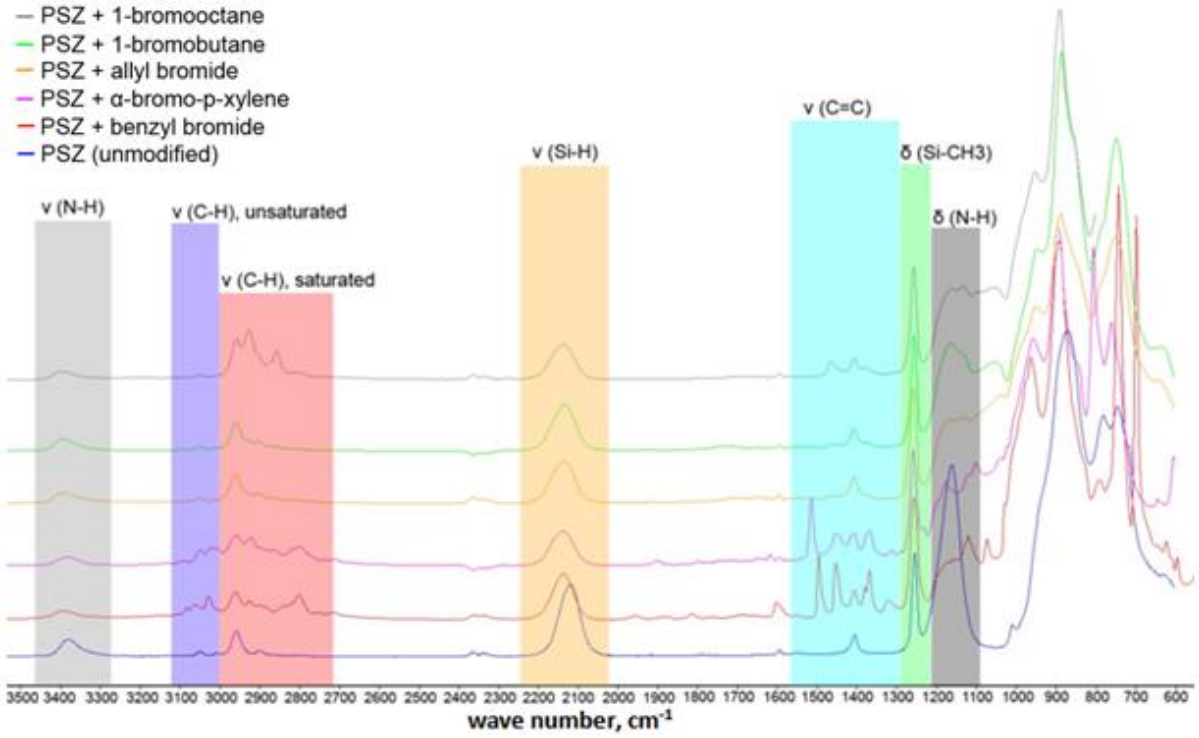

Fig. 13 IR spectra of samples modified with five different bromides

In the case of the "PSZ + 1-bromooctane" sample, additional peaks compared to the unmodified polymer can be seen in the region of the saturated carbon-hydrogen bonds (2750-3000 cm^{-1}, marked in red), in the samples "PSZ + 1-bromobutane" and "PSZ + allyl bromide" no additional peaks in this area occur. This makes sense for the "PSZ + 1-bromooctane" sample since additional carbon-hydrogen bonds should be introduced by the nucleophilic substitution, but it is surprising that no additional carbon-hydrogen peaks occur in the other two samples, although additional carbon-hydrogen peaks should also be introduced into these samples.

The bands of N-H bonds (deformation vibrations 1100-1200 cm^{-1}, stretching vibrations 3300-3450 cm^{-1}, both marked in gray) are still present in the modified polymers. Although they are weaker than in the unmodified polymer, they are still clearly visible in all samples, indicating that the reactions were not complete.

In the case of the samples "PSZ + benzyl bromide" and "PSZ + α-bromo-p-xylene", the indication of the presence of N-H bonds is in contradiction to the findings from the mass losses during pyrolysis (see 4.1.4) and the elemental analysis (see 4.1.5), which indicate a degree of substitution near 100 % for these two modifications. A degree of substitution of 100 % would in turn mean that every hydrogen atom at the nitrogen atoms got substituted through an organic group, which is why no N-H bonds should be visible in the IR spectra of these samples. Since this is not the case, the substitution may take place differently than it was assumed in 2.3.

4.1.4 Mass change during cross-linking and pyrolysis

The samples were weighed before and after cross-linking and pyrolysis, and the relative mass losses were calculated with Eq.4 (see 3.4.2). The mass losses during cross-linking and pyrolysis are listed in Tab. 6. For better comparison, the unmodified polymer was also cross-linked and pyrolyzed with the same temperature program (see 3.2.2). The theoretical mass losses were calculated with Eq.5 (see 3.4.2).

Tab. 6 Mass change during cross-linking and pyrolysis of experiments with different bromides

Sample	Mass change during cross-linking, %	Mass change during pyrolysis, %	Theoretical mass change, %
PSZ	-25.3	-14.8	/
PSZ + benzyl bromide	-21.7	-61.8	-59.0
PSZ + α-bromo-p-xylene	-28.2	-63.5	-62.4
PSZ + allyl bromide	-11.7	-17.1	-39.3
PSZ + 1-bromobutane	-15.4	-13.2	-47.4
PSZ + 1-bromooctane	-23.4	-17.2	-64.1

In the mass losses during cross-linking no clear trend can be seen, they are always in a range between 10 and 30 %. Since the unmodified polymer is also in this range, it can be assumed that the modification of the polymer has no significant influence on these mass losses.

In the further course of this work, it was found that the mass losses during cross-linking increase with increasing storage times, which indicates that mainly decomposition products volatilize during cross-linking (see 4.4.1).

In the case of the mass losses during pyrolysis, the significantly higher mass loss in the polymers modified with the aromatic bromides is particularly noticeable. These mass losses also agree well with the calculated theoretical mass losses, suggesting that the aromatic groups decompose during pyrolysis.

In the case of the samples modified with the non-aromatic bromides, the mass loss is significantly lower than it would be expected according to the theoretical calculations. This can have different causes: Either the substitution was not complete, which consequently results in a lower mass loss, or the substituted groups are not or not completely eliminated during pyrolysis.

4.1.5 Elemental analysis

Subsequently, elemental analysis (see 3.3.1) was performed on all samples (on the uncrosslinked, cross-linked and pyrolyzed samples). In the following, the analysis of the carbon content (see 4.1.5.1) and subsequently the analysis of the oxygen content (see 4.1.5.2) will be discussed.

4.1.5.1 Carbon content

In this section the measured carbon contents will be examined, which can provide information about the degree of substitution of the samples. For better comparison, the theoretical carbon contents were calculated with Eq.6 (see 3.4.3), which are shown together with the measured carbon contents in Tab. 7.

Tab. 7 Carbon contents of experiments with different bromides

Sample	C_uncrosslinked, %	C_crosslinked, %	C_pyrolyzed, %	th. C, %
PSZ	16.3 ± 1.7	26.5 ± 0.9	14.6 ± 1.0	26.13
PSZ + benzyl bromide	67.0 ± 4.1	62.8 ± 2.2	16.8 ± 2.6	65.33
PSZ + α-bromo-p-xylene	67.0 ± 3.7	69.8 ± 4.4	18.3 ± 1.7	67.03
PSZ + allyl bromide	30.2 ± 2.8	27.0 ± 1.5	17.0 ± 0.7	50.63
PSZ + 1-bromobutane	32.8 ± 3.7	30.7 ± 2.0	16.4 ± 1.3	53.87
PSZ + 1-bromooctane	39.4 ± 3.5	34.2 ± 1.2	16.9 ± 1.1	63.99

Looking at Tab. 7, the following points are noticeable: First, the carbon content of the modified polymers changes only slightly as a result of cross-linking, and tends to decrease slightly. On the other hand, in the case of pyrolysis, the carbon content decreases sharply and, regardless of the bromide used in the modification, reaches a value between 16 and 19 %. This suggests that the substituted groups decompose completely or at least almost completely during pyrolysis, leaving behind ceramics which are very similar to each other in elemental composition.

Second, it is noticeable that only the two polymers modified with the two aromatic bromides have a carbon content close to the theoretically calculated carbon content in uncrosslinked and crosslinked state. All other polymers have a significantly lower carbon content both before and after crosslinking. This indicates that only the samples modified with the aromatic bromides possess a degree of substitution near 100 %, while the other samples seem to have much lower degrees of substitution. In order to be able to estimate the degree of substitution achieved with the individual bromides, the degree of substitution was calculated with Eq.7 (see 3.4.4).

The results of the calculations are summarized in Tab. 8. The standard deviations were calculated with the standard deviations of the elemental analysis (see Tab. 7).

Tab. 8 Calculated degree of substitution of uncrosslinked and crosslinked samples based on carbon content of experiments with different bromides

Sample	X_uncrosslinked, %	X_crosslinked, %
PSZ + benzyl bromide	110.8 ± 29.0	85.8 ± 11.4
PSZ + α-bromo-p-xylene	99.8 ± 24.1	119.9 ± 36.9
PSZ + allyl bromide	10.9 ± 8.1	2.2 ± 3.9
PSZ + 1-bromobutane	14.5 ± 9.1	9.5 ± 4.5
PSZ + 1-bromooctane	16.4 ± 5.6	9.0 ± 1.6

From the results in this table, it can be seen that the carbon contents indicate, in the case of the polymers modified with aromatic bromides, a almost complete degree of substitution, which is consistent with the findings in 4.1.4. Some calculated degrees of substitution are even higher than 100 %, which is theoretically impossible. However, the theoretical maximal possible degree of 100 % is always within the range of the very high standard deviations.

In contrast, the degrees of substitution of the polymers modified with non-aromatic bromides are very low, in all cases under 20 %, which also explains the significantly lower mass losses during pyrolysis (see Tab. 6).

4.1.5.2 Oxygen content

Next, the measured oxygen contents will be discussed, which are summarized in Tab. 9.

Tab. 9 Oxygen contents of experiments with different bromides

Sample	O_uncrosslinked, %	O_crosslinked, %	O_pyrolyzed. %
PSZ	4.1 ± 0.7	4.9 ± 0.7	3.5 ± 0.8
PSZ + benzyl bromide	5.7 ± 0.2	7.4 ± 0.6	10.5 ± 0.5
PSZ + α-bromo-p-xylene	6.0 ± 0.2	8.5 ± 0.3	12.0 ± 1.8
PSZ + allyl bromide	13.1 ± 1.2	11.7 ± 1.5	14.3 ± 1.8
PSZ + 1-bromobutane	14.6 ± 1.8	11.4 ± 1.2	13.6 ± 1.0
PSZ + 1-bromooctane	13.4 ± 1.5	10.2 ± 1.2	13.7 ± 1.4

From the oxygen measurements it can be concluded that the oxygen content of the polymer is increased by the chemical modification. Since the modified polymers also have a higher oxygen content after cross-linking than the unmodified polymer, adsorbed moisture can be excluded from the samples as sole cause and it can be assumed that undesirable side reactions have occurred.

The possible periods during which these side reactions can take place are: First, during the reaction, second, during the processing of the product or third, during storage. An occurrence of side reactions during storage can almost be ruled out since no influence of the storage time on the oxygen content could be found (see 4.4.2).

As the polymers whose reactions lasted seven days ("PSZ + allyl bromide", "PSZ + 1-bromobutane" and "PSZ + 1-bromooctane", see also 4.1.2) have a higher oxygen content than the polymers whose reactions lasted three days, this could indicate that the increase of the oxygen content occurred, despite the nitrogen atmosphere, during the nucleophilic substitution.

On the other hand, it can also be argued that the polymers modified with the non-aromatic bromides could, due to the incomplete substitution, subsequently have a higher oxygen affinity, which could lead to an oxygen input during processing.

Furthermore, it can be seen from Tab. 9 that the oxygen contents of the modified samples increase during pyrolysis. Since this increase cannot be observed in the unmodified samples, it is reasonable to assume that the cause for this increase is not an oxygen entry during pyrolysis, but that the groups separated during pyrolysis have a lower oxygen content than the polymer before pyrolysis on average, whereby the oxygen content increases relatively.

In order to test this theory it was calculated with Eq.8 how high the oxygen content of the pyrolyzed samples would be if no oxygen would split off during pyrolysis.

$$O_{p,th} = \frac{O_v}{1 + m_P} \qquad \textbf{Eq. 8}$$

$O_{p,th}$.....theoretical maximal possible oxygen content after pyrolysis with no additional oxygen entry during pyrolysis, %

O_v.....measured oxygen content after crosslinking, % (see Tab. 9)

m_P.....mass change during pyrolysis, % (see Tab. 6)

The results of these calculations can be seen in Tab. 10 and are compared with the measured values of the elemental analysis. For the two polymers which were modified with the aromatic bromides, the oxygen values of the pyrolyzed samples are significantly lower than those calculated with Eq.5. For these samples the explanation that the cause for the increase in the oxygen content is the elimination of oxygen-poor groups seems to be plausible.

In the case of the polymers modified with the non-aromatic bromides, on the other hand, the oxygen values of the pyrolyzed samples are even higher than those calculated with Eq.8. However, taking into account the standard deviations, it is also possible to explain the increase in the oxygen content due to the splitting off of oxygen-free groups.

Tab. 10 Comparison of oxygen contents with theoretical oxygen contents after pyrolysis

Sample	O_crosslinked, %	O_pyrolyzed, %	O_pyrolyzed (th.), %
PSZ + benzyl bromide	7.4 ± 0.6	10.5 ± 0.5	19.4 ± 1.6
PSZ + α-bromo-p-xylene	8.5 ± 0.3	12.0 ± 1.8	23.3 ± 0.8
PSZ + allyl bromide	11.7 ± 1.5	14.3 ± 1.8	14.1 ± 1.8
PSZ + 1-bromobutane	11.4 ± 1.2	13.6 ± 1.0	13.1 ± 1.4
PSZ + 1-bromooctane	10.2 ± 1.2	13.7 ± 1.4	12.3 ± 1.4

4.1.6 NMR analysis

The uncrosslinked samples were analyzed by NMR spectroscopy (see 3.3.3), with ^{1}H and ^{13}C spectra taken from each sample. Only the sample "PSZ + allyl bromide" could not be measured by NMR as this sample was not sufficiently soluble in $CDCl_3$, possibly due to already occurring cross links.

4.1.6.1 Unmodified polysilazane

From the unmodified sample only a ^{1}H NMR spectrum was recorded, which can be seen in Fig. 14 and will be discussed first.

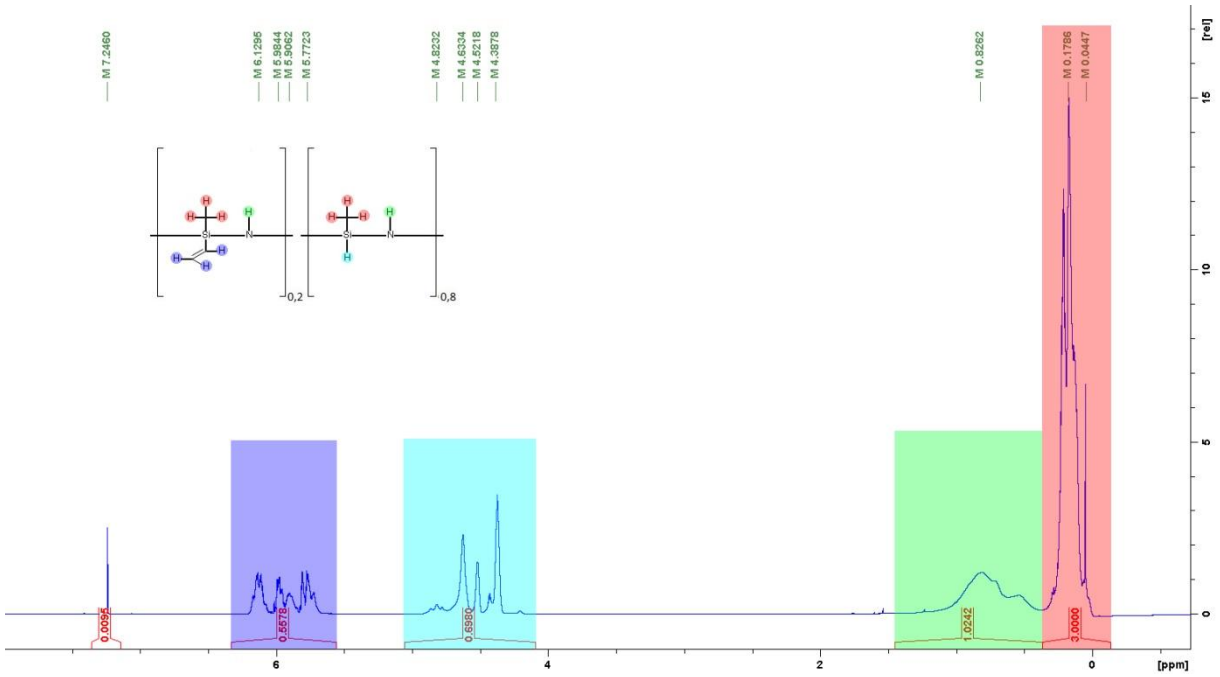

Fig. 14 ^{1}H NMR spectrum of the unmodified polysilazane HTT1800; uncrosslinked sample

As can be seen from this spectrum, all peaks could be assigned to hydrogen atoms in the structural formula of the polymer. The unmarked peak at 7.24 ppm corresponds to the solvent peak of $CDCl_3$. Here, as with all other ^{1}H NMR spectra, all integrals were calibrated with the $SiCH_3$ peak at approximately 0 ppm (marked in red), caused by three equivalent hydrogen atoms. This gives a relatively good match in the integrals (N-H: 1.02, th .: 1, Si-H: 0.70, th .: 0.8, vinyl-H: 0.56, th .: 0.6). The size of the solvent peak is not significant with 0.0095 hydrogen atoms.

4.1.6.2 PSZ + benzyl bromide

Next, the NMR spectra of the sample "PSZ + benzyl bromide" will be discussed, which are shown in Fig. 15 and Fig. 16.

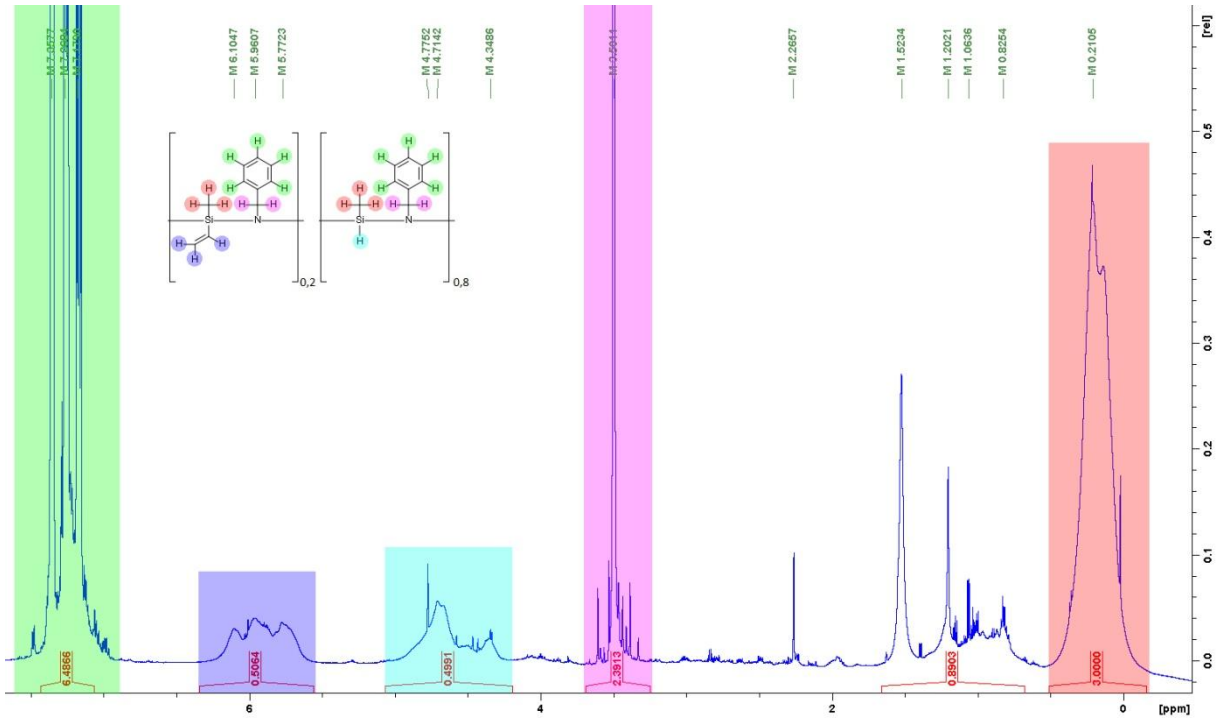

Fig. 15 ^{1}H NMR spectrum of the sample "PSZ + benzyl bromide"; uncrosslinked sample

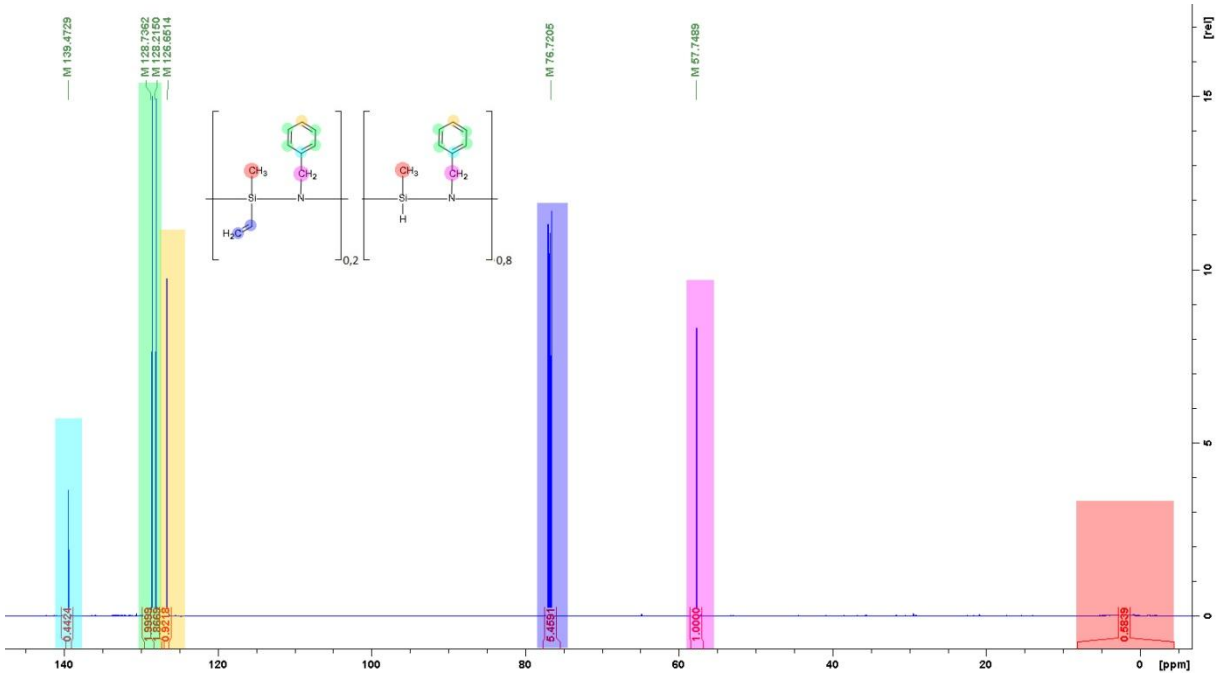

Fig. 16 ^{13}C NMR spectrum of the sample "PSZ + benzyl bromide"; uncrosslinked sample

In the ^{1}H spectrum of this sample occur two additional complex multiplets in comparison to the ^{1}H spectrum of the unmodified polymer: The peaks at about 7.0-7.5 ppm (marked in green) can be assigned with great certainty to the aromatic hydrogen atoms of the benzene ring, while the multiplet at 3.5 ppm (marked in violet), can be assigned to the two hydrogen atoms of the methylene bridge between the benzene ring and the nitrogen atom.

The integrals of these two multiplets are both slightly too high (aromatic: 6.49, th .: 5, CH_2: 2.39, th.: 2). Although the solvent peak is included in the integral of the aromatic hydrogen atoms, its effect should be insignificant.

In contrast, the integrals of the multiplets between 4 and 6.5 ppm are smaller in relation to the NMR spectrum of the unmodified polymer (Si-H: 0.50 instead of 0.70, vinyl-H: 0.51 instead of 0.56). It is therefore possible that the benzyl bromide partially reacts with the vinyl groups and/or the silicon atoms, whereby more benzyl groups are present in the modified polymer than would be expected from the reaction equation (see Fig. 6). The calculated degrees of substitution in Tab. 8 indicate that this could be a possibility.

The complex multiplet between 0.7 and 1.7 ppm could not be assigned without doubt. It could be related to hydrogen atoms bound directly to the nitrogen. These NH groups should theoretically no longer be present at the very high degree of substitution (see Tab. 8) of this sample, but were also clearly recognizable in the IR analyzes (see Fig. 13).

However, since the peak in Fig. 15 differs significantly in its appearance from that in Fig. 14, it cannot be exclusively assigned to NH groups. Therefore, byproducts (e.g. with oxygen) are most likely responsible for this peak group.

The assignment of the peaks of the ^{13}C spectrum was more problematic. The peaks between 125 and 140 ppm (marked in turquoise, green and yellow) are in the range of the aromatic carbon atoms, which can therefore be assigned to the benzene ring. The carbon atom of the methylene bridge between the nitrogen atom and the benzene ring is visible at 57.7 ppm (marked in violet), which also meets the expectations.

The assignment of the remaining peaks was more difficult. The very broad peak at about 0 ppm (marked in red) may be assigned to the carbon atom of the methyl group on the silicon, although its appearance is untypically broad.

The two carbon atoms of the vinyl group on the silicon would have to result in two peaks at about 100 ppm. These two peaks may occur at a lower shift and overlap with the solvent peak at about 77 ppm (marked in blue). Even if the integral of the solvent peak is sufficiently large, it seems unlikely that all three peaks occur at the same shift.

Since no further peaks occurred, the carbon atoms of the vinyl group were assigned in all ^{13}C spectra to the peak group at 77 ppm, but this assignment may be inapplicable.

For the calibration of the integral sizes, the peak of the methylene bridge at 57.7 ppm (marked in violet) was used, resulting for the peaks of five of the six carbon atoms of the benzene ring (marked in green and yellow) an integral size as would be expected (from left to right: 2.00 ; 1.87; 0.92), for the peak of the sixth carbon atom of the benzene ring (marked in turquoise) and the peak of the carbon atom of the methyl group on the silicon (marked in red), on the other hand, the integral sizes are significantly too low (aromatic carbon: 0.44, methyl carbon: 0.58).

Mainly due to the very broad peak of the methyl group and the resulting unreliable integral size, the ^{13}C spectrum of this sample is unsuitable for determining the degree of substitution.

4.1.6.3 PSZ + α-bromo-p-xylene

Next, the NMR spectra of the sample "PSZ + α-bromo-p-xylene" will be discussed, which are shown in Fig. 17 and Fig. 18.

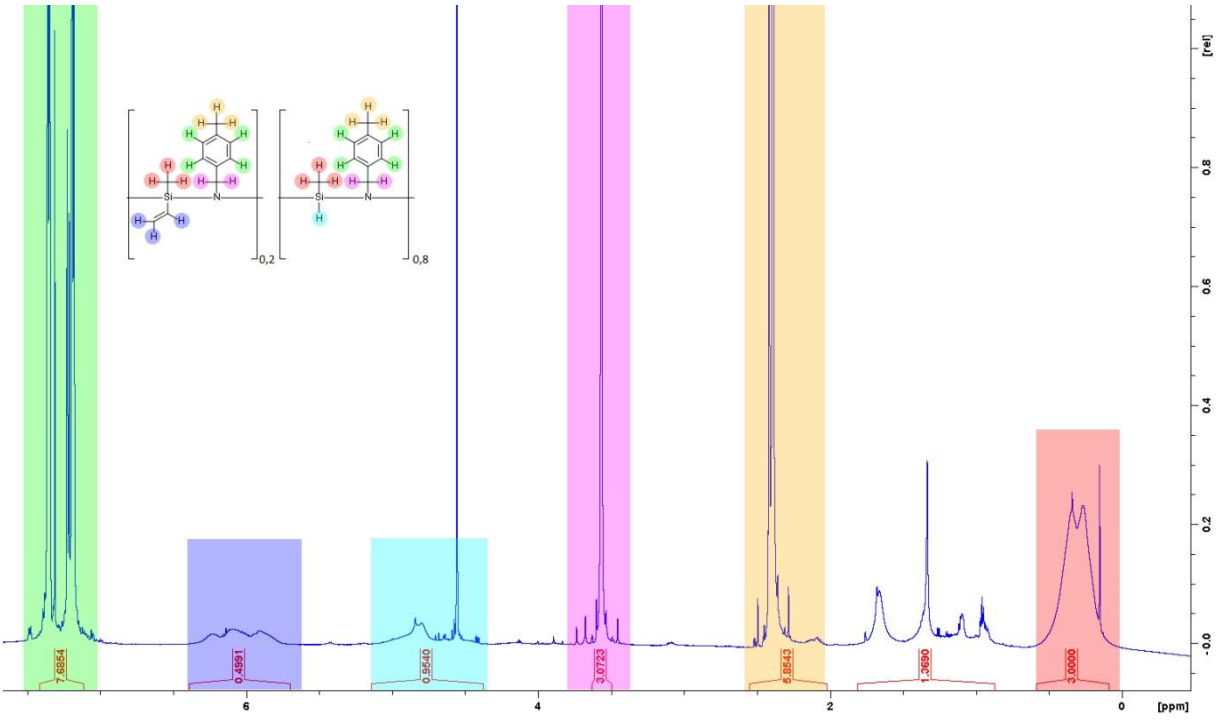

Fig. 17 ^{1}H NMR spectrum of the sample "PSZ + α-bromo-p-xylene"; uncrosslinked sample

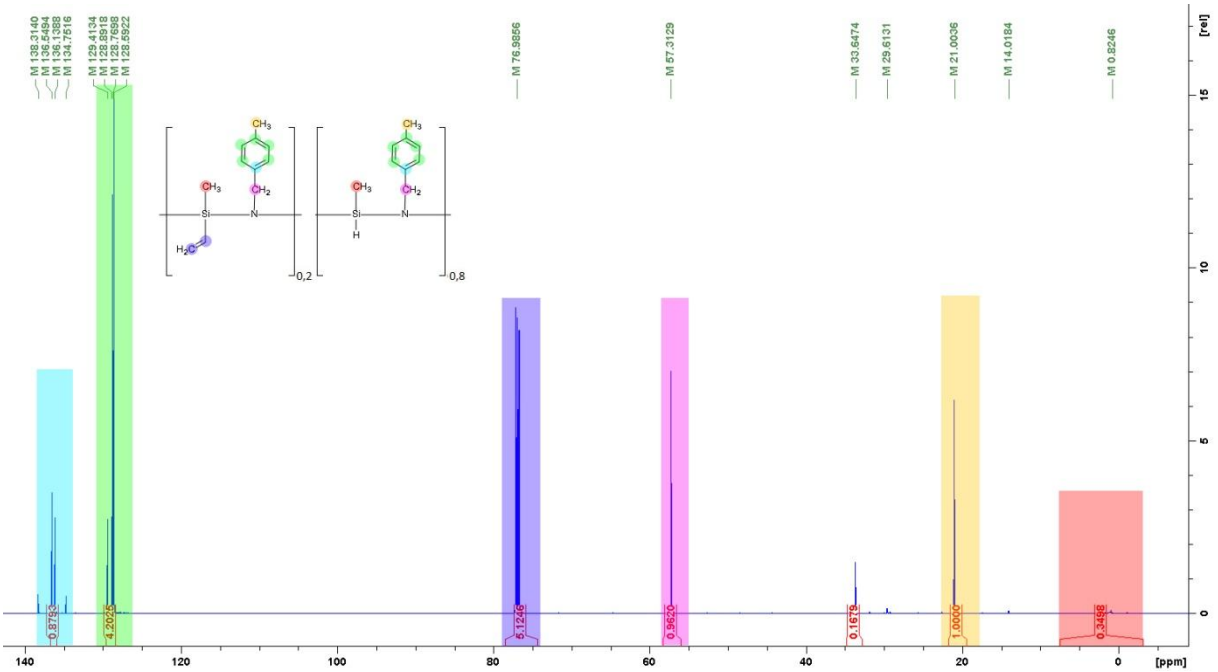

Fig. 18 ^{13}C NMR spectrum of the sample "PSZ + α-bromo-p-xylene"; uncrosslinked sample

The ^{1}H NMR spectrum of this sample is similar to that of the sample "PSZ + benzyl bromide", which was to be expected due to the chemical similarity.

The biggest difference is the peak occurring at 2-2.5 ppm (marked in yellow), which can be assigned to the additional methyl group on the benzene ring. However, the integral of this peak is larger than would be expected (5.85, th.: 3), which also applies to all other integrals relatable to the p-xylene group (aromatic: 7.69, th.: 4; CH_2: 3.07, th.: 2).

These values, which are much too high in relation to the Si-CH_3 integral, would indicate a degree of substitution of 150-200 %, which contradicts the calculated values in Tab. 8 and can therefore be excluded.

Another explanation would be that α-bromo-p-xylene has such a high boiling point (218-220 °C [25]) that the distillation step during processing (see 3.2.1) was not sufficient to remove the educt completely from the product. However, since the excessive integral values are also observed in the sample "PSZ + 1-bromobutane" (see Fig. 19), with 1-bromobutane having a much lower boiling point (100-104 °C [25]), this explanation is not sufficient to clarify this phenomenon.

It was also suspected that the relaxation delay in the NMR measurement was too short, resulting in an inefficient signal buildup. An increase of the relaxation delay, however, brought no significant change to the NMR spectra.

The ^{13}C spectrum of the sample "PSZ + α-bromo-p-xylene" has compared to the spectrum of the sample "PSZ + benzyl bromide" (see Fig. 15) an additional peak at around 20 ppm (marked in yellow), which can be assigned to the carbon atom of the methyl group on the benzene ring.

The integral sizes of this spectrum were calibrated after this peak, giving a peak size of 0.96 for the peak of the methylene bridge (marked in violet). The remaining integrals, however, are smaller than expected, particularly striking is again the peak of the carbon atom of the methyl group on the silicon (marked in red), which has with 0.35 only about one-third of the expected size.

At about 33 ppm, a small peak occurs in this spectrum (integral size 0.17), which could not be assigned. Possibly residues of the educt were still present here due to the high boiling point of α-bromo-p-xylene.

4.1.6.4 PSZ + 1-bromobutane

Next, reference is made to the NMR spectra of the sample "PSZ + 1-bromobutane", which are shown in Fig. 19 and Fig. 20.

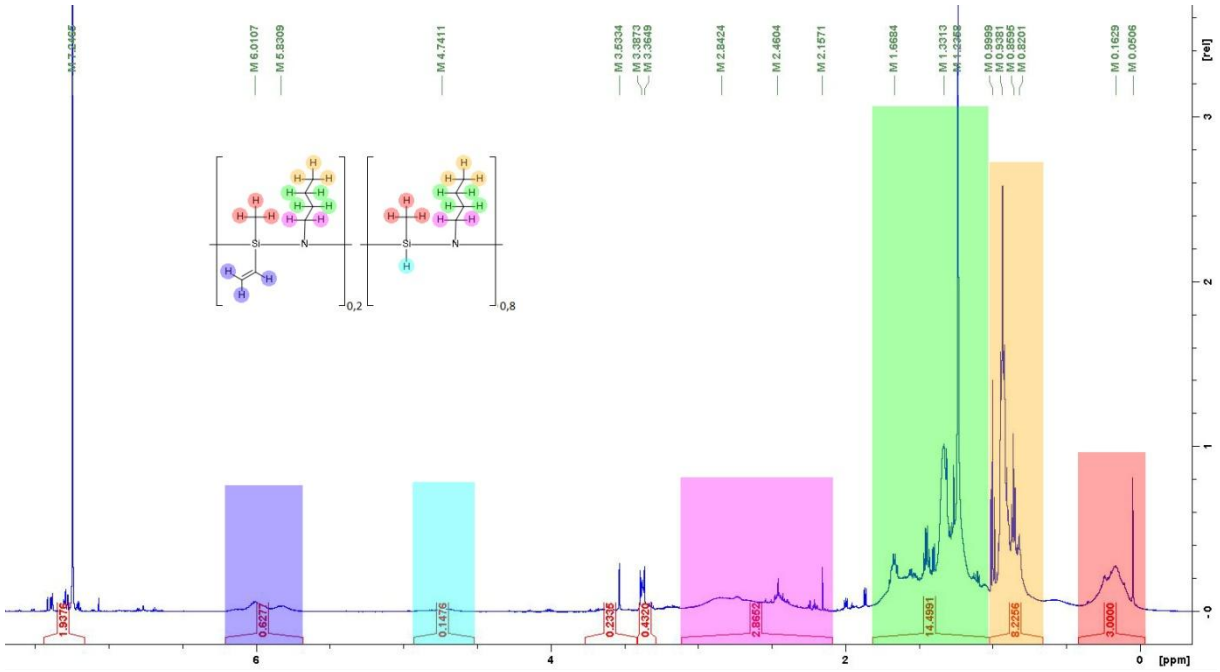

Fig. 19 ^{1}H NMR spectrum of the sample "PSZ + 1-bromobutane"; uncrosslinked sample

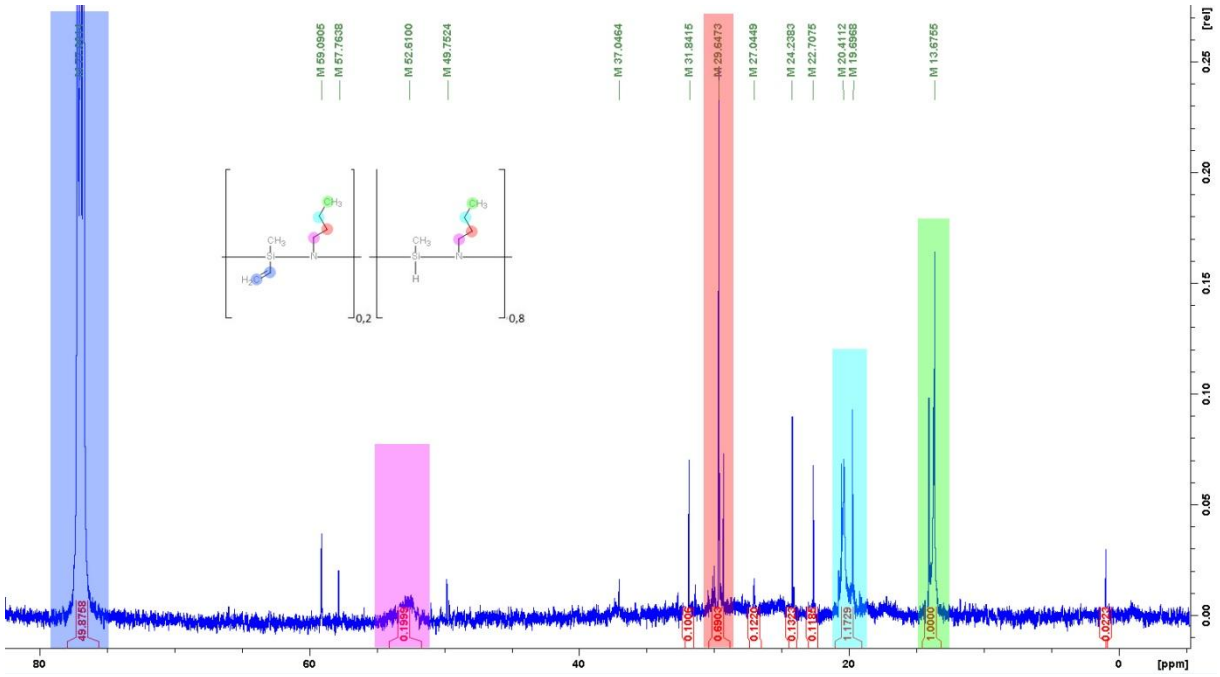

Fig. 20 ^{13}C NMR spectrum of the sample "PSZ + 1-bromobutane"; uncrosslinked sample

Compared to the ^{1}H spectrum of the unmodified polymer (see Fig. 14), the spectrum of this sample shows additional peaks between 0.7 and 3.1 ppm, which corresponds to the range expected from this sample. However, the integrals of these peaks are clearly too large in relation to the other integrals (from left to right: 2.87, th.: max 2, 14.50, th.: max 4, 8.23, th.: max 3), suggesting that high amounts of byproducts are present or that NMR is in this case not suitable for quantification.

What speaks for the existence of byproducts is that the spectra of the samples "PSZ + benzyl bromide" and "PSZ + α-bromo-p-xylene" showed also peaks in the range between 0.7 and 1.7 ppm, which could not be assigned (see Fig. 15 and Fig. 17). However, the yellow and green marked integrals in Fig. 19 are so large that more than ten times as many byproducts would be present than in the samples "PSZ + benzyl bromide" and "PSZ + α-bromo-p-xylene", if byproducts would be the sole cause for these peaks.

According to Tab. 9, the sample "PSZ + 1-bromobutane" has a higher oxygen content than these two samples and therefore probably contains more unwanted byproducts, but not to the extent that it could explain the size of the integrals in Fig. 19.

At first glance, the ^{13}C spectrum of this sample seems to have a much greater noise than the two previous ^{13}C spectra. However, this is only due to the much smaller peaks, due to which it was zoomed in (see y-axis). This may be because the sample did not dissolve sufficiently. This is also supported by the very strong solvent peak (marked in blue), in relation to the other peaks.

The assignment of the peaks of this spectrum is problematic. The peak of the carbon atom of the methyl group on the silicon should occur around 0 ppm. Although there is one peak at about 0 ppm, it is too small to be assigned to the product (integral size: 0.022). The peak is more likely to be an impurity or a byproduct.

Possibly the peak of this methyl group, which was already very broad and flat in the two previous spectra (see Fig. 16 and Fig. 18), disappears in the measurement noise.

The peaks of the butyl group occur between 13 and 52 ppm (marked in purple, red, turquoise and green). The integral sizes were calibrated after the peak at 13.6 ppm (marked in green), resulting in integral values of the other peaks from left to right: 0.20; 0.69; 1.17. The broad peak at 52 ppm (marked in violet) is therefore clearly too small in relation to the other peaks.

4.1.6.5 PSZ + 1-bromooctane

Lastly, the NMR spectra of the sample "PSZ + 1-bromooctane" will be discussed, which are shown in Fig. 21 and Fig. 22.

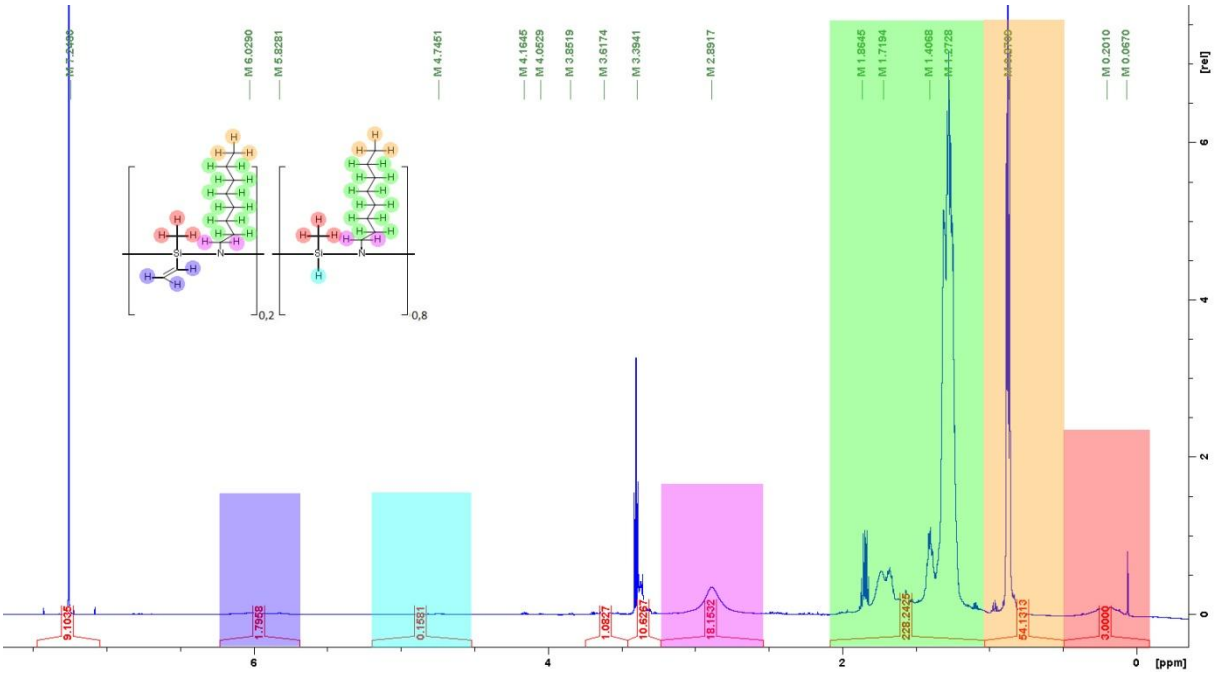

Fig. 21 ^{1}H NMR spectrum of the sample "PSZ + 1-bromooctane"; uncrosslinked sample

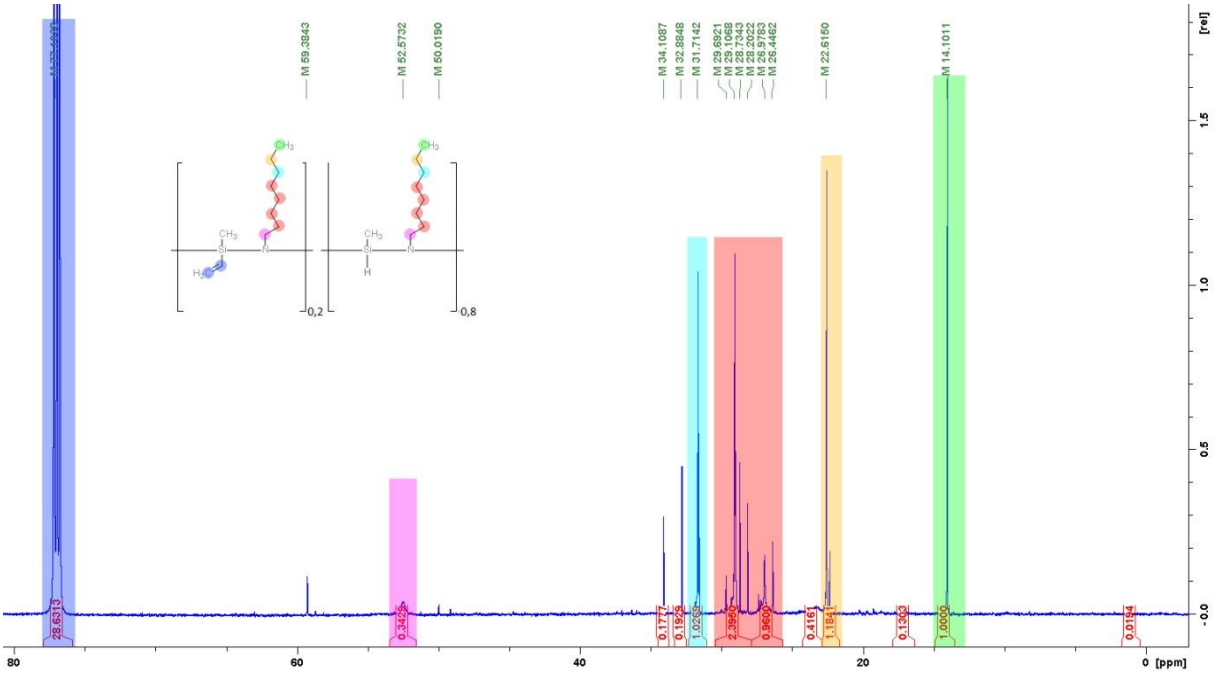

Fig. 22 ^{13}C NMR spectrum of the sample "PSZ + 1-bromooctane"; uncrosslinked sample

The ^{1}H spectrum of this sample is similar to that of the sample "PSZ + 1-bromobutane" (see Fig. 19), except that the integrals assigned to the octyl chain (marked in violet, green and yellow) are even larger in relation to the integral of the $SiCH_3$ group (marked in red).

For this sample, the same applies as for the sample "PSZ + α-bromo-p-xylene": Due to the very high boiling point of 1-bromooctane (201 ° C [25]), educt residues could be present in the product, but not such high amounts that it could explain the sizes of the integrals.

Another considerable feature of this spectrum is that the solvent peak is exceptionally big. That could be already observed with the sample "PSZ + 1-bromobutane", but occurs here even more clearly. This indicates that these two samples aren't completely soluble in $CDCl_3$. Therefore, it could be that the high integral sizes could occur due to a much higher solubility of the byproducts in comparison to the solubility of the modified polymers.

The ^{13}C spectrum of this sample is in all respects similar to that of the sample "PSZ + 1-bromobutane". The expected peak of the carbon of the methyl group on the silicon at about 0 ppm is again not visible and the solvent peak (marked in blue) is again exceptionally strong, although not quite as strong as in the sample "PSZ + 1-bromobutane" (see Fig. 20).

The peaks of the octyl group, however, could be assigned without problems. The integral size of the peak of the carbon, which is bound directly to the nitrogen, (marked in violet) is clearly too small in relation to the other integrals of the octyl group. The other integral sizes, however, at least concur approximately with each other (from left to right: 1.03, th .: 1, 3.36, th .: 4, 1.18, th .: 1).

In addition to the assigned peaks, two small peaks occur at 32.8 and 34.1 ppm, which could not be assigned to a carbon atom. These are possibly educt residues.

4.1.7 Pore analysis

The specific surface area and the pore size distribution of pyrolyzed samples were measured by nitrogen physisorption (see 3.3.4). It should be noted that the measurements of the unmodified polymer were not performed by the author of this work due to limited measurement time. However, since they were performed on the same device and using the same procedure, it should still be possible to use these measurements as reference values.

4.1.7.1 BET surface area

First, the BET surface area of the samples, summarized in Tab. 11, will be discussed.

Tab. 11 BET surface area of samples modified with different bromides and pyrolyzed at 600 °C

Sample	BET surface area, m^2/g
PSZ (unmodified)	13.1 ± 0.1
PSZ + benzyl bromide	218.6 ± 10.6
PSZ + α-bromo-p-xylene	233.2 ± 13.7
PSZ + allyl bromide	107.1 ± 3.4
PSZ + 1-bromobutane	221.7 ± 11.7
PSZ + 1-bromooctane	201.6 ± 17.9

From this table it can be seen that the modification of the polymer significantly increases the BET surface area of the resulting ceramics (by a factor of about 10-20). The BET surface areas of all samples are approximately equal (in the range 200-235 m^2 / g), except for the sample "PSZ + allyl bromide", whose BET surface area is only about half as high as of the other samples.

Compared to the results from previous investigations, it is surprising that the BET surface areas of the samples differ so little, since it would be expected that samples with a five times higher degree of substitution (see Tab. 8) would also lead to a higher BET surface area.

4.1.7.2 Pore size distribution

The pore size distributions (PSD) of the samples were calculated from the adsorption isotherms with the data reduction software SAEIUS (see 3.3.4). The isotherms used for the calculation are shown in Fig. 23.

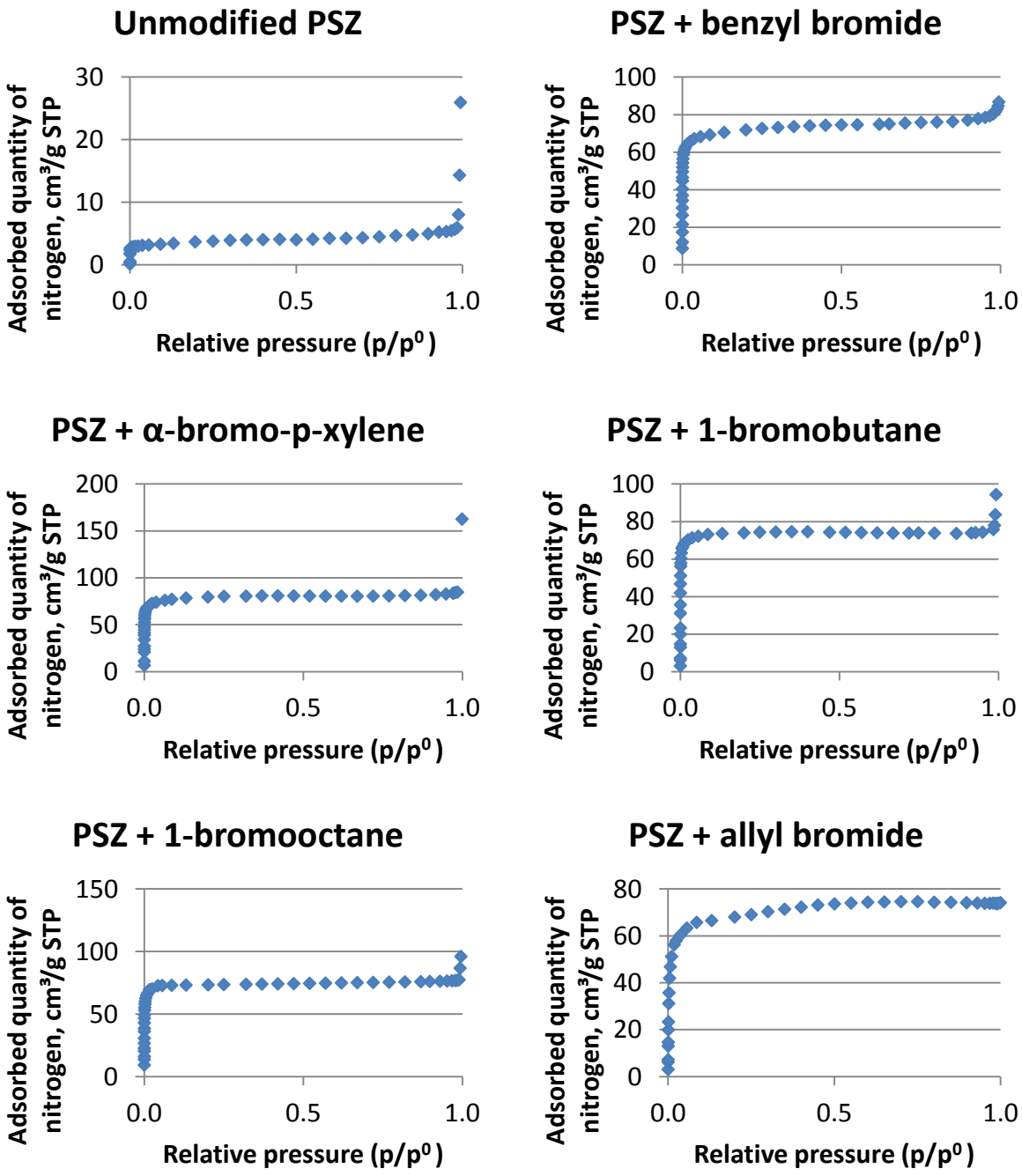

Fig. 23 Adsorption isotherms of samples modified with different bromides

As can be seen, the adsorption isotherms of all samples are similar to each other. After IUPAC classification all of these would be classified as isotherm type I [26], which indicate microporous solids with narrow micropores. Only the adsorption isotherm of the sample "PSZ + allyl bromide" (bottom right) differs slightly, indicating that mesopores are also present. The adsorbed quantity of nitrogen is similar for all samples, except for the unmodified polymer (top left), which adsorbed a much lower quantity of nitrogen.

The calculated pore size distribution (PSD) are shown in Fig. 24 and Fig. 25. In the first figure all samples are summarized, with the exception of the sample "PSZ + allyl bromide", which had pores in a different size range and is therefore shown in a separate figure.

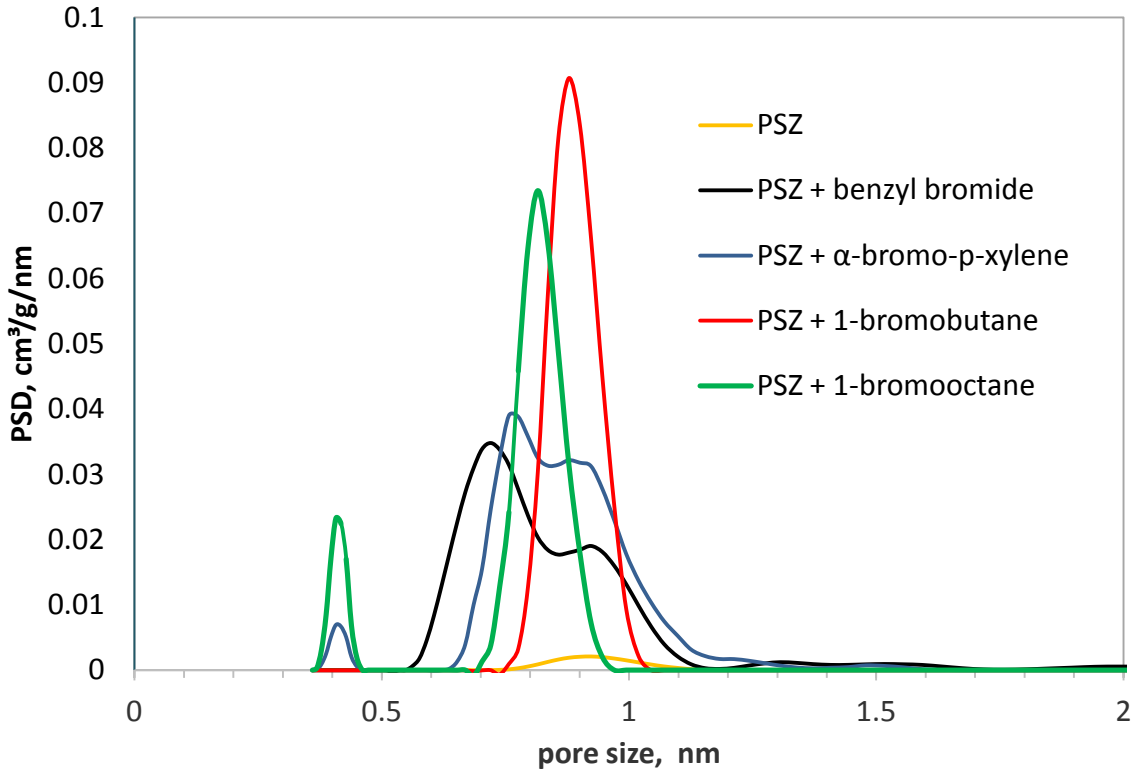

Fig. 24 Pore size distribution of samples modified with different bromides; measured by nitrogen physisorption, calculated with SAEIUS (using NLDFT models)

From this figure it can be seen that the samples all have a very similar pore size distribution, having their maxima in the range 0.7-0.9 nm. The pore size is unchanged compared to the unmodified sample ("PSZ", marked in orange), only the amount of pores is much higher.

The size of the substituent obviously has no influence on the pore size of the resulting ceramics. The sample which has been modified with the largest substituent ("PSZ + 1-bromooctane") even has a minimal lower average pore size than the sample modified with the much smaller substituent 1-bromobutane.

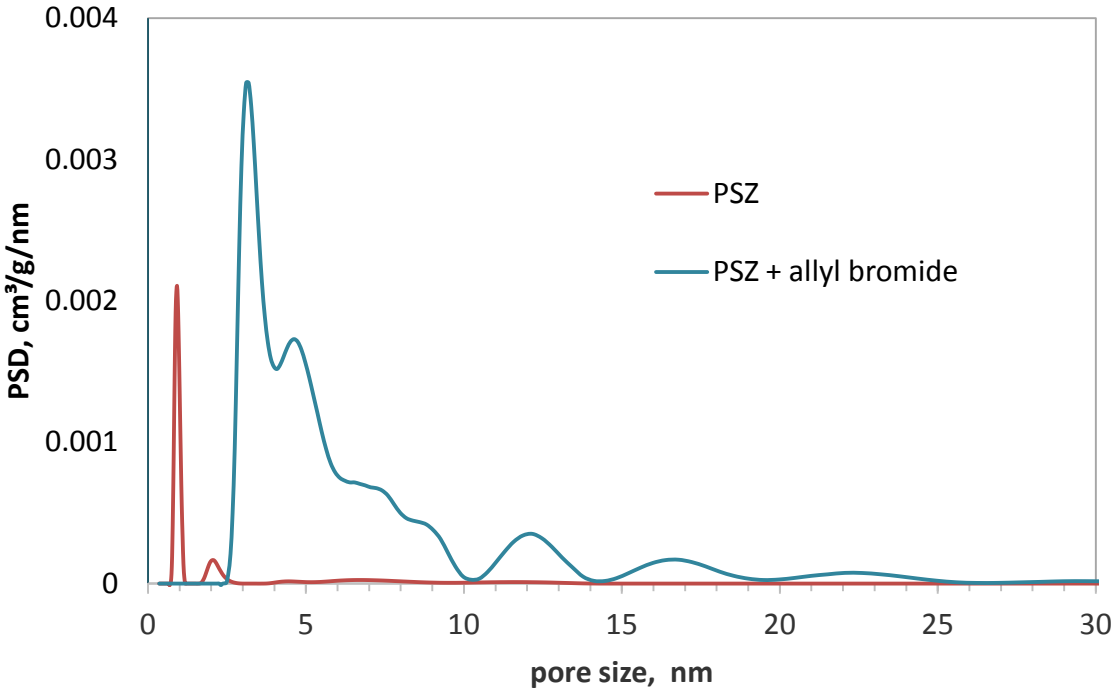

Fig. 25 Pore size distribution of the sample "PSZ + allyl bromide"; measured by nitrogen physisorption, calculated with SAEIUS (using NLDFT models)

In the case of the sample "PSZ + allyl bromide" the pores are significantly larger than in the other samples, as can be seen from

Fig. 25. No microporosity (<2 nm) was measured, the sample consists mainly of mesopores in the range 2-10 nm, even pores bigger than 10 nm are present.

The processes during pyrolysis may be different for this sample because it is more cross-linked by the introduced double bonds and because the substituents are not connected to the polymer via one bond but through two bonds, resulting in a different pore size distribution.

4.1.8 Summary

In the experiments with different bromides several observations were made, which will be summarized at this point:

First, the experiments with the aromatic bromides (benzyl bromide and α-bromo-p-xylene) seem to have worked better than the experiments with non-aromatic bromides (1-bromobutane, 1-bromooctane and allyl bromide). The following results indicate this:

- They had a higher yield after a shorter reaction time (see 4.1.2) than the samples modified with non-aromatic bromides. The benzene ring is therefore beneficial to the reaction rate of the nucleophilic substitution.
- The oxygen content of these two samples was lower than that of the other samples (see 4.1.5.2).
- The degree of substitution of the modified polymers is higher, indicated by the mass losses during pyrolysis (see 4.1.4), and the carbon content (see 4.1.5.1).

Second, modification of the polymer significantly increases the BET surface area of the resulting ceramics (see 4.1.7.1). While the number of pores is increased, the size of the pores remains almost unchanged (see 4.1.7.2), except for the sample "PSZ + allyl bromide", whose pore analysis did not reveal any micropores but only mesopores (see

Fig. 25).

Third, the nature and size of the substituent does not significantly affect the BET surface area (see Tab. 11) or the pore size distribution (see Fig. 24). Based on this finding, only two bromides were used in the further course of this work, representative of the two bromide groups: benzyl bromide for the aromatic bromides and 1-bromobutane for the non-aromatic bromides.

4.2 Effect of precursor/bromide ratio

In this section, experiments were carried out with two different bromides (benzyl bromide and 1-bromobutane). In contrast to previous experiments (see 4.1), in which the bromide was added in excess (to be exact twice the amount that would have been necessary for the complete modification of the precursor), the precursor/bromide ratio was varied in the experiments of this section.

The reaction time for the samples modified with benzyl bromide was three days, while the reaction time for those samples modified with 1-bromobutane was seven days. The reaction durations were chosen based on the results of section 4.1.2.

The motivation behind the experiments in this section was to examine how the variation of the precursor/bromide ratio affects the results of the executed analyzes.

4.2.1 Yield

The yields of the experiments in this section were again calculated as in section 4.1.2 using Eq.1. The calculated yields are summarized in Tab. 12. The sample descriptions contain the bromide used for the modification and the molar ratio of precursor to bromide.
"PSZ + benzyl bromide 1:0.25" means that the precursor was modified with 25 % of the equimolar amount of benzyl bromide respective to the monomer of the precursor.

The received mass of product was calculated with Eq.2 and the theoretical receivable mass of product was calculated with Eq.3. Both quantities are dimensionless, since they were divided by the mass of PSZ used for the respective experiment.

Tab. 12 Yields of experiments with different precursor/bromide ratios

Sample	Received mass of product, g/g PSZ	th. receivable mass of product, g/g PSZ	Yield, %
PSZ + benzyl bromide 1:0.25	0.68	1.35	50.3
PSZ + benzyl bromide 1:0.5	0.98	1.70	57.8
PSZ + benzyl bromide 1:1	1.47	2.41	61.0
PSZ + benzyl bromide 1:2	1.41	2.41	59.6
PSZ + 1-bromobutane 1:0.5	0.54	1.44	37.3
PSZ + 1-bromobutane 1:2	0.63	1.88	33.8

Larger amounts of product are obtained when more bromide is added, which was to be expected. However, the yield stays almost the same and seems to be independent of the precursor/bromide ratio. For the samples modified with benzyl bromide the yield is 50-60%, for the samples modified with 1-bromobutane the yield is between 30 and 40%.

4.2.2 IR analysis

From the modified samples, IR spectra of four samples were subsequently measured. In order to better estimate whether the intensity of the peaks caused by the substituent change, the spectra were superimposed and normalized again (as in 4.1.3) with respect to the peak of the bending vibrations of the Si-C bonds at a wavenumber of about 1250 cm^{-1} (marked in green in Fig. 26).

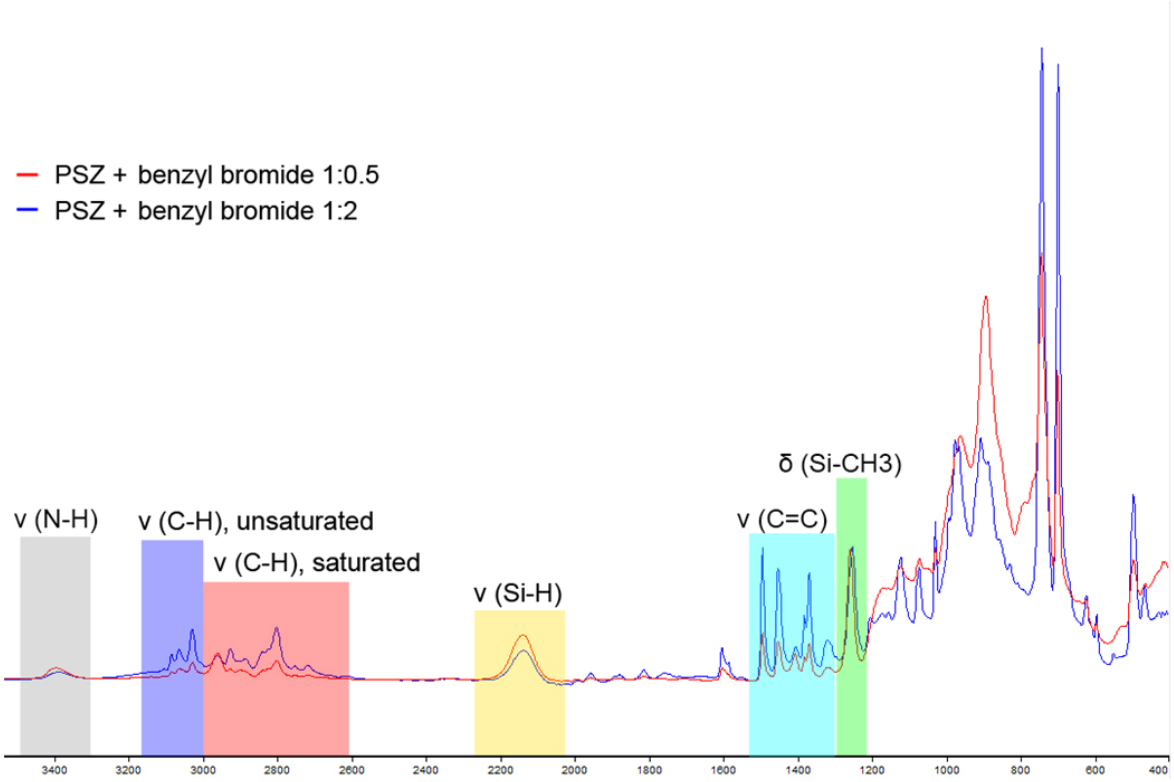

Fig. 26 IR spectra of benzyl bromide experiments with different bromide ratios

In Fig. 26, it can be clearly seen that the peaks, which are mainly caused by the benzene ring (unsaturated carbon-hydrogen bonds between 3000-3150 cm^{-1} and carbon-carbon double bonds between 1200 and 1450 cm^{-1}; marked in blue and turquoise), are significantly weaker in the sample with the lower precursor/bromide ratio (shown in red in Fig. 26) than in the sample with the higher precursor/bromide ratio (marked in blue in Fig. 26).

This clearly indicates that the sample "PSZ + benzyl bromide 1:0.5" has a lower degree of substitution than the sample "PSZ + benzyl bromide 1:2". This was expected due to the higher precursor/bromide ration of the sample "PSZ + benzyl bromide 1:2" and also coincides with the calculations of the degree of substitution of these samples in section 4.2.4.1, whose results are illustrated in Tab. 15.

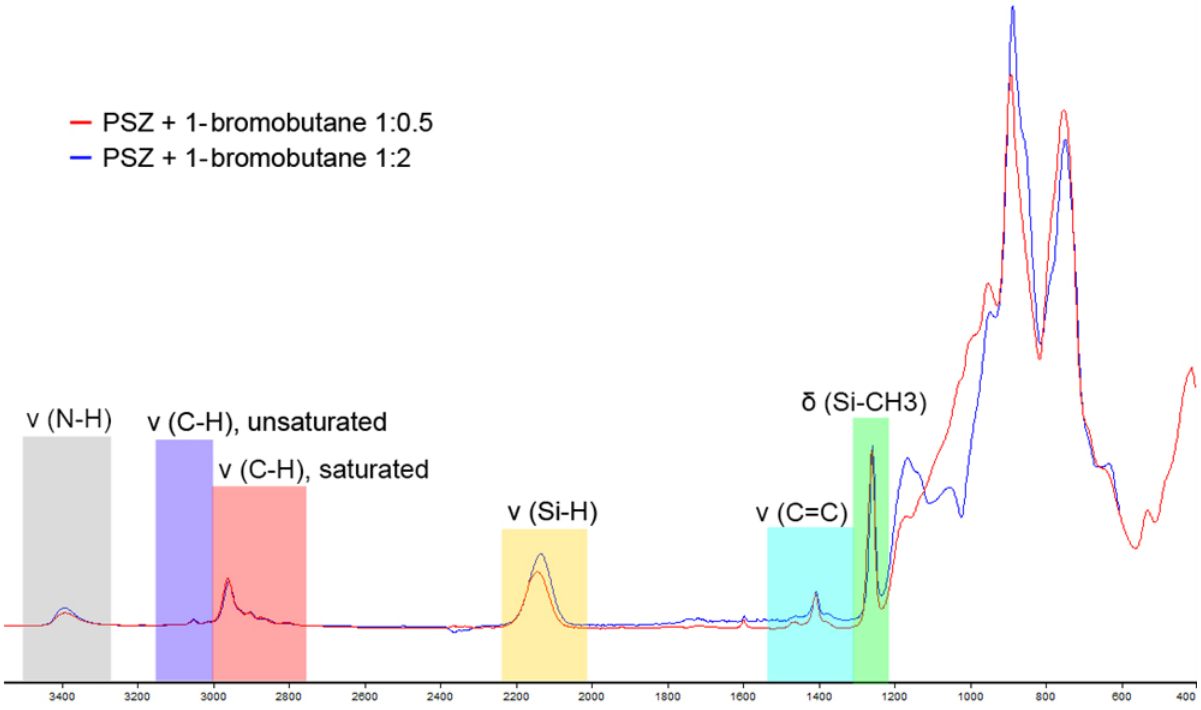

Fig. 27 IR spectra of 1-bromobutane experiments with different bromide ratios

In Fig. 27 the spectra of the samples, which were modified with 1-bromobutane, are shown. Despite the different precursor/bromide ratios, the two spectra are nearly identical, so it seems that these two samples do not differ in their degree of substitution.

However, it should be noted that differences between the sample modified with 1-bromobutane and the unmodified sample in section 4.1.3 (see Fig. 13) were only visible in the fingerprint range (<1000 cm^{-1}). It is therefore impossible to make a reliable statement regarding the degree of substitution from Fig. 27.

4.2.3 Mass change during cross-linking and pyrolysis

The samples were then cross-linked and pyrolyzed (see 3.2.2). To calculate the percent mass losses, the samples were weighed before and after each heat treatment step. The theoretical mass losses were, as in Section 4.1.4, calculated with Eq.2. The mass losses during cross-linking and pyrolysis as well as the calculated theoretical mass losses are summarized in Tab. 13.

Tab. 13 Mass change during heat treatment for experiments with different bromide ratios

Sample	Mass change during cross-linking, %	Mass change during pyrolysis, %	Theoretical mass change, %
PSZ + benzyl bromide 1:0.25	-25.2	-20.4	-26.1
PSZ + benzyl bromide 1:0.5	-25.4	-36.1	-41.3
PSZ + benzyl bromide 1:1	-19.9	-56.1	-58.5
PSZ + benzyl bromide 1:2	-17.4	-68.7	-58.5
PSZ + 1-bromobutane 1:0.5	-9.8	-11.4	-30.9
PSZ + 1-bromobutane 1:2	-12.1	-12.8	-47.2

The mass loss during pyrolysis of the samples modified with benzyl bromide increases with increasing precursor/bromide ratio, which in turn must be due to the higher degree of substitution. This confirms the assumption from 4.1.4 that the substituted groups are split off during pyrolysis. Consequently, at lower degrees of substitution, fewer substituted groups are split off, which then results in a lower relative mass loss.

For the samples modified with 1-bromobutane, on the other hand, no correlation between mass loss during pyrolysis and precursor/bromide ratio was observed, indicating that these samples have almost the same degree of substitution.

The mass losses during cross-linking could not be correlated with the degree of substitution. These probably depend mainly on the storage time of the samples (see 4.4.1).

4.2.4 Elemental analysis

4.2.4.1 Carbon content

Subsequently, the samples were subjected to elemental analysis (see 3.3.1). First, the carbon contents will be discussed, which are summarized in Tab. 14. The theoretical carbon contents were calculated as in section 4.1.5.1 with Eq.6 (see 3.4.3).

Tab. 14 Carbon contents of experiments with different bromide ratios determined by elemental analysis

Sample	C_before heat treatment, %	C_crosslinked, %	C_pyrolyzed, %	th. C-Content, %
PSZ	16.3 ± 1.7	26.5 ± 0.9	14.6 ± 1.0	26.13
PSZ + benzyl bromide 1:0.25	37.5 ± 2.1	29.3 ± 0.2	14.3 ± 1.9	43.55
PSZ + benzyl bromide 1:0.5	44.9 ± 3.3	41.5 ± 1.3	21.8 ± 0.9	53.81
PSZ + benzyl bromide 1:1	54.3 ± 4.4	54.8 ± 2.1	19.2 ± 0.6	65.33
PSZ + benzyl bromide 1:2	64.0 ± 1.2	68.5 ± 2.1	22.5 ± 1.1	65.33
PSZ + 1-bromobutane 1:0.5	30.3 ± 0.6	28.7 ± 1.9	18.7 ± 0.6	44.21
PSZ + 1-bromobutane 1:2	33.7 ± 1.4	32.9 ± 1.7	17.6 ± 1.3	53.87

The carbon content of the samples, modified with benzyl bromide, increases with increasing amount of bromide, the theoretical carbon contents being reached only when the bromide is added in excess. This corresponds to expectations, since the increase of the amount of bromide in the reaction mixture leads to a higher degree of substitution and thus to a higher carbon content.

The fact that the theoretical carbon contents were only reached in the sample "PSZ + benzyl bromide 1:2", indicates that the reaction is not complete in the case of the remaining samples. This may be because the reaction rate decreases so much in the course of the reaction that the reaction is not completed after three days or because the bromide partly undergoes side reactions (for example with the base).

In the samples modified with 1-bromobutane, the influence of the bromide ratio is much weaker. However, it must be remembered that these samples already have a significantly lower degree of substitution (see Tab. 8), which results in a smaller difference in the carbon content.

In order to better estimate the effects of the bromide ratio on the degree of substitution, the degree of substitution was again calculated with Eq.4, the results are summarized in Tab. 15. The standard deviations were calculated from the standard deviations of the elemental analysis in Tab. 14.

Tab. 15 Calculated degrees of substitution for experiments with different bromide ratios

Sample	Calculated degree of substitution_as synthesized, %	Calculated degree of substitution_crosslinked, %
PSZ + benzyl bromide 1:0.25	14.5 ± 3.4	3.5 ± 0.2
PSZ + benzyl bromide 1:0.5	27.7 ± 7.2	21.2 ± 2.4
PSZ + benzyl bromide 1:1	65.6 ± 19.7	53.1 ± 7.2
PSZ + benzyl bromide 1:2	92.2 ± 7.0	121.8 ± 17.9
PSZ + 1-bromobutane 1:0.5	8.6 ± 1.4	5.2 ± 4.1
PSZ + 1-bromobutane 1:2	16.7 ± 3.6	14.7 ± 4.3

The calculated degree of substitution increases significantly with increasing precursor/bromide ratio, even for the samples which have been modified with 1-bromobutane. However, the difference between the samples is lower than for the benzyl bromide samples.

The theoretically achievable degree of substitution is only achieved by the sample "PSZ + benzyl bromide 1:2", while the other samples possess significantly lower degrees of substitution. The samples modified with 1-bromobutane have a much lower calculated degree of substitution than the samples modified with benzyl bromide, which is in accordance with the results of section 4.1.5.1 (see Tab. 8).

For better illustration, the calculated degrees of substitution were plotted against the associated precursor/bromide ratios. The resulting graph is shown in Fig. 28. There seems to be a nearly linear interrelationship between the precursor/bromide ratio and the calculated degree of substitution. Although it must be mentioned that more data points would be required for a reliable statement.

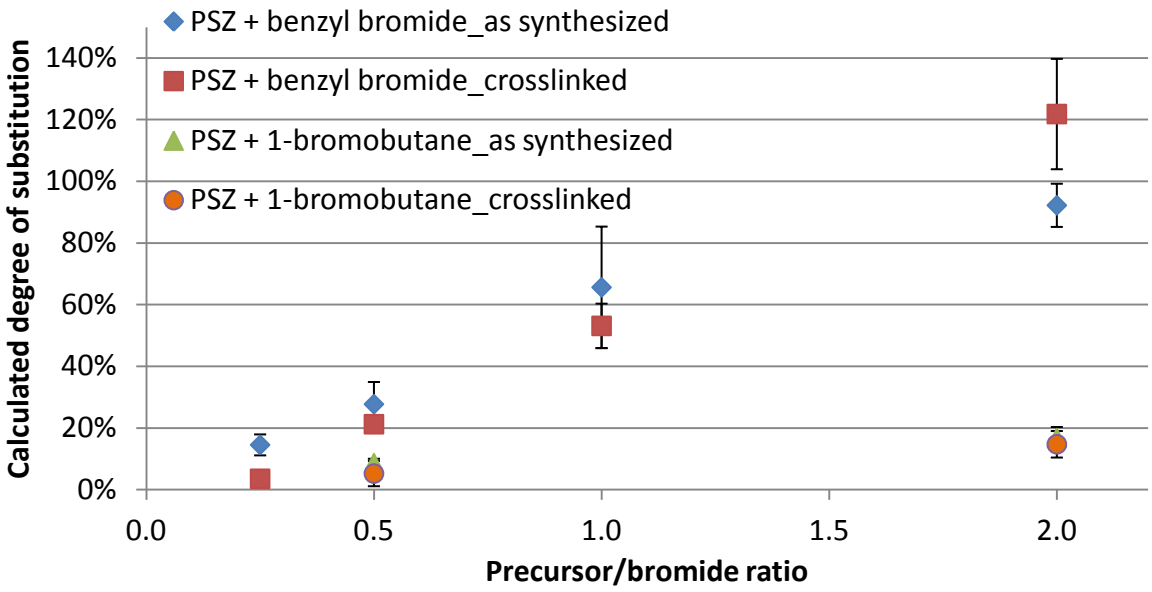

Fig. 28 Degree of substitution (calculated from carbon content) as a function of the precursor/bromide ratio for samples before (as synthesized) and after cross-linking

4.2.4.2 Oxygen content

Next, the oxygen contents of the samples will be discussed, which are summarized in Tab. 16.

Tab. 16 Oxygen contents of experiments with different precursor/bromide ratios

Sample	O_before heat treatment, %	O_crosslinked, %	O_pyrolyzed, %
PSZ	4.1 ± 0.7	4.9 ± 0.7	3.5 ± 0.8
PSZ + benzyl bromide 1:0.25	8.5 ± 0.7	8.5 ± 0.6	13.0 ± 1.2
PSZ + benzyl bromide 1:0.5	10.2 ± 0.8	9.8 ± 0.4	16.6 ± 0.8
PSZ + benzyl bromide 1:1	8.5 ± 0.2	10.3 ± 1.0	15.0 ± 0.2
PSZ + benzyl bromide 1:2	5.4 ± 0.4	5.5 ± 0.1	10.5 ± 0.5
PSZ + 1-bromobutane 1:0.5	14.9 ± 0.2	12.6 ± 0.8	15.0 ± 1.0
PSZ + 1-bromobutane 1:2	14.3 ± 0.8	11.2 ± 0.9	14.6 ± 1.1

No direct relationship between precursor/bromide ratio and oxygen content can be derived from Tab. 14. The only sample that shows a significant deviation from the other samples (with the same bromide) is the "PSZ + benzyl bromide 1:2" sample, which has a lower oxygen content than the other samples modified with benzyl bromide. At first glance, one might think this sample could be an outlier, but other samples with the same reaction conditions had similar levels of oxygen (see, for example, Tab. 9), so it is highly unlikely to be an outlier.

Since the sample "PSZ + benzyl bromide 1:2" is the only sample with approximately 100% degree of substitution (see Tab. 15), it seems likely that the lower oxygen content of this sample can be related to its high degree of substitution. The nucleophilic substitution of the polymer may prevent the attack of oxygen during processing.

However, if this would be the case, then it would be expected that the oxygen content decreases with increasing degree of substitution. From the data of Tab. 16, however, this seems not to be the case. Instead the oxygen content is approximately constant with increasing degree of substitution and decreases only at a degree of substitution of 100 %.

Apparently, the samples thus appear to have better protection against the incorporation of oxygen only with a complete or almost complete substitution.

4.2.5 NMR analysis

^{1}H NMR spectra were recorded from the uncrosslinked samples to investigate how the precursor/bromide ratio affects the size of the peaks, which are assigned to the substitution group, in relation to the other peaks. ^{13}C spectra of these samples were also taken, but these are unsuitable for such an analysis, mainly because the peak of the methyl group on the silicon is very unreliable (see 4.1.6).

The ^{1}H spectra of the samples modified with benzyl bromide are shown in Fig. 29 - Fig. 32.

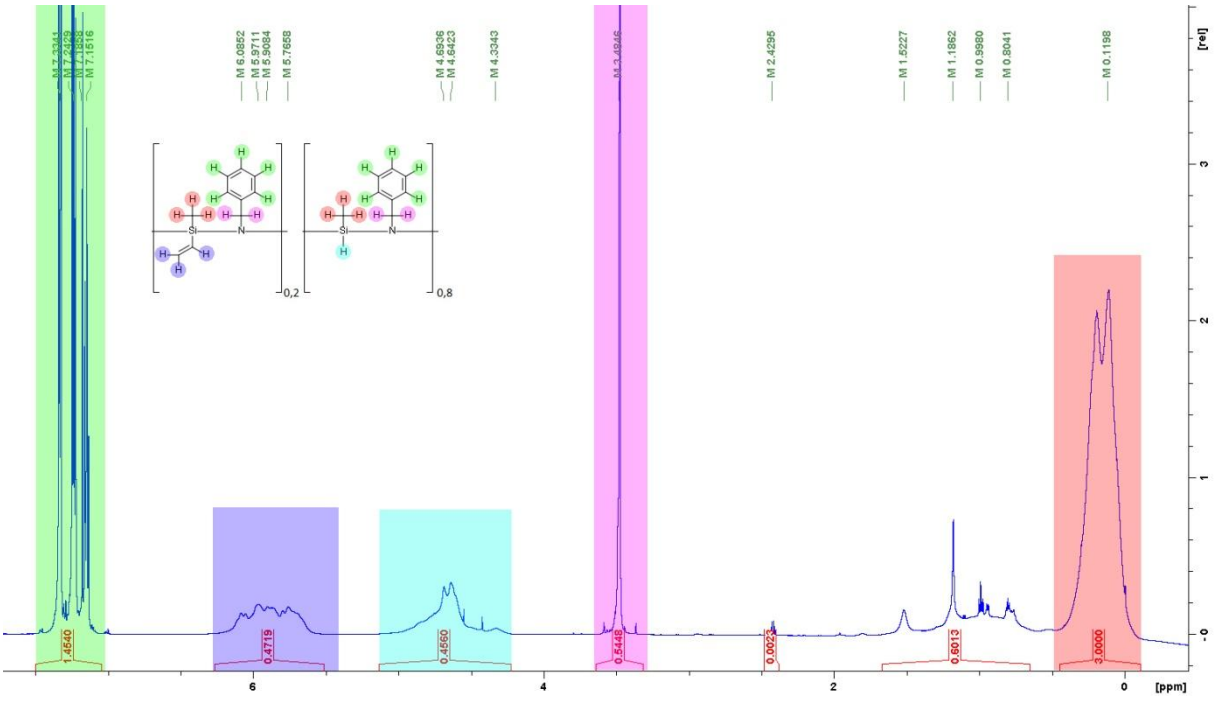

Fig. 29 ^{1}H NMR spectrum of the sample "PSZ + benzyl bromide 1:0.25"

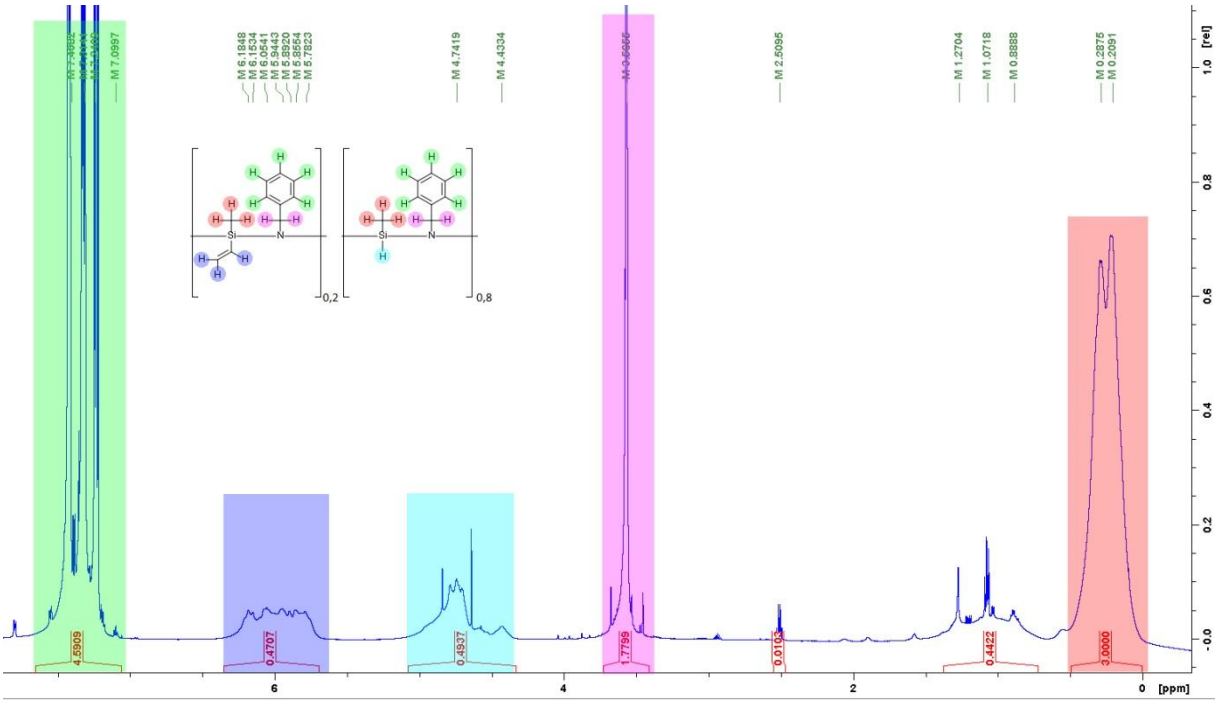

Fig. 30 ^{1}H NMR spectrum of the sample "PSZ + benzyl bromide 1:0.5"

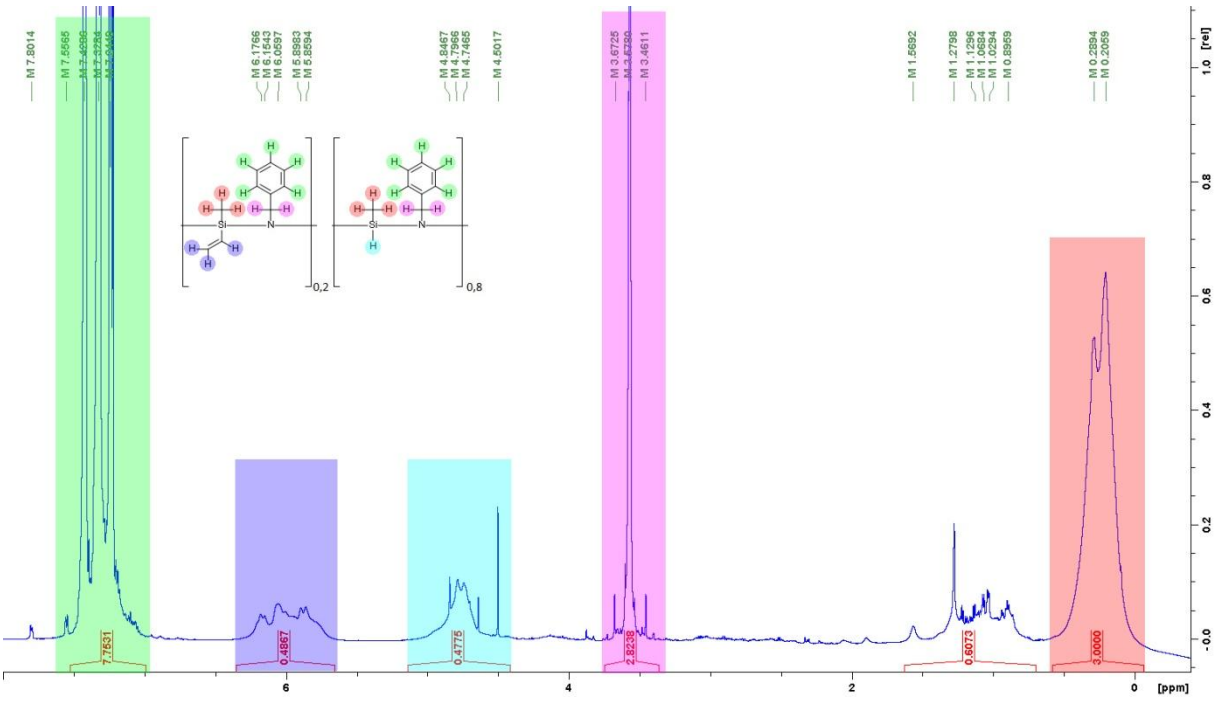

Fig. 31 ^{1}H NMR spectrum of the sample "PSZ + benzyl bromide 1:1"

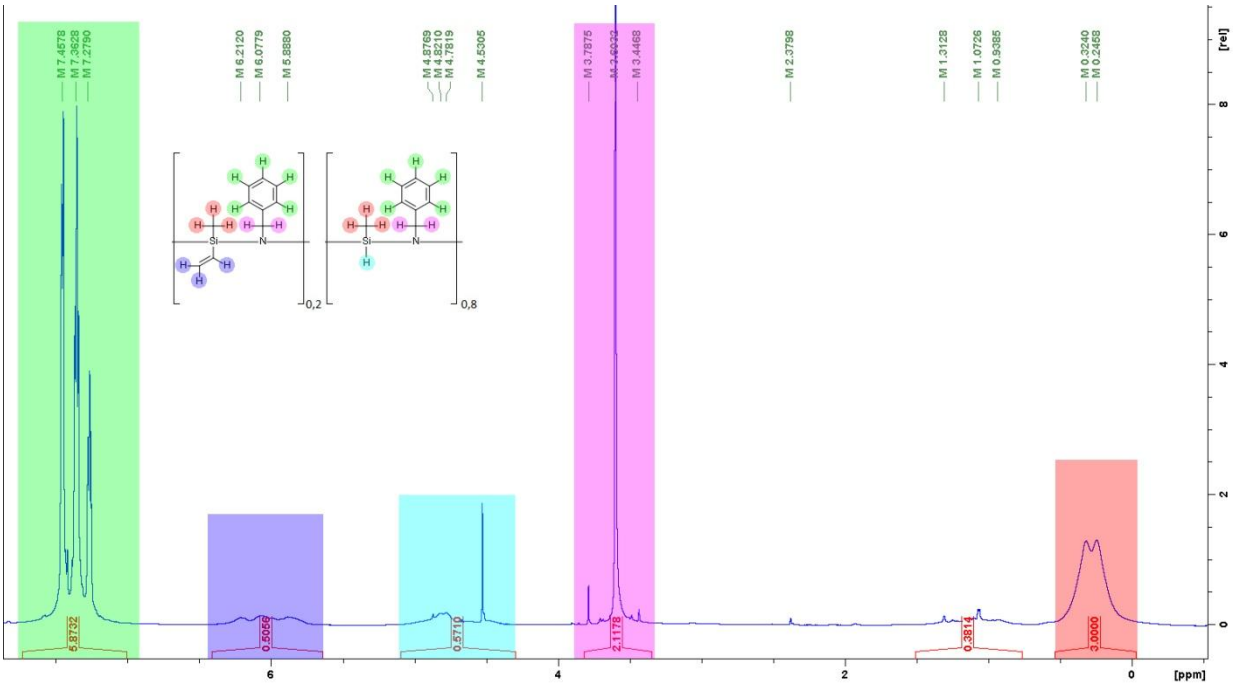

Fig. 32 ^{1}H NMR spectrum of the sample "PSZ + benzyl bromide 1:2"

All spectra were normalized with respect to the peak of the methyl group on the silicon (marked in red). The resulting integral sizes of the peaks of the methylene bridge (marked in violet) and the aromatic hydrogen atoms on the benzene ring (marked in green) are summarized in Tab. 17. For a better orientation the theoretical integral sizes (with complete conversion of the added educts and a degree of substitution of maximal 100 %) and the calculated degrees of substitution from section 4.2.4 (see Tab. 15), calculated with Eq.6 (see 3.4.4), were added.

Tab. 17 Integral sizes of ^{1}H spectra with different precursor/benzyl bromide ratios, normalized by Si-CH_3 peak at 0.5 ppm

Sample	Calculated degree of substitution (based on carbon content), %	methylene bridge (3.5 ppm)	th.	benzene ring (7 ppm)	th.
PSZ + benzyl bromide 1:0.25	14.5 ± 3.4	0.54	0.50	1.45	1.25
PSZ + benzyl bromide 1:0.5	27.7 ± 7.2	1.78	1.00	4.59	2.50
PSZ + benzyl bromide 1:1	65.6 ± 19.7	2.82	2.00	7.75	5.00
PSZ + benzyl bromide 1:2	92.2 ± 7.0	2.12	2.00	5.87	5.00

From this table it can be seen that the integral sizes of the ^{1}H spectra are basically correlated with the bromide ratio, but not to the extent that would be expected. With increasing bromide ratio the integral sizes increase (exception: "PSZ + benzyl bromide 1:2"), but all integral sizes are higher than expected.

Only the integral values of the sample "PSZ + benzyl bromide 1:0.25" show approximately the theoretically calculated values, but these refer to the maximum possible degree of substitution of 25% and not to the value calculated in section 4.2.4 of 14.5 ± 3.4 %, which is why even these integral sizes are higher than they should be.

The values of the samples "PSZ + benzyl bromide 1:0.5" and "PSZ + benzyl bromide 1:1" are significantly higher than expected, while the integral values of the sample "PSZ + benzyl bromide 1:2" are significantly closer to the theoretically calculated values. On the other hand, it is surprising that this sample has lower integral sizes than the sample "PSZ + benzyl bromide 1:1", which appears to have a much lower degree of substitution. This indicates that the integral sizes of the ^{1}H spectra have a very large deviation. This is supported by the fact that the sample "PSZ + benzyl bromide", which was analyzed in section 4.1.6, shows integral values of 2.39 and 6.49 (see Fig. 15), which are more than 10 % higher than the integral values of the sample "PSZ + benzyl bromide 1:2", although these two samples were synthesized using the same precursor/bromide ratio.

Similarly, the same analysis was performed on the 1-bromobutane samples. In Fig. 33 and Fig. 34 the ^{1}H spectra of the two samples modified with 1-bromobutane are shown.

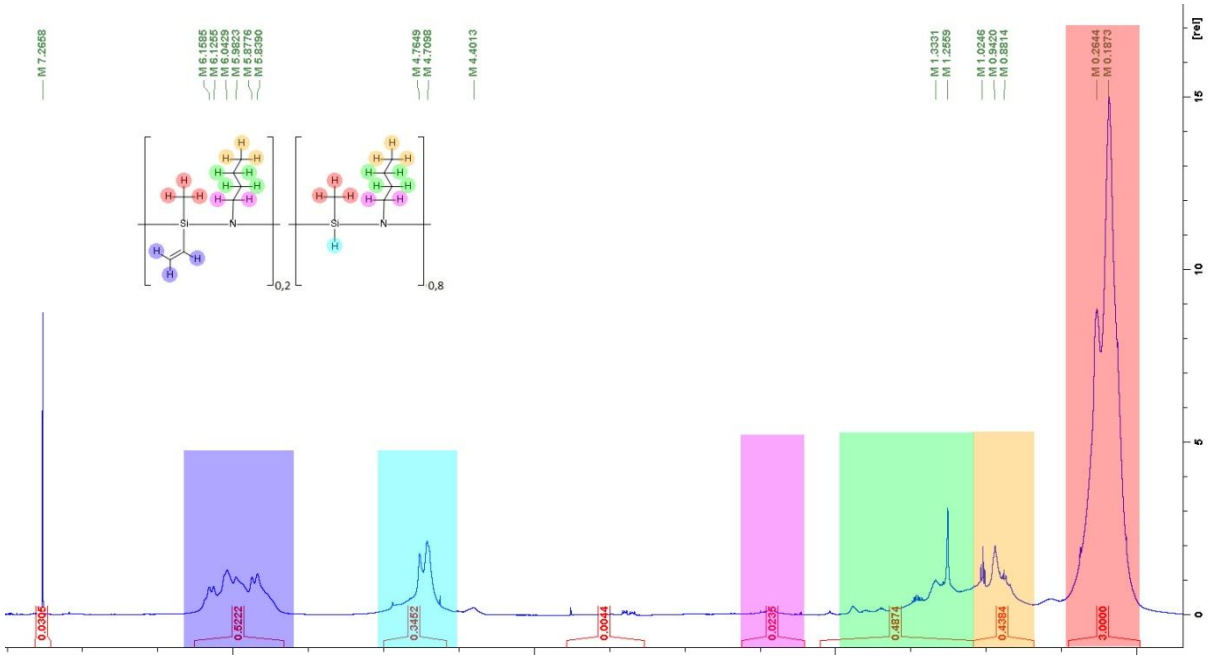

Fig. 33 ^{1}H NMR spectrum of the sample "PSZ + 1-Bromobutane 1:0.5"

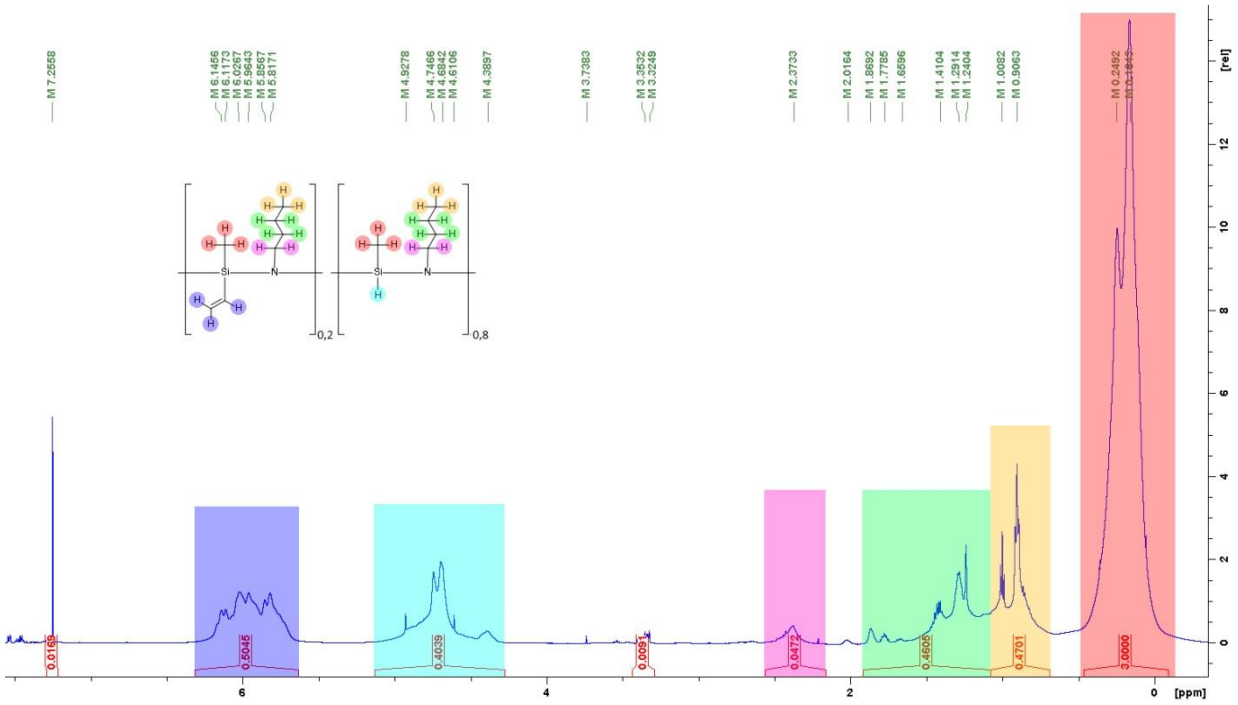

Fig. 34 ^{1}H NMR spectrum of the sample "PSZ + 1-Bromobutane 1:2"

The integral values of these spectra were normalized with respect to the peak of the methyl group on the silicon (marked in red). Since they are not clearly separable, the integral values of all the peaks that could be assigned to the butyl group (marked in violet, green and yellow) were added up and the combined integral sizes were analyzed. The data are listed in Tab. 18 next to the calculated degree of substitution. The theoretically calculated values here refer to the calculated degree of substitution and not to the maximum possible degree of substitution as in Tab. 17. This is due to the apparently very low degree of substitution of these samples, which don't come anywhere close to the theoretical achievable values.

Tab. 18 Integral sizes of ^{1}H spectra with different precursor/1-bromobutane ratios

Sample	Calculated degree of substitution (based on carbon content), %	integral size butyl group	th.
PSZ + 1-bromobutane 1:0.5	8.6 ± 1.4	0.95	0.77 ± 0.13
PSZ + 1-bromobutane 1:2	16.7 ± 3.6	0.98	1.50 ± 0.32

From this table it can be seen that the integral sizes from the peaks caused by the butyl group do not appear to change with the bromide ratio. However, it should be noted that spectra without a substituted butyl group (e.g. Fig. 32) showed also peaks in the range between 0.7 and 1.7 ppm, which could not be assigned. They are possibly caused by byproducts, which could distort the integral sizes in this range. In addition, two samples are too few to draw conclusions about a correlation.

It is also noticeable that the combined integral size of the sample "PSZ + 1-bromobutane 1:2" is smaller than expected, whereas in the benzyl bromide samples all integrals assigned to the substitution group were larger than theoretically calculated. Considering that the examined peaks may include peaks of byproducts and would be even smaller without them, this is very surprising.

The comparison with the spectrum of the sample "PSZ + 1-bromobutane" (Fig. 19), which was analyzed in section 4.1.6.4, is also remarkable. Although these samples were prepared nearly identically, the integral size of the peaks assigned to the butyl group is here more than one magnitude larger (25.59). The cause of this extreme difference in the size of the peaks can only be guessed. The storage time may play a role here (see also section 4.4), as a result of which the samples become partly insoluble, which distorts the integral sizes.

4.2.6 Pore analysis

The pyrolyzed samples were measured by physisorption (see 3.3.4). Due to limited measurement time the samples "PSZ + benzyl bromide 1:2" and "PSZ + 1-bromobutane 1:2" were not analyzed with pyhsisorption, instead the measurements from the experiments of 4.1.7 were used for comparison with the other samples. This should be unproblematic, because these samples were also prepared with a bromide ratio of 1:2. From the other samples (except "PSZ + benzyl bromide 1:0.25") only the BET surface area was measured, but not the pore size distribution.

4.2.6.1 BET surface area

First, the BET surface area of the samples, summarized in Tab. 19, will be discussed.

Tab. 19 BET surface area of pyrolyzed samples (pyrolyzed at 600 °C) modified with different precursor/bromide ratios

Sample	BET surface area, m^2/g
PSZ	13.1 ± 0.1
PSZ + benzyl bromide 1:0.25	80.7 ± 4.0
PSZ + benzyl bromide 1:0.5	120.8 ± 7.7
PSZ + benzyl bromide 1:1	187.4 ± 5.8
PSZ + benzyl bromide 1:2	218.6 ± 10.6
PSZ + 1-bromobutane 1:0.5	136.6 ± 6.6
PSZ + 1-bromobutane 1:2	221.7 ± 11.7

It can be seen that the BET surface area increases with increasing precursor/bromide ratio, whereas it appears to be almost independent of the type of bromide. To illustrate the relationship, the BET surface area was plotted against the bromide ratio in Fig. 35.

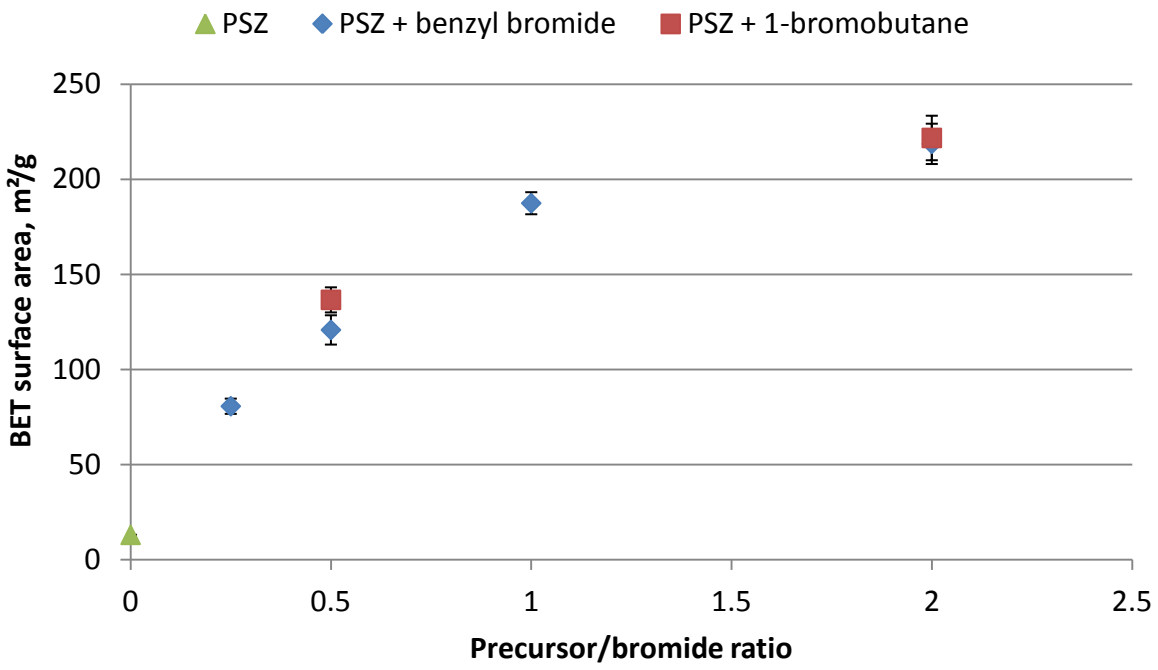

Fig. 35 BET surface area of samples plotted against precursor/bromide ratio

This figure illustrates the conclusions drawn from Tab. 19: The BET surface area seems to be directly related to the precursor/bromide ratio, but is almost independent of the bromide used for the modification. Up to a precursor/bromide ratio of 1:1, even an approximately linear relationship seems to exist. The fact that the BET surface area does not increase that much from here on is probably due to the fact that the degree of substitution does not increase that much anymore. To test this consideration, the BET surface area was plotted in Fig. 36 against the calculated degree of substitution (see Tab. 15) of the samples before heat treatment.

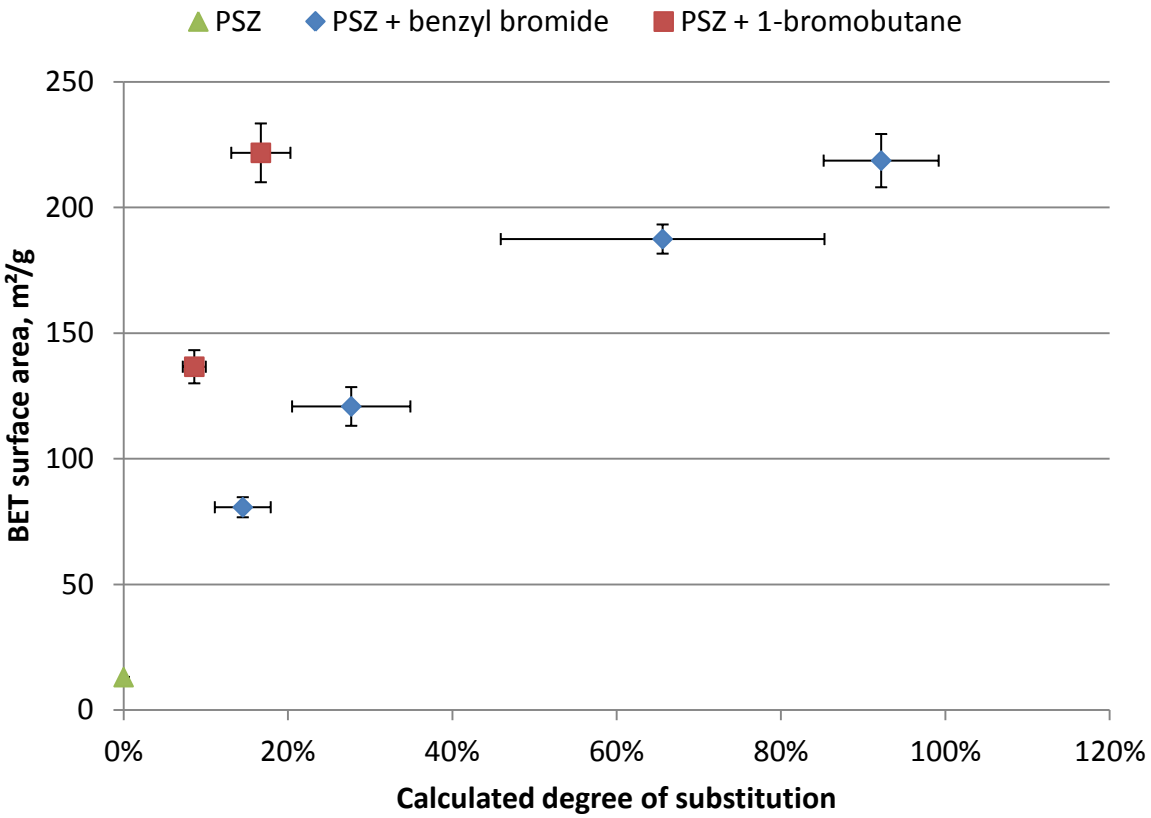

Fig. 36 BET surface area of samples modified with different precursor/bromide ratio plotted against calculated degree of substitution (based on carbon content)

Fig. 36 confirms that there is a direct correlation between the BET surface area and the degree of substitution. The higher the degree of substitution, the higher the BET surface area. This is consistent with the theory that the separation of the substituted groups during pyrolysis leads to the formation of pores and thus to an increase in the BET surface area. The higher the degree of substitution, the more groups are split off during pyrolysis and thus more pores are formed, which results in a higher BET surface area

On the other hand, it can also be seen in Fig. 36 that in the case of the "PSZ + 1-bromobutane" samples, the BET surface area is significantly higher for the same calculated degree of substitution. The reason for this is not clear, but the size of the substituents and thus the size of the resulting pores should not play a role here, as the pore size analysis has shown that the pore sizes are for all samples in the same size range (see 4.1.7.2 and 4.2.6.2).

4.2.6.2 Pore size analysis

As already indicated in 4.2.6, the pore size distribution was measured only for 3 samples: the two samples with a bromide ratio of 1:2 and the sample "PSZ + benzyl bromide 1:0.25". The adsorption isotherms of these three samples are shown in Fig. 37, the calculated pore size distribution (PSD) can be seen in Fig. 38.

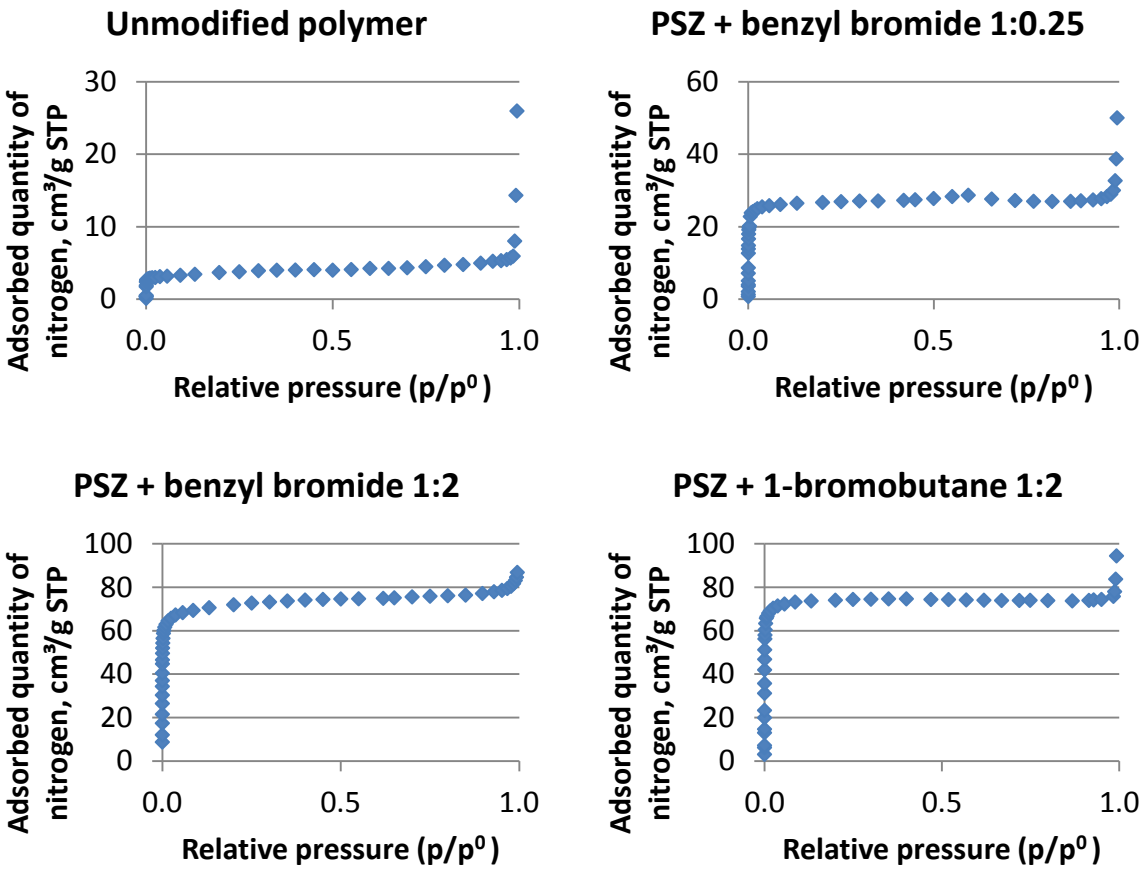

Fig. 37 Adsorption isotherms of samples modified with different precursor/bromide ratio

The shape of these adsorption isotherms are again (as in 4.1.7) very similar to each other and all of them can be classified after IUPAC classification as isotherms of type I [26], indicating microporous solids with narrow micropores. The only significant difference between these adsorption isotherms is the adsorbed quantity of nitrogen.

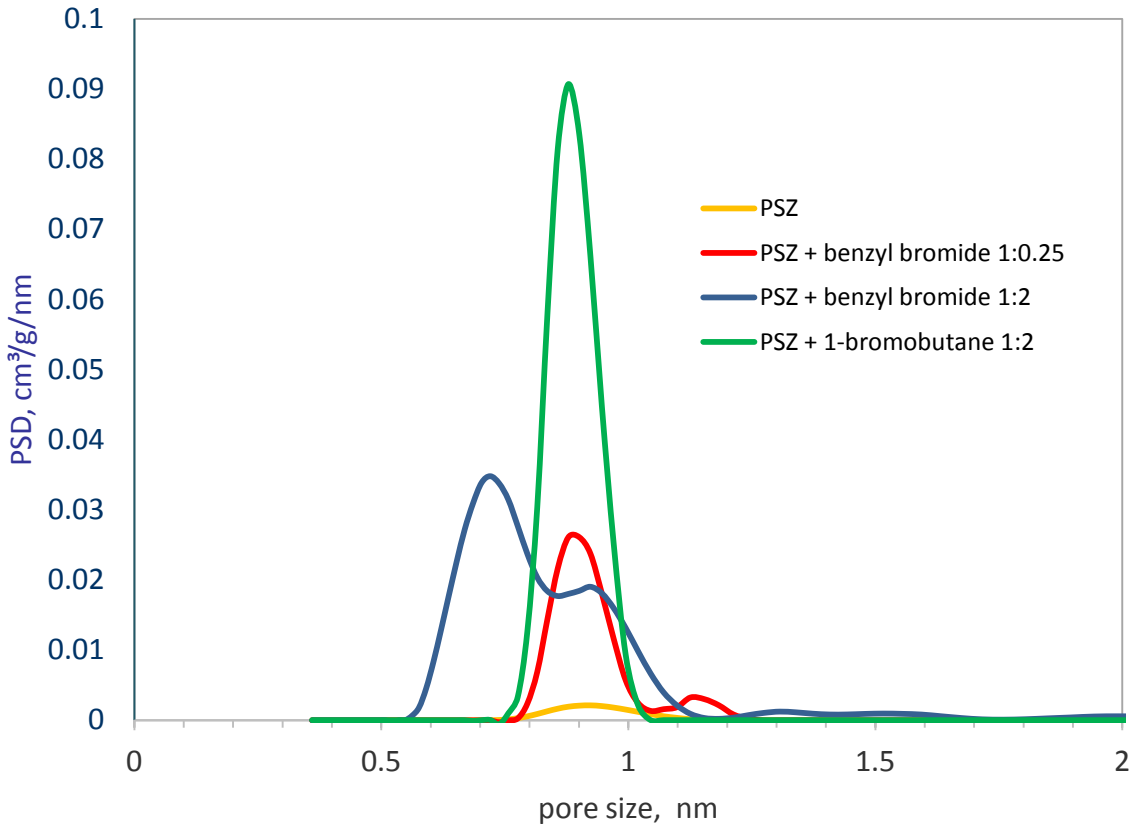

Fig. 38 Pore size distribution of experiments with different precursor/bromide ratio

The conclusion that can be drawn from Fig. 38 is that the precursor/bromide ratio does not appear to affect the pore size distribution. It only changes the number of pores (and therefore the pore volume and the BET surface area), but not the pore size. Nothing else was to be expected since the modification had no influence on the pore size either (see also 4.1.7.2).

4.2.7 Summary

At this point, the results of this section will be summarized.

The goals of the experiments carried out in this section were to determine how the precursor/bromide ratio in the reaction mixture affects the degree of substitution and how it affects BET surface area and pore size distribution.

At least for the PSZ + benzyl bromide samples it can be clearly stated, after evaluation of the results, that the degree of substitution correlates with the bromide ratio. If the bromide ratio increases, then the degree of substitution increases too. The following results indicate this:

- In the IR spectra (see 4.2.2) and the NMR spectra (see 4.2.5) of the uncrosslinked samples, the size of the peaks assigned to the benzyl group increases relative to the other peaks, if the bromide ratio is increased.
- The carbon content increases with increasing precursor/bromide ratio (see 4.2.4.1). Since the substituted polymer has a higher carbon content than the unsubstituted polymer, this suggests a correlation between bromide ratio and degree of substitution.
- Those samples with a higher bromide ratio show a higher mass loss during pyrolysis (see 4.2.3), which in turn indicates a higher degree of substitution since it can be assumed that the substitution groups are split off during pyrolysis.

For the samples which were made with 1-bromobutane, the picture was not so clear. Although there was evidence indicating a correlation between bromide ratio and degree of substitution, the differences between the samples were not as clear as in the samples made with benzyl bromide. This is presumably due to the lower degrees of substitution of the PSZ + 1-bromobutane samples (see Tab. 15), whereby the differences are naturally lower.

An influence of the precursor/bromide ratio and thus the degree of substitution on the BET surface area could be shown for all samples (see 4.2.6.1). This is significant because it helps to understand how the porosity can be controlled. The higher the degree of substitution, the more groups are split off during pyrolysis and the more pores are formed. In contrast, an influence of the degree of substitution on the pore size could not be determined (see 4.2.6.2).

Another observation made in this section was that for samples with nearly complete substitution, the oxygen content is lower than for samples with incomplete substitution (see 4.2.4.2). This insight can help to find out how such large amounts of oxygen enter the system unintentionally.

4.3 Effect of processing methods

In addition to the processing with n-hexane described in 3.2.1, another method of processing with dichloromethane was also investigated. Therefore the solid residue after the removal of the solvent (acetonitrile) was dissolved in dichloromethane instead of n-hexane. Since the quaternary ammonium salt partially dissolves in dichloromethane, it had to be removed by liquid-liquid extraction with water. Subsequently, the organic phase was dried with $MgSO_4$, which was separated by centrifugation and the dichloromethane was distilled off.

The two processing methods had in some aspects very similar results, which will not be mentioned. Instead, only the resulting differences will be discussed.

Objective of this section was to investigate how the processing method influences the results and if this processing method leads to better or worse results than the processing method used in 4.1 and 4.2.

4.3.1. Oxygen content

The oxygen contents of the samples were measured by elemental analysis (see 3.3) and are shown in Tab. 20.

Tab. 20 Oxygen content of uncrosslinked samples prepared with different processing methods

Sample	Oxygen content before heat treatment, %
PSZ	4.1 ± 0.7
PSZ + benzyl bromide dichlormethane	10.3 ± 0.9
PSZ + benzyl bromide hexane	7.1 ± 0.5
PSZ + 1-bromobutane dichlormethane	16.9 ± 1.2
PSZ + 1-bromobutane hexane	14.8 ± 0.2

It can be clearly seen that the oxygen content of the samples processed with dichloromethane is higher than those processed with n-hexane. This is probably due to the liquid-liquid extraction with water, which introduces additional oxygen into the system. Furthermore, the liquid-liquid extraction wasn't performed under nitrogen atmosphere, which could also be a reason for the higher increase in oxygen.

It is interesting to observe that the processing method strongly influences the oxygen content of the samples. Perhaps the oxygen content can be lowered even further by another processing method.

4.3.2. NMR analysis

In addition, the two ^{1}H spectra of the two samples prepared with 1-bromobutane, which are shown in Fig. 39 and Fig. 40, will be discussed.

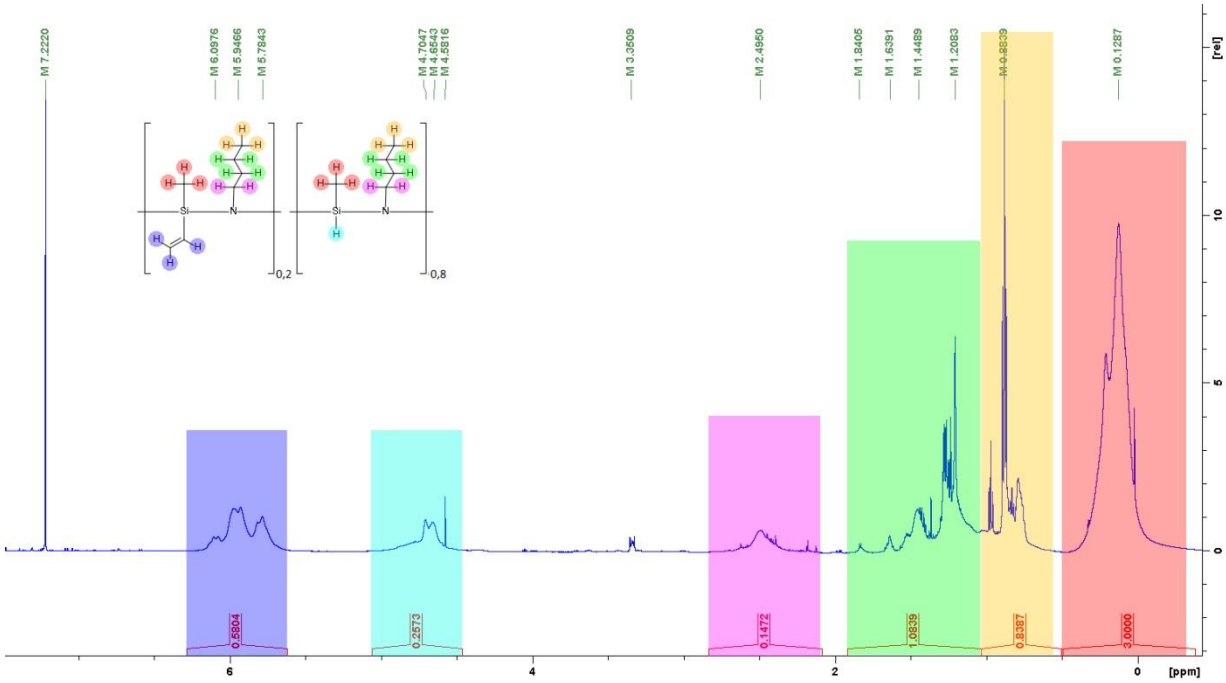

Fig. 39 ^{1}H NMR spectrum of the sample "PSZ + 1-bromobutane hexane"

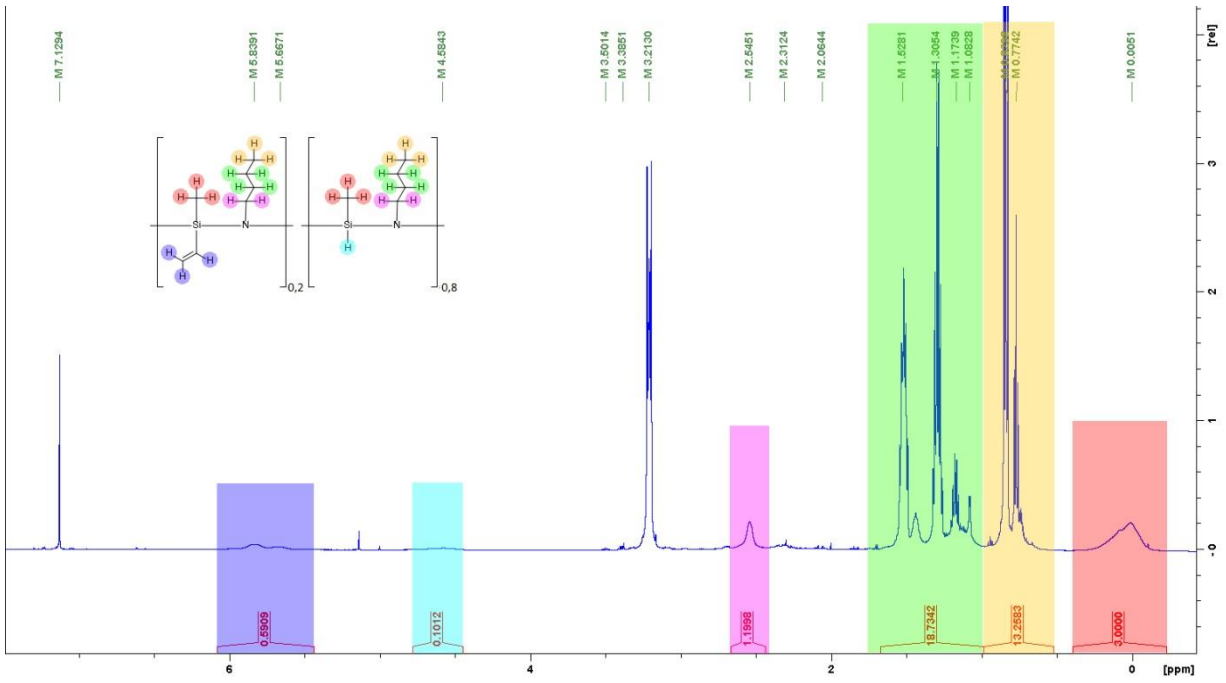

Fig. 40 ^{1}H NMR spectrum of the sample "PSZ + 1-bromobutane dichlormethane"

The peaks in the range between 0.7 and 1.7 ppm (marked in green and yellow) are significantly higher for the sample processed with dichlormethane. This could indicate a greater number of byproducts or a lower solubility of the second sample. An influence of the storage time can be excluded here, since both samples were produced and measured simultaneously.

It is also noticeable that the sample, which was processed with dichloromethane, had a strong peak at 3.2 ppm, which could not be assigned. This peak is also visible in the sample processed with n-hexane, but is very weak here.

4.3.3. Summary

In summary, the alternative processing method with dichloromethane does not appear to be very promising, because the oxygen levels were higher and the NMR spectra indicated that the samples were of poorer quality than the samples processed with n-hexane. This processing method was therefore rejected and was not applied in the further course of this work.

However, an interesting observation has emerged from the experiments in this section: the type of processing seems to have a significant influence on the oxygen content of the samples. This knowledge may be helpful to reduce the oxygen content of the samples.

4.4 Effect of storage time

For storage, the samples were transferred into screwable glass vials. These were flushed with nitrogen and stored at + 4 °C in a refrigerator. In general the processing and analysis of the samples was executed as soon as possible to minimize time dependent effects. However, to estimate these effects, some samples were processed and analyzed after longer storage times (> 100 days).

4.4.1 Mass change during cross-linking and pyrolysis

To examine the influence of the storage time on the mass loss during cross-linking, the mass change was plotted against the storage time (= number of days between the end of nucleophilic substitution and beginning of cross-linking), see Fig. 41.

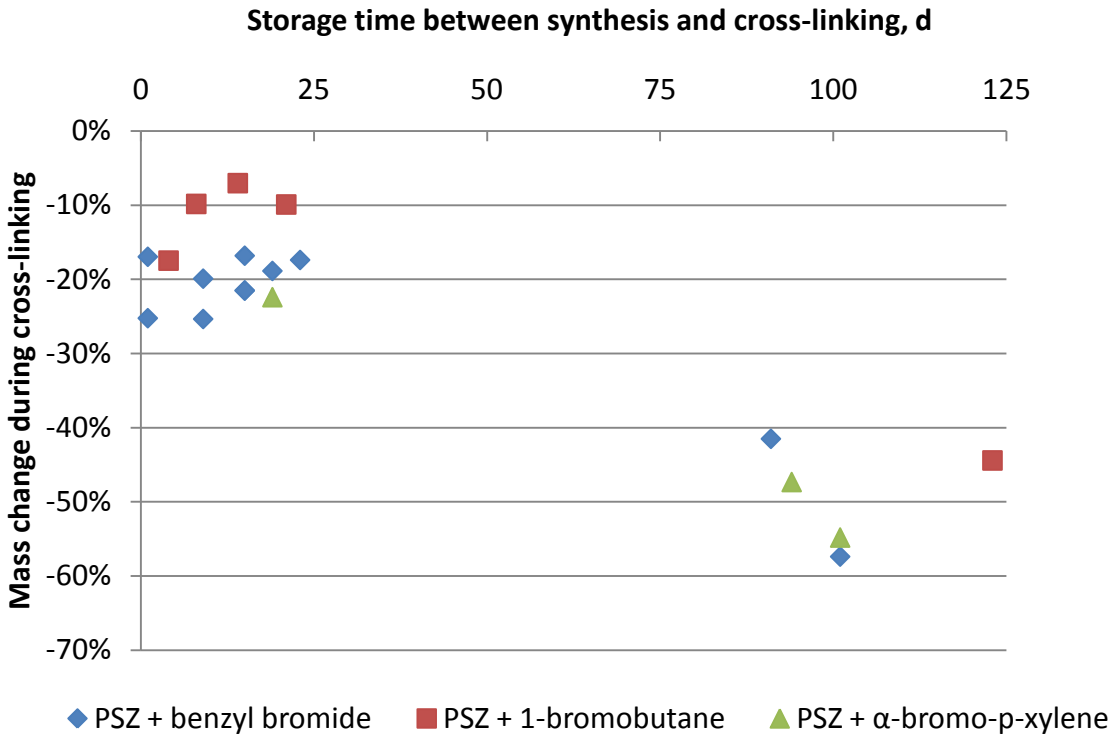

Fig. 41 Mass change during cross-linking as a function of storage time between synthesis and cross-linking

Several conclusions can be drawn from this figure: While the mass loss at low storage times (<25 days) is relatively constant or even slightly decreasing, it increases considerable at high storage durations. Furthermore, the chemically similar samples (PSZ+ benzyl bromide and PSZ + α-bromo-p-xylene) show a very similar behavior, while PSZ + 1-bromobutane - samples show in general a lower mass change.

Fig. 41, therefore, indicates that the modified polymers undergo chemical reactions during storage, resulting in a higher amount of volatile components after long duration of storage. These volatile components volatilize during heating, leading to a higher mass loss during cross-linking.

The same plot was applied for the pyrolysis-experiments, which is shown in Fig. 42.

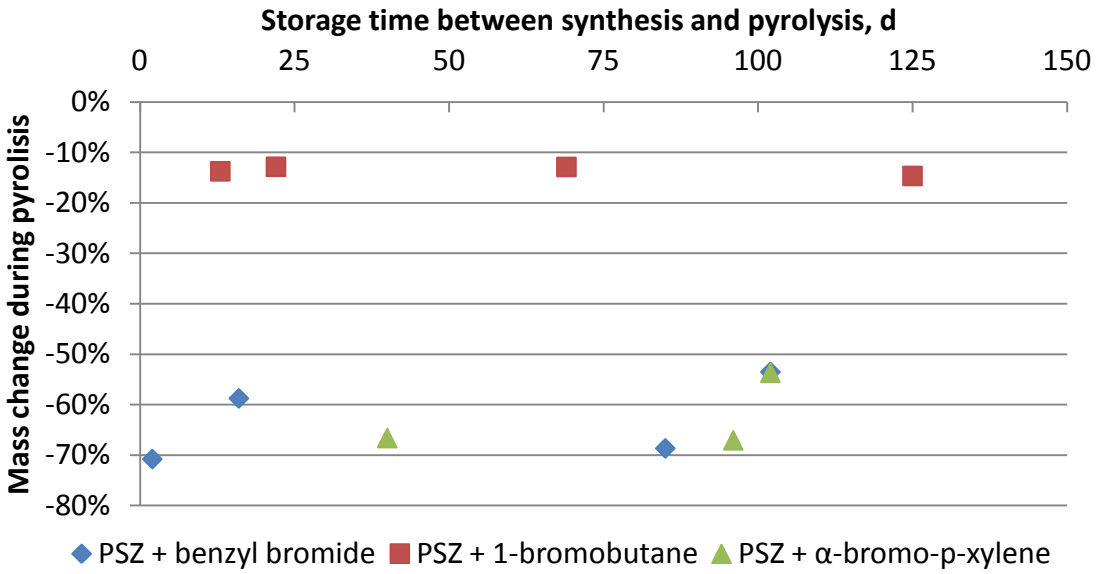

Fig. 42 Mass change during pyrolysis as a function of storage time between synthesis and pyrolysis

From this figure the conclusion can be drawn that mass loss during pyrolysis depends only on the substituted species (see also 4.1.4), but is independent from the duration of storage. However, it must be considered that the storage time in Fig. 42 relates to the time between the nucleophilic substitution and the pyrolysis, not taking into account that the volatile components were already separated during cross-linking.

To check if the volatile components also form during storage of the cross-linked samples, the mass loss during pyrolysis was additionally plotted against the storage time of the cross-linked samples (= days between cross-linking and pyrolysis), which is shown in Fig. 43.

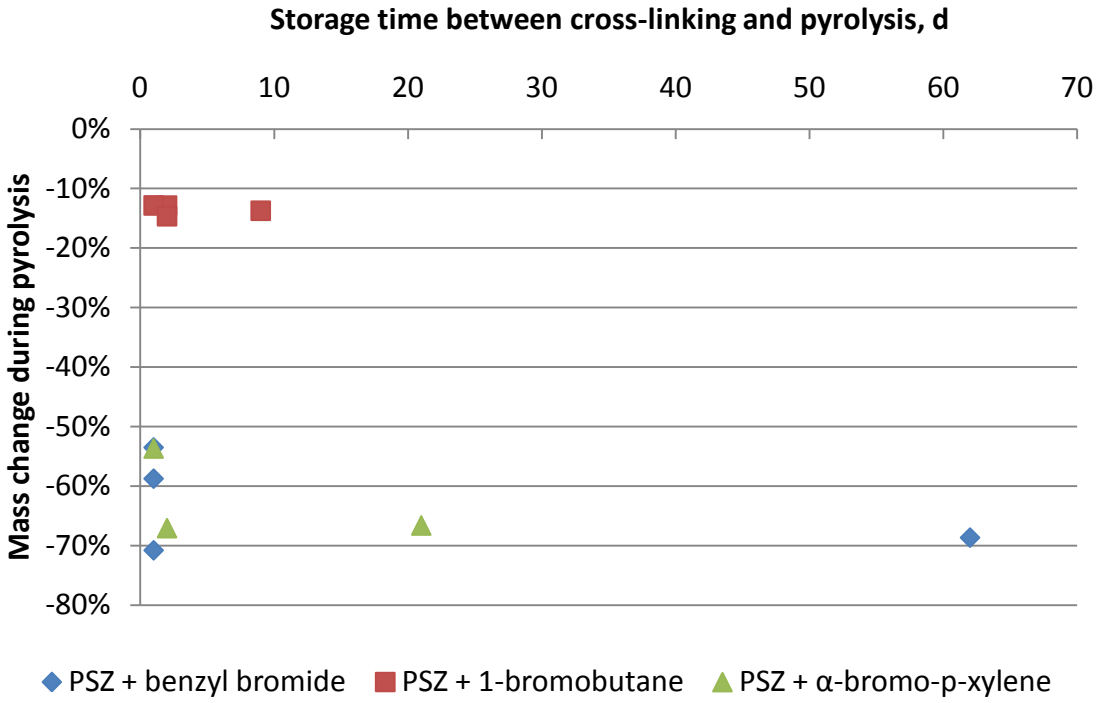

Fig. 43 Mass change during pyrolysis as a funtion of storage time between cross-linking and pyrolysis

Again, no influence of the storage time on mass loss during pyrolysis could be observed. The decomposition, which seems to occur during storage of the modified (and uncrosslinked) samples, doesn't seem to occur with the cross-linked samples.

4.4.2 Oxygen content

Given that the unmodified polymer is sensitive towards hydrolysis, it is likely to suppose that the increasing mass loss during cross-linking results from the hydrolysis sensitivity of the modified polymers. Although the modified samples were stored under nitrogen atmosphere, the possibility of air (including air moisture) in the sample vials cannot be eliminated.

A hydrolytic decomposition would inevitably increase the oxygen content, which is why the oxygen contents of the samples, which were modified with benzyl bromide, were plotted against the storage time (see Fig. 44).

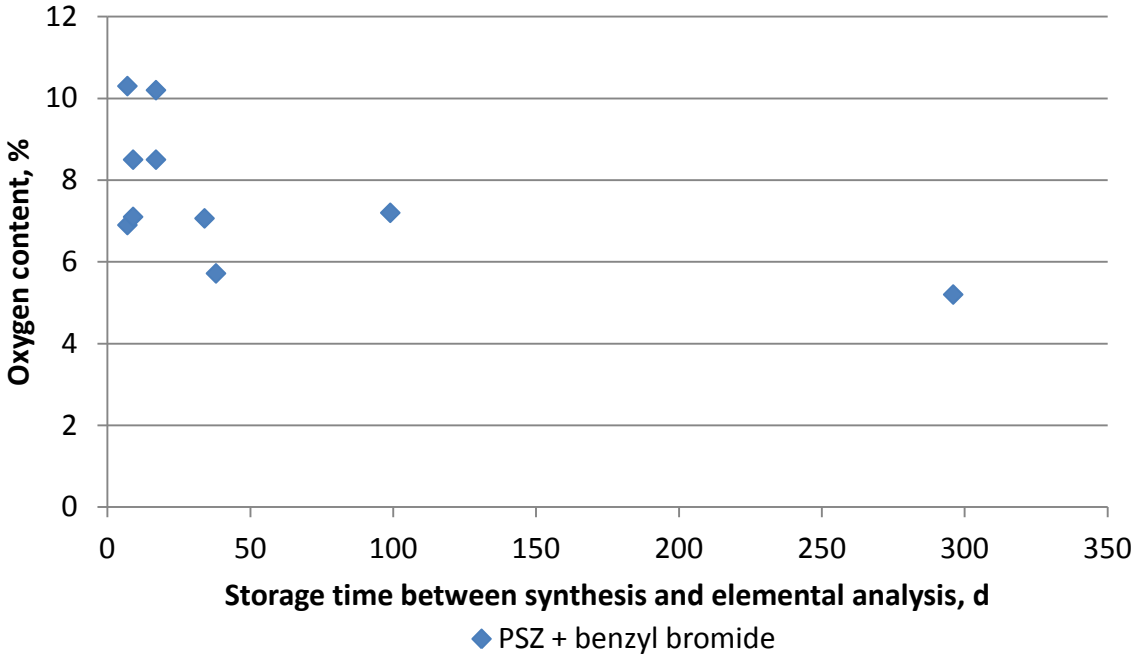

Fig. 44 Oxygen content of uncrosslinked samples modified with benzyl bromide as a function of storage time

Although the oxygen content varies very widely (mainly due to different reaction conditions), it isn't possible to infer that the oxygen content increases with higher storage times. To eliminate the influence of different reaction conditions and to get a better comparability, two samples were illustrated on their own in Fig. 45. The numbers "1112" and "2606" refer thereby to the date on which the samples were synthesized.

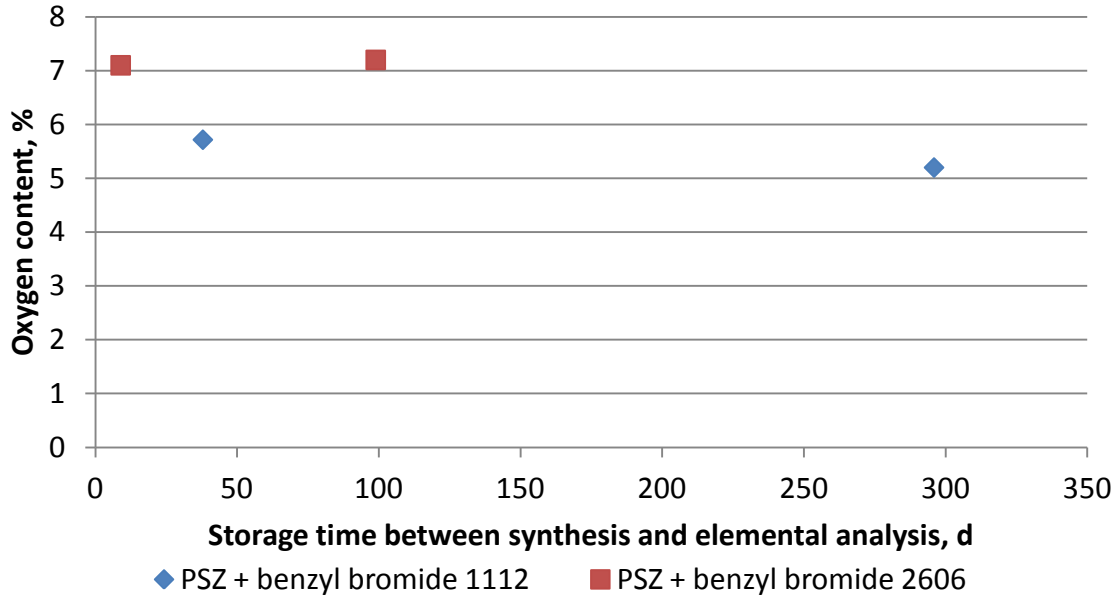

Fig. 45 Oxygen content of two uncrosslinked samples modified with benzyl bromid as a function of storage time

Fig. 45 shows again that the oxygen content doesn't change significantly with time, indicating that the samples were not hydrolyzed.

4.4.3 Carbon content

Since the decomposition reaction during storage does not seem to be a hydrolysis (see 4.4.2), it seems likely that the substituted organic groups split off again in a reverse reaction of the nucleophilic substitution (see Fig. 6). If this would be the case, however, this decrease in the degree of substitution would have to result in a significantly decrease in the carbon content after cross-linking.

Therefore, the carbon contents of the crosslinked samples shown in Fig. 45 were plotted against the storage time between synthesis and cross-linking, which is shown in Fig. 46. It can be seen that the carbon content does not change significantly as a function of the storage time. It therefore appears that there is no reverse reaction of the nucleophilic substitution, instead it is more likely that the polymer chain breaks down into smaller parts during storage. The reason why this phenomenon only occurs in the modified samples, but not in the unmodified polymer, could not be clarified. A possible explanation could be that the increased oxygen content of the modified samples weakens the polymer chain, causing it to decompose over time.

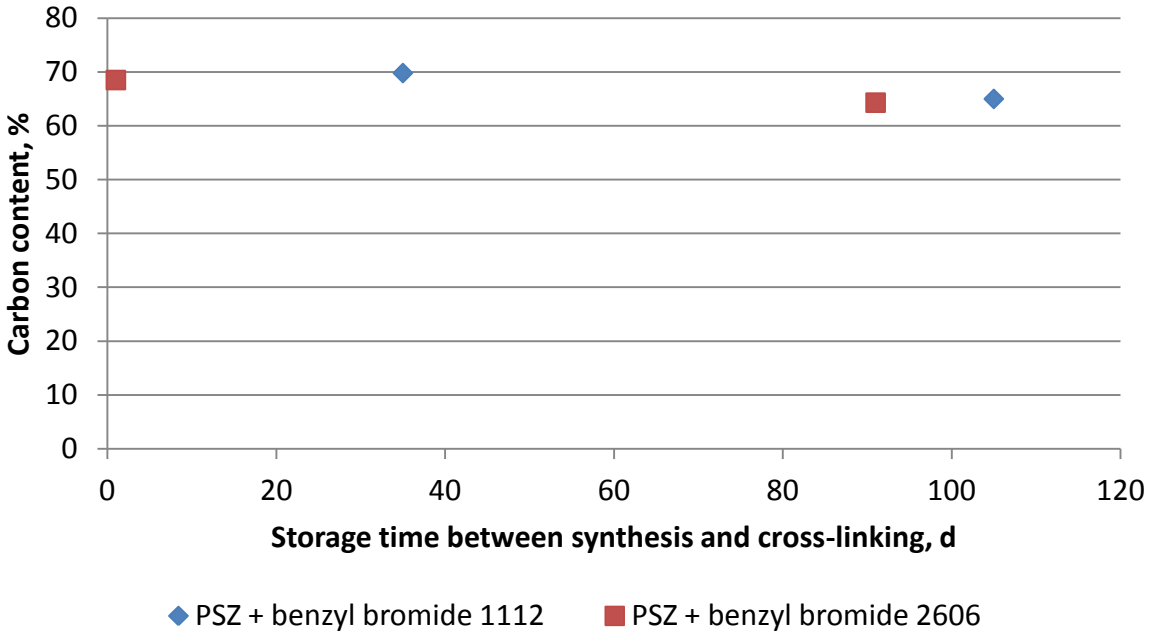

Fig. 46 Carbon content of two crosslinked samples modified with benzyl bromide as a function of storage time between synthesis and crosslinking

4.4.4 Summary

The following observations were made investigating the influence of storage time:

- Mass loss during cross-linking increases with increasing storage time, indicating that the modified samples slowly decompose under the chosen storage conditions.
- Mass loss during pyrolysis does not seem to correlate with the storage time, indicating that the cross-linked samples don’t decompose or decompose much slower than the uncrosslinked samples.
- The oxygen contents of the samples remain unaltered with long storage times, indicating that the decomposition reaction is not a hydrolysis.
- The carbon contents of the samples doesn't change with the duration of storage, which contradicts the assumption that the decomposition reaction is a reverse reaction of the nucleophilic substitution.

During this work, it was not clarified what causes the decomposition of the uncrosslinked samples during storage, but it is possible that incorporation of oxygen during the chemical modification weakens the polymer chain, causing decomposition over time.

5. Conclusions

In summary, it can be said that the aim of this work has been achieved, which was a significant increase of the microporosity of the resulting ceramics through chemical modification of the precursor polymers. The ceramics resulting from the modified samples had a significantly higher BET surface area than ceramics obtained by pyrolysis of the unmodified polymer (see 4.1.7.1). The pore size distribution of the resulting ceramics does not change as a result of the modification and, according to NLDFT analysis, is in the desired range around or just below 1 nanometer (see 4.1.7.2).

The observations made in this work indicate that the modification basically works as expected. By chemical modification, organic groups were attached to the polymer, which were split off during pyrolysis (see 4.1.4), increasing the number of micropores (see 4.1.7 and 4.2.6). By adding less or more bromide, therefore, the degree of substitution and thus the resulting porosity can be controlled (see 4.2.6).

In addition to these promising results, however, there is still room for improvement. The oxygen content, which should be kept as low as possible, was higher than expected and increased significantly by the modification compared to the unsubstituted polymer (see 4.1.5.2), although the reactions were carried out under nitrogen atmosphere. There are indications that the oxygen enters the samples during processing (see 4.3.1).

Surprisingly, the IR spectra of all samples showed the peak of the NH group (see 4.1.3), although this hydrogen atom should be split off during nucleophilic substitution (see Fig. 6), whereby the peak was not expected, at least for the samples with almost complete substitution. Since the peak can be seen nevertheless, it is possible that the substitution takes place in a different manner than assumed in section 2.3.

Although the NMR spectra basically showed the peaks that were to be expected, the size of the peaks deviated considerably from the theory (see 4.1.6). The reasons behind this phenomenon could not be clarified.

It was also analyzed which bromides are best suited for the achievement of the objectives of this work. In the experiments with different bromides (see 4.1), it was found that the aromatic bromides (benzyl bromide and α-bromo-p-xylene) performed better than the remaining bromides, as the reactions proceeded faster (see Tab. 5), the degree of substitution was higher (see Tab. 8) and the oxygen levels lower (see Tab. 9). The NMR spectra (see 4.1.6) also speak for the aromatic bromides, since the NMRs were the closest to the expectations here.

The only argument in favor of the non-aromatic bromides (e.g., 1-bromobutane) would be that they had at a much lower degree of substitution a BET surface area as high as the aromatic bromides (see Fig. 36). One might therefore assume that with these bromides an even higher BET surface area would be possible if it could be managed to further increase the degree of substitution. However, this is only speculative and it is more than questionable whether this can outweigh the disadvantages.

In conclusion, it can therefore be said that the idea underlying this work seems promising. At the same time, however, additional work must be invested to be able to understand and to eliminate the problems that still occur.

List of references

[1] "Englisch Oxford living Dictionaries," Oxford, [Online]. Available: https://en.oxforddictionaries.com/definition/us/PORE. [Accessed 6 March 2019].

[2] J. R. Nimmo, "Porosity and pore size distribution," *Encyclopedia of Soils in the Environment,* vol. 3, pp. 295-303, 2004.

[3] R. Haynes, "Effect of porosity content on the tensile strength of porous materials," *Powder Metallurgy,* vol. 14, no. 27, pp. 64-70, 1971.

[4] M. Scheffler and P. Colombo, Cellular Ceramics: Structure, Manufacturing, Properties and Applications, Wiley-VCH, 2006.

[5] A. R. Studart, U. T. Gonzenbach, E. Tervoort and L. J. Gauckler, "Processing Routes to Macroporous Ceramics: A Review," *Journal of the American Ceramic Society,* vol. 89, no. 6, pp. 1771-1789, 2006.

[6] P. Liu and G.-F. Chen, "Applications of Porous Ceramics," in *Porous materials: processing and applications*, Elsevier, 2014, pp. 303-344.

[7] C. Vakifahmetoglu, D. Zeydanli and P. Colombo, "Porous polymer derived ceramics," *Materials Science and Engineering R,* vol. 106, pp. 1-30, 2016.

[8] A. Stankiewicz and J. A. Moulijn, Re-engineering the chemical processing plant: process intensification, CRC Press, 2003.

[9] A. Stankiewicz, "Reactive separations for process intensification: an industrial perspective," *Chemical Engineering and Processing,* vol. 42, no. 3, pp. 137-144, 2003.

[10] J. Hansen, P. Narbel and D. Aksnes, "Limits to growth in the renewable energy sector," *Renewable and Sustainable Energy Reviews,* vol. 70, pp. 769-774, 2017.

[11] R. Baker, "Baker, Richard W. "Future directions of membrane gas separation technology," *Industrial & engineering chemistry research,* vol. 41, no. 6, pp. 1393-1411, 2002.

[12] T. Konegger, C.-C. Tsai, H. Peterlik, S. E. Creager and R. K. Bordia, "Asymmetric polysilazane-derived ceramic structures with multiscalar porosity for membrane applications," *Microporous and Mesoporous Materials,,* vol. 232, pp. 196-204, 2016.

[13] T. Isobe, Y. Kameshima, A. Nakajima, K. Okada and Y. Hotta, "Gas permeability and mechanical properties of porous alumina ceramics with unidirectionally aligned pores," *Journal of the European Ceramic Society,* vol. 27, no. 1, pp. 53-59, 2007.

[14] "Institute of Chemical Technologies and Analytics," TU Wien, 23 July 2018. [Online]. Available: https://www.cta.tuwien.ac.at/division_chemical_technologies/hlk/. [Accessed 6 March 2019].

[15] T. Konegger, P. Rajesh and R. Bordia, "A novel processing approach for free-standing porous non-oxide ceramic supports from polycarbosilane and polysilazane precursors," *Journal of the European Ceramic Society,* vol. 35, no. 9, pp. 2679-2683, 2015.

[16] P. Colombo, G. Mera, R. Riedel and G. D. Sorarù, "Polymer-Derived Ceramics: 40 Years of Research and Innovation in Advanced Ceramics," *Journal of the American Ceramic Society,* vol. 93, no. 7, pp. 1805-1837, 2010.

[17] P. Colombo, "Engineering porosity in polymer-derived ceramics," *Journal of the European Ceramic Society,* vol. 28, no. 7, p. 1389.1395, 2008.

[18] J. Dismuukes, J. Johnson, J. Bradley and J. Millar, "Chemical synthesis of microporous nonoxide ceramics from polysilazanes," *Chemistry of materials ,* vol. 9, no. 3, pp. 699-706, 1997.

[19] P. Greil, " Polymer derived engineering ceramics," *Advanced engineering materials,* vol. 2, no. 6, pp. 339-348, 2000.

[20] M. Zaheer, T. Schmalz, G. Motz and R. Kempe, "Polymer derived non-oxide ceramics modified with late transition metals," *Chemical Society reviews,* vol. 41, no. 15, pp. 5102-5116, 2012.

[21] Q. Li, X. Yin, W. Duan, L. Kong, X. Liu, L. Cheng and L. Zhang, "Improved dielectric and electromagnetic interference shielding properties of ferrocene-modified polycarbosilane derived SiC/C composite ceramics," *Journal of the European Ceramic Society,* vol. 34, no. 10, pp. 2187-2201, 2014.

[22] M. S. Bazarjani, H.-J. Kleebe, M. M. Müller, C. Fasel, M. B. Yazdi, A. Gurlo and R. Riedel, "Nanoporous Silicon Oxycarbonitride Ceramics Derived from Polysilazanes In situ Modified with Nickel Nanoparticles," *Chemistry of Materials,* vol. 23, no. 18, pp. 4112-4123, 2011.

[23] M. S. Bazarjani, M. M. Müller, H.-J. Kleebe, Y. Jüttke, I. Voigt, M. B. Yazdi, L. Alff and A. Gurlo, "High-Temperature Stability and Saturation Magnetization of Superparamagnetic Nickel Nanoparticles in Microporous Polysilazane-Derived Ceramics and their Gas Permeation Properties," *ACS applied materials & interfaces,* vol. 6, no. 15, pp. 12270-12278, 2014.

[24] J. L. Moore, S. M. Taylor and V. A. Soloshonok, "An efficient and operationally convenient general synthesis of tertiary amines by direct alkylation of secondary amines with alkyl halides in the presence of Huenig's base," *Arkivoc,* vol. 6, pp. 287-292, 2005.

[25] "Chemical Search Engine," [Online]. Available: https://www.chemicalbook.com/. [Accessed 6 March 2019].

[26] M. Thommes, K. Kaneko, A. V. Neimark, J. P. Olivier, F. Rodriguez-Reinoso, J. Rouquerol and K. S. Sing, "Physisorption of gases, with special reference to the evaluation of surface area and pore size distribution (IUPAC Technical Report)," *Pure and Applied Chemistry,* vol. 87, no. 9-10, pp. 1051-1069, 2015.

[27] J. A. Moulijn, A. Stankiewicz, J. Grievink and A. Górak, "Process intensification and process systems engineering: A friendly symbiosis," *Computers & Chemical Engineering,* vol. 32, no. 1-2, pp. 3-11, 2008.